Australian Government

Department of Defence

Defence Science and

Technology Organisation

Development of the Larzac Engine Rig for Compressor Stall Testing

A M Abdel-Fattah and A S Vivian

Air Vehicles Division
Defence Science and Technology Organisation

DSTO-RR-0377

ABSTRACT

The development and upgrade of test installations, instrumentation and the data acquisition system of an existing turbofan engine test rig are described for an experimental program which was planned and initiated to investigate the transient unsteady operation of gas turbine engines with an emphasis on compressor operation. The objective of the program was to examine aerodynamic instabilities such as stall and surge. Of particular interest were the pre-stall behaviour of the compressor and the generation and the detection of gas-path stall/surge precursors. Methods used to invoke compressor stall/surge and to detect stall/surge precursors are described and examples of results of the observed stall/surge phenomena and their precursors are included. However, the precursor pressure pulses are of small amplitude and occur only several milliseconds prior to the point of stall initiation. Additional work is required to incorporate these results in a practical stall warning device.

RELEASE LIMITATION

Approved for public release

UNCLASSIFIED

APPROVED FOR PUBLIC RELEASE

UNCLASSIFIED

Development of the Larzac Engine Rig for Compressor Stall Testing

Executive Summary

Stall and surge of turbo-machinery compressors has been a major concern to aircraft operators since the first gas turbine engines were introduced into service. Stall, on its own, sometimes undetected and unsuspected, is always detrimental to engine efficiency and performance. Combined with surge it can be sudden in onset, giving no warning and very rapidly lead to flameout, thrust loss and catastrophic mechanical failure. This is likely to occur in the presence of air flow disturbance, whilst the aircraft is manoeuvring or the pilot is demanding rapid changes of thrust. High ambient temperature is also a potential contributing factor. Stall and surge is unacceptable to a civil operator of multi-engined aircraft; to a military operator such an occurrence, particularly at low altitude, can be fatal. Unfortunately the circumstances where stall and surge are most likely to occur are frequently unavoidable during military operations, where, in addition to naturally occurring atmospheric and manoeuvring effects, another possible source of intake disturbance is ingestion of hot gases from gun discharge or missile launch.

Decades of development have produced engines with reduced stall and surge susceptibility, but have not eliminated stall and surge as potential causes of aircraft loss. Studies of the phenomena make it clear that it is unlikely to ever achieve total elimination of the problem. However, it may be possible to detect pressure disturbances in the engine intake air flow which provide a warning that the engine is approaching stall. Detected early enough these precursor disturbances might be used to initiate avoidance action.

This report describes the further development of an existing engine performance test rig to provide the capability to investigate stall and surge occurrences and to identify stall precursors. The rig is one of a very small number of such rigs in the world and is currently unique in Australia. The report details the operation of the overall rig and of the test engine and its control system. It also details the procedures for successful experimental testing and presents a selection of results obtained. These results show evidence of stall precursors, however these are of small amplitude and occur only a few milliseconds prior to the point of stall initiation. The report includes recommendations for future studies of stall and surge onset detection.

This page is intentionally blank

Authors

Dr. Adnan M. Abdel-Fattah
Air Vehicles Division

Dr Abdel-Fattah Graduated with a B.Mech.Eng. (Cairo)-1970, and M.Eng.Sc. Sydney)-1976, and Ph.D, (Sydney)-1978. He lectured in Mathematics May/1971 - Jul/1973 in S.I.T.C. - Ministry of Labour – Kuwait - United Nations Development Programs, and later at UTC Sydney and Sydney University. He joined James Howden Australia Pty. Ltd. – Sydney as Research and Development Engineer, Aug/78 - Oct/82. The R&D Work included the development of a patented anti stall device capable of eliminating the stall margin from any axial and mixed flow fan operation. He joined DSTO in 1982 as Research Scientist and was promoted to Senior Research Scientist in 1987. Research included work on thrust augmenting ejectors, confined jet mixing, aerodynamics of aircraft-engine run-up facilities, turbojet engine air intake duct, modelling of stall/surge prediction, and experiments to detect and identify stall and surge precursors in the operation of multi stage compressors in aero engines. He received the ASME Best Paper Award, 2007, Atlas Copco Prize, Best Thesis, Sydney Uni, 1976. He retired in 2007

_____   _____

Andrew S. Vivian
Air Vehicles Division

Mr. Andrew Vivian joined what was then known as the Mechanical Engineering Division of Aeronautical Research Laboratories in 1964; Aeronautical Research Laboratories subsequently became DSTO-Melbourne. Mr Vivian currently works in Air Vehicles Division. Mr Vivian studied at Melbourne University and Latrobe University, graduating BSc in physics and mathematics. Mr. Vivian has been involved in all of DSTO's major engine performance research programs and RAAF engine investigations since 1980.

_____   _____

This page is intentionally blank

Contents

This page is intentionally blank

Nomenclature

Abbreviations and Acronyms

Casella	Brand of high accuracy barometer
DAQ	Data Acquisition
DSTO	Defence Science and Technology Organisation
EGT	Exhaust Gas Temperature
HPC	High Pressure Compressor
Hz	Hertz (frequency)
Kulite	Brand of very high-response rate pressure transducer
LPC	Low Pressure Compressor
N	Newton
PC	Personal Computer
PCI	Peripheral Component Interconnect
psia	pounds per square inch absolute
SETH	Small Engine Test House
SNECMA	Major French Aerospace and Engine Manufacturing Company

Symbols

$dP_{s\text{-}d}$	Reduction due to stall of static pressure at fan exit
$dP_{s\text{-}u}$	Increase due to stall of static pressure at fan inlet
f1, f2, etc	Designators for various frequency peaks in measured pressure spectra
N_{HPC}	HPC rotational speed
N_{LPC}	LPC rotational speed

This page is intentionally blank

1. Introduction

Instabilities encountered during the operation of a gas turbine engine normally originate in the axial flow compressor, and can be triggered by non uniformities or distortion in the intake air flow at the engine face. Intake flow distortion, in a variety of forms and sources, has increasingly become a key issue affecting engine performance and stability. The most common form of axial compressor instability is rotating stall, which, depending on engine type, loading and application, can lead to fully developed surge with ultimately serious and damaging effect.

Stall is a result of flow separation on the blades in the hub or tip region of the stator or compressor rotor. This separation could be steady or unsteady. In either case inlet flow distortion could cause this separation. This in turn leads to effective alteration of the compressor maps, in the form of reduced mass flow, shift in efficiency contours, and a depression of the surge line with an equivalent reduction in the stall margin of the compressor. The distortion amplitude, depending on application and circumstances, may lead to compressor stall and surge, References 1 to 8. In the case of an installed compressor, inlet flow distortion may produce significant rematching with resulting operating line shifts reducing the surge margin and potentially destabilising the engine. The progression, possibly very rapid, from flow separation through stall to surge and severe mechanical damage to the subject engine serves to maintain interest in this phenomenon.

Aerodynamic stability is a fundamental limit in both the compressor design and operation process. Increasing this limit would permit higher loading and deliver higher efficiency, in turn increasing mission safety and tolerance to stage mismatch during part speed operation and speed transients. A major research topic for the last six decades has been investigation of the transient unsteady operation of gas turbine engines with emphasis on compressor operation. A particular focus has been inlet flow distortion and its effect on the performance and stability of the compression system, coupled with examination of the aerodynamic instabilities leading to the inception of stall or surge.

It has long been observed that surge is almost always preceded by stall. More recently the pre-stall behaviour of the compressor has become a major concern, especially the identification and detection of stall/surge precursors in the flow, with the ultimate goal being active stability enhancement of the compressor. Precursor pulsations in the gas path flow might serve as a stall/surge warning, and be used to initiate avoidance, recovery or suppression of compressor stall possibly by means of active stall control of the engine. Active control could be achieved internally through the main engine controls, or externally, by some interference with or modification of the air flow at the inlet. For reliable stall warning or stall onset recognition, it is therefore important that a reliable real-time precursor detection capability be investigated.

This report describes the development of a turbofan engine test rig with additional capabilities to generate, detect, capture, and ultimately analyse compressor flow instabilities leading to the inception, growth and propagation of stall and surge.

2. Test Facility:

The test engine used in this investigation is the Larzac 04-C4B engine installed in the Small Engines Test House, DSTO Melbourne and is shown in Figure 1. It is a two-spool low bypass ratio turbofan engine, which was designed and manufactured by Turbomeca-Snecma, and is used in the Alpha Jet trainer and ground attack aircraft. The engine operated by DSTO was previously used by Snecma as a development engine.

The Larzac engine consists of a two-stage fan or low pressure compressor (LPC) driven by a single-stage low pressure turbine; a four-stage high pressure compressor (HPC) driven also by a single-stage high pressure turbine; an annular pre-vaporising combustor exhausting through, firstly, the high pressure turbine and then through the low pressure turbine. The core and bypass flows stay unmixed and exhaust through concentric separate nozzles. Two bleed valves behind the second stage of the HPC are used to reduce the blade loading at part-speeds ranging up to 80% speed of the HPC. When open these bleed valves allow some of the high pressure flow to escape into the bypass duct.

Performance parameters at design speed and sea-level static conditions are shown in the following table.

Table 1 Performance parameters at design speed and sea-level static conditions

LPC Speed	17311 rpm
HPC Speed	22914 rpm
LPC Pressure Ratio	2.26
HPC Pressure Ratio	4.6
Mass flow rate	28.1 kg/s
Bypass ratio	1.14
LPC blade number	23
HPC blade number	29
Engine thrust	13181 N

2.1 Test Rig Development

The aim of the program was to modify and upgrade the Larzac test rig in the Small Engine Test House (SETH) in order to develop additional capabilities to generate, detect, and capture the initial compressor flow instabilities presaging the inception and propagation of stall.

2.1.1 Original Experimental Setup:

The Larzac engine with a section depicting locations for the original suite of conventional low speed engine instrumentation is shown in Figure 2. The original specification and limitations of both sensors and Data Acquisition system (DAQ) is described in the following sections:

2.1.1.1 Instrumentation:

Standard engine operation and aircraft cockpit instrumentation was used extensively in the original setup of the engine test rig. Relatively few internal parameter measurements were available through the standard instrumentation. However, where possible, these were accessed electronically for experimental purposes. Thus, both engine high and low spool speeds were captured from the "phonic wheel" speed-sensors. These generate pulse-rate signals from magnetic sensors detecting the passage of multi-splined sections of each spool shaft. Turbine exit temperature was captured directly as a low-level voltage signal, (subsequently amplified), from the standard thermocouple loom fitted immediately downstream of the turbine exit.

Pressures were measured indirectly via pressure probes connected by external tubes to pressure transducers. The transducers were located off the engine and generally a little distant from measurement points although as close as reasonably possible. This separation was to reduce the possibility of transducers failing due to high vibration levels. Most pressure and all temperature sensors were of conventional type, providing analogue output signals, but of inherently low frequency response capability.

Static pressure and temperature were measured in the volume between the test cell air intake splitters and the debris screen in front of the engine bell mouth. The total pressure in the test cell at the start of the bell mouth was measured with a total pressure probe. Temperature was measured at the same point using a single microchip sensor.

Pressure in the intake duct was measured with a radial total pressure rake having four radially located, forward looking, pitot-type entries. These entries were positioned radially so that the annuli between were of equal area. Static pressure was measured at the same axially located cross sectional plane as the total pressure rake, with four static pressure ports spaced around the circumference of the duct, with the static pressures being averaged by being connected to a common tube feeding to a pressure transducer.

A specially designed rake was installed through the engine casing via a borescope inspection port at the exit of the fan (or LPC). This rake covered the inlet of both the by-pass duct and the HPC with total pressure measured by five pitot type probes. Total temperature was measured by five separate type K thermocouples of smallest possible diameter inserted one into each of the pitot type probes. A view of the rake is shown in Figure 3. Static pressure was measured at the inner surface of the casing wall with the sensing orifice located in a flush-fitting plug installed into a second borescope port located in exactly the same cross-sectional plane.

Another specially designed rake was fitted at the HPC exit. As a result of the very constricted cross-sectional area of the exit nozzle it was only possible to fit this rake with one total pressure pitot, with an included total temperature sensing thermocouple and a single static pressure sensing port.

Again, a specially designed arrangement of total pressure pitot and static pressure sensing port were fitted at the entrance to the core-engine exit duct, downstream of the high and low-pressure turbines. The normal factory incorporated ring of rapid response total

temperature thermocouples used by the engine's fuel controller are also installed at this location. These were adapted to simultaneously provide the same voltage signal to the experimental data acquisition system. The location of the various gas path sensors- rakes, static pressure ports, etc, are shown in Figure 2.

Temperature and pressure conditions were measured at the by-pass duct exit, where the by-pass flow re-enters the surrounding atmosphere. Four rakes were located at ninety degree intervals around the circumference of the duct exit. Each rake consisted of three total pressure pitot probes with included total temperature sensing thermocouples, facing upstream within the exit annulus, together with a static pressure tapping in the outer wall of the duct. The three total pressure probes were located at various radii from the outer wall. The radii were selected to ensure equal annular cross-sectional areas between the probes and between probes and duct walls. Details are shown in Figure 4.

Engine rotational speeds for both the low pressure fan spool and for the high pressure compressor spool were obtained from the inbuilt sensing system used by the electronic engine control system. In both cases the sensing was provided by a magnetostrictive circuit with an electromagnetic pickup located very close to and activated by the passage of equally spaced teeth of splines cut accurately into the spool shafts. The pulse-rate signals were fed to the DAQ system via frequency to voltage converters.

Ambient conditions for the test engine were measured inside the test cell, between the air entry splitters and the engine. The air pressure was measured using an accurate electronic Casella barometer with a digital output. The air temperature was simultaneously measured across the cell at mid-height using four suspended microchip sensors whose circuitry was designed to combine the four outputs to produce a single average-value analogue signal. These sensors were open toward the incoming air-flow and to the rear but were each shielded with multiple surrounding radiation screens.

2.1.1.2 *Computer and Data Acquisition:*

The original DAQ system incorporated Data Translation Inc DT-2839 and DT-2896 analogue to digital conversion boards and could accommodate 64 differential input channels, albeit at only one sampling rate. The highest rate possible, at 224 kHz overall, gave a sample rate per channel of 224kHz divided by the number of connected channels or 3.5 kHz per channel if all 64 channels were in use. Higher rates could be achieved only by reducing the number of connected channels. Previous use of the system captured 30 channels at 32 Hz per channel for up to 35 minutes. Higher sample rates were precluded due to inherent inabilities of the instrumentation. Thus, the instruments (probes, tubing, transducers, etc) themselves could only deliver response times of the order of 0.1 to 0.07 sec, so that 32 Hz per channel was an appropriate sample rate. With a response time of 0.07 sec, a sensor was unable to detect and track a parameter change faster than 15 Hz. Thus a sampling rate of 32 Hz was actually over-sampling, but not excessively so, and guaranteed that observed changes had been tracked to the full capability of the sensor. On the other hand an advantage of this situation was that the problem of aliasing (which always arises in the presence of parameter change rates in excess of sampling rate) was largely avoided; the sensors themselves functioned as effective low-pass filters. A further limitation inherent in the earlier data acquisition system was that real-time display of data during the actual acquisition process was severely constrained. With these limitations and

constraints, only operational transients resulting from operator inputs, and control system failures could be studied; transient phenomena, such as rapid changes of gas-path parameters due to internal physical processes within the engine were beyond the capability of the system.

2.1.2 Revised Experimental Setup:

Development of the revised test rig involved the following issues and requirements:

■ The approach was to build on and make use of the components of the existing experimental setup as far as possible. Careful consideration of how to make use of the pre-existing setup showed that it would be possible to build on all the required extra capability whilst maintaining backward compatibility.

■ New DAQ circuit boards (from Data Translation Inc) enabled the connection of up to 8 channels per board, and gave a maximum sample rate per channel of 100 kHz divided by the number of connected channels. Thus, with all 8 available channels accepting data the maximum possible sample rate on any one channel would be 12.5 kHz. These new boards were compatible with the previously installed boards and software. With a triggering link installed, the new boards could acquire data at their maximum speed, simultaneously, and synchronised with, the older boards capturing data at 32 Hz per channel.

■ Investigation of compressor flow instabilities dictated the need for very high response pressure transducers, coupled as closely as possible to the point of measurement in order to eliminate or at least minimise the effect of the coupling. The best possible arrangement was to locate the transducer at the measurement location, which could only be achieved using miniaturised Kulite transducers of such small size that they could be built into the compressor walls or into pitot tubes etc., in pressure rakes with the sensitive end face of each transducer open directly to the gas flow. The use of these sensors is described in greater detail later in this report.

■ The decision to utilise Kulite transducers having a nearly flat frequency response to beyond 65 kHz necessitated the installation of adjustable low-pass anti-aliasing filters on each high speed channel. Without such filters, and with the certain presence of blade passing frequencies and even higher turbulence and acoustic generated pressure fluctuations, aliasing and noise would certainly swamp any measurements related to stall and surge instability. As the instability related phenomena were not expected to occur at frequencies greater than the rotational speed of the engine a roll-off frequency of about 1 to 2 kHz was prescribed for the filters.

■ Fitting miniature Kulite transducers generated significant problems due to the geometrical constraints involved in gaining access to internal passages of the engine in order to insert the new sensors in the gas path. Access to the plane immediately prior to the fan entry was simple. Some limited access to the gas path at the fan outlet into the bypass duct and upstream of the HPC was possible through existing borescope ports through the engine casing in this area. Kulite sensors upstream and downstream of the fan could be incorporated using specially designed and manufactured new probes or by modifying existing ones. These arrangements permitted the extension of the previous low speed

measurement system to measure pressures (effectively average pressure, that is) at the same locations as the Kulite transducers.

■ To gain access to internal engine components and passages between the fan stages and in the high pressure region of the HPC and in the hot end of the engine, some special additional engine tooling to separate engine modules was required. These tools were acquired from "SNECMA", the manufacturer of the engine. No further detailed planning for further instrumenting the less accessible regions of the engine was undertaken.

■ A compressor throttling device or other means to force the engine gas generator operating point off the standard operating line towards the surge line and into the region of reduced surge margin was to be designed, built and installed in the rig in SETH. Similarly a device was required to throttle the bypass duct, to force the fan toward its surge line

■ The revised and upgraded engine test rig was to include the following new features:

   • Miniaturised high speed sensors and transducers capable of installation at the point of measurement to provide the necessary dynamic sensing capability.
   • Special probes and fittings designed and built to allow the installation of the high speed sensors in the engine.
   • DAQ boards with the highest acquisition rate possible.
   • Anti-aliasing filters fitted to all dynamic high speed signal lines.
   • System of real-time display of a selection of any channels, permitting some inspection of the signal levels and capable of recording all high and low speed channels with sufficient capacity to store all recordings.
   • Externally controllable electro-mechanical devices to throttle both the gas generator exit flow and to throttle the exit flow from the bypass duct.
   • Externally controllable means for over-riding the arrangements built into the engine control system to prevent over temperatures and to prevent compressor stall.

2.1.2.1 Instrumentation:

Flow disturbances and distortions leading to or causing the inception of compressor stall result in rapid variation of velocity and pressure in the compressor flow field. The stall phenomena itself is always preceded by the development of stall cells which move in the circumferential direction at a speed of up to 70% of rotor speed. To detect the stall cells and the flow disturbances responsible for their generation, and to minimise time lag and damping in measuring the pressure fluctuations, it is essential to directly measure these at the point where the fluctuations were located within the compressor. This is called the ''direct measurement method'', to achieve which the sensors or pressure transducers must be directly facing the fluid flow at the disturbance location. In the harsh environment of gas turbine engines, these sensors must simultaneously satisfy the following requirements:

1. Small in size so as not to interfere with the flow.
2. High natural frequency to eliminate resonance between the transducer and changes in facing pressure.

3. Must have enough thermal stability to withstand the flow temperature at the particular location.
4. Must be stable in relation to engine vibration.
5. Must not be affected by the particulates or molecules in the flow field.
6. Very sensitive with very high speed transient response to changes in pressure.

Piezo-resistive Kulite miniaturized pressure transducers, capable of delivering excellent high frequency response were found to satisfy all of the above requirements and were therefore selected for addition to the 'standard' instrumentation.

The Kulite transducers selected for both upstream and downstream of the LPC (the fan), were types XCQ-093-25 (25 psia max) and XCQ-093-50 (50 psia max) respectively. These transducers were approximately 2.0 mm in diameter and 10 mm in length. In terms of size and shape these are shown in Figure 5 for comparison with the conventional low speed pressure transducers used on the rig.

New rakes and fittings were designed and built to accommodate the miniature Kulite transducers for internal gas path measurement, with the rakes to be installed upstream and downstream of the fan.

To avoid drilling holes in the fan casing, a spacer ring was designed and built to accommodate the miniature Kulite transducers for direct dynamic pressure measurements immediately upstream of the first stage of the fan. The ring was incorporated in the rig between the cylindrical fan casing and inlet duct with details shown in Figure 6. The ring can accommodate ten miniature Kulite transducers giving five static and five total pressure measurements at a cross section plane 6mm upstream of the edge of the first fan stage. However, five static and only two total pressure sensors were connected and activated. The total pressure sensors were mounted inside appropriate lengths of close fitting steel tube with the outer end capped closed. A small entry hole was bored through the wall of the tube close to the closed off end with the edges of the hole chamfered to minimise entry flow disturbance. The sensing transducer was fastened into the tube so that the sensing end face of the transducer was 2 mm in from the entry hole plane. The connecting wires were run out through the tube which was mounted into the circumferential ring so that the entry hole faced directly upstream. The static pressure transducers were flush mounted with the casing or the inner diameter of the spacer ring. To achieve this they were fastened into close fitting radial holes in the ring with their pressure sensing end face just below the inner face of the ring. Due to geometrical constraints, the sensors could not be uniformly distributed around the circumference of the spacer ring. The angular locations of the sensors in the ring are also shown in Figure 7.

Direct measurement of static pressure downstream of the fan was achieved through an existing inspection hole with a newly designed "probe", actually a close fitting metal plug completely filling the inspection port, accommodating a single miniature Kulite transducer which was flush mounted to the curved inner face of the plug so as to sense static pressure in the flow path. Details are shown in Figure 6.

The specially designed conventional pitot type total pressure and temperature rake shown in Figure 3, included provision to accommodate two miniature Kulite transducers located at different radial positions and fitted with their own pitot entries, one for the direct

measurement of transient total pressure upstream of the HPC and the other for entry into the bypass duct. These locations are also indicated in Figure 3.

The Larzac test rig with the location of the new dynamic high speed instrumentation is shown schematically in Figure 8.

2.1.2.2 *Computer and data acquisition:*

To match the improved capabilities of the instrumentation and to accommodate the selected high performance pressure sensors it was necessary to upgrade the supporting PC-based data acquisition system. The PC system used the Windows98-SE operating system. Data acquisition, real time display and subsequent data analysis were all handled by Agilent HP-VEE and Data Translation DT-VPI software.

Low-speed data acquisition continued to use Data Translation DT-2839 and DT-2896 boards. High speed data acquisition was carried out using two of Data Translation's DT-3002 DAQ boards, with which acquisition rates of 12 kHz, or higher, were possible. Details of signal distribution signal collection and data acquisition are shown in Figure 12. Each of the signals from the Kulite pressure transducers was amplified to a higher level range of voltages (0 to 10 VDC), and was subsequently filtered and digitized with a sampling rate of (12500 Hz) and 12-bit resolution.

The low speed DAQ boards and the two high speed DAQ boards were synchronised together by an external link conductor and were started by one trigger signal, from one of the high speed boards, designated as "master' for the entire system. On receipt of the triggering signal, signals in all 16 high speed channels together with signals connected to the low speed boards were synchronously sampled and recorded. Some details of the board synchronisation problem and its resolution are presented in Figure 13.

To eliminate high frequency noise and aliasing, all of the high speed channel signals were filtered with analogue low-pass 8-pole Modified Elliptic Filters, one per channel, with a cut off adjusted at 1200 Hz, before being digitized and the digitised values transferred to a data storage device.

The revised system is capable of recording a minimum of 8 channels for each of the two high speed DAQ boards, together with 64 low speed channels. Continuous data acquisition and recording for a test condition can be extended, if necessary, for prolonged periods of more than 20 minutes.
Real-time display of all high speed channels and at least 10 low speed channels can be easily achieved. The software also displays a real-time, moving tabulation of all the signals connected to the computer using signal voltages as a common scale, by means of which the operator can closely check on the continuing proper functioning of all the connected instrumentation. This is a useful and important capability; the test instruments and sensors, and, in, particular, the various pressure transducers, have been found to be more or less delicate and occasionally fail in use, an indication of the extreme operating environment associated with a jet engine. Monitoring of the test instrumentation can provide an important saving in time and resources if evidence of instrument failure is promptly identified, thereby permitting testing to be immediately discontinued, and the fault repaired.

2.2 Test Rig Operation

2.2.1 Stall Generation.

The operating point for each compressor was traversed from the normal equilibrium state on the standard, or design operating line for a given speed, into the off-design region (or surge margin) between the operating line and surge line by increasing the exit pressure of the subject compressor. Additionally, on occasion, it was also found necessary to introduce screen-generated inlet flow distortion because the compressors were found to be quite resistant to stalling and surge. Increase of compressor exit pressure was achieved through the activation of independent, controllable, engine exhaust throttling devices fitted to the respective exit nozzles. In theory the use of back-pressuring devices, together with a degree of inlet flow distortion should be sufficient to provoke stall and subsequent surge. In practice, despite employing all the above additional devices, invoking LPC or HPC stall was found to be impossible without overriding the engine's control system. Even with the control system overridden as far as practicable, it was found impossible to drive the engine along the final part of a constant speed line as that line closed on the surge line. The engine control system function and the overrides used are discussed in a later section of this report, together with an explanation for the difficulties experienced as a constant speed line approaches the surge line.

2.2.1.1 Compressor Throttling:

Separate mechanisms were installed to throttle the by-pass duct and the core engine exhaust nozzle.

In the case of the LPC, back-pressuring was achieved through the use of a controllable actuator-driven blockage mechanism throttling the by-pass flow. The mechanism functioned similarly to an iris or a camera shutter and achieved its throttling by the gradual reduction of the effective area of the by-pass exit annulus surrounding the nozzle or core duct, Figure 9.

Back-pressuring the HPC was achieved through the use of an actuator driven blockage mechanism throttling the core flow at its exit. Under operator control an actuator could slowly drive an external mounted parabolic body of revolution- a stainless steel bung- into the engine nozzle until the compressor stalled and surged, Figure 10.

The mechanical and metered actuation of the blockage mechanisms for both the core and by-pass flows, allowed steady controlled throttling, with reproducible results of compressor stall onset and characteristics. Since the purpose of the work was to investigate stall and surge of the individual compression components of the engine, rather than the overall stall and surge behaviour of the engine, it was unnecessary to introduce any mechanism to allow both throttling mechanisms to operate in tandem, thereby simultaneously maintaining the same elevated back-pressure at the respective exits of both ducts.

2.2.1.2 Inlet Flow Distortion:

In addition to tests without any inlet flow distortion extensive tests were carried out with distortion devices at the inlet to simulate engine operation during cross wind flights

resulting from the usual military aircraft manoeuvres, or with inlet being subjected to other inlet distortion effects.

Total pressure distortion at the compressor entry face was simulated by placing multiples of 60° sectors of perforated sheet metal having 36% open area at about one rotor diameter upstream of the first stage rotor in the inlet duct, Figure 11. The extent of this circumferential distortion at the compressor face varied between 60° and 240° (one to four sectors of screen).

2.2.2 Engine Control and Operation

The Larzac engine control system uses an electronic unit and a hydro-mechanical fuel control unit. Between them these units sense atmospheric pressure, exhaust gas temperature, rotor speeds, HPC delivery pressure and fuel flow and, by controlling fuel flow rate, act to prevent over speeds and over temperatures and correct for altitude effects. Normally the controls also prevent excursions of the engine operation into the off-design region where the surge margin is seriously reduced. The control system maintains the stall margin by (i), limiting fuel flow and (ii), by opening the engine's HPC bleed; although mutually independent mechanically, on occasion both operations occur simultaneously. Limiting, or further, reducing fuel flow, limits EGT (its primary purpose) but also assists to reduce HPC speed thereby tending to reduce outlet pressure. Opening the HPC bleed allows air to escape into the by-pass duct from the intermediate stages of the HPC, reducing the overall pressure ratio and shifting the operating condition away from the surge line toward the standard operating condition. With these limiting functions available and operating to maintain surge margin it proved impossible to move the operating point any perceptible distance from the standard operating line.

There is also another limiting process built into the control system. If the HPC bleed system and the normal EGT limiting protection achieved by restricting fuel flow were both inoperative and the operating condition moved close to the surge line, the altitude compensating system will almost certainly intervene. This component of the fuel controller senses the increased pressure ratio not as a higher pressure at the compressor outlet, but as though the compressor inlet pressure were reduced, as would happen if the engine was operating at altitude. In such circumstances the controller interprets this condition as resulting in reduced air-flow so that the fuel/air mixture is becoming excessively rich and with combustion threatening to occur at increasingly high and unacceptable temperatures. Accordingly the fuel controller reduces the fuel flow to prevent the higher temperature and as a result the engine speed falls away. This function of the engine controller was carefully designed to be fool-proof, consequently is very difficult to override, and makes it impossible, in practice, to follow a constant speed line all the way up to a clearly defined point of surge. Indeed it was found that as the surge line is approached no amount of coaxing will keep the engine at the desired constant speed; instead the speed falls away so that when the compressor finally stalls or surges it does so at a turbine entry temperature which, while high, is not disastrously so.

2.2.3 Overriding the Engine Control System

To be able to invoke a compressor stall it was necessary to override some of the engine controls prior to the commencement of compressor throttling by inserting some non-

standard modifications into the control system sensing circuits. These modifications provided carefully judged falsifying signals to the control system to fool it into misjudging the values of the control parameters, thereby preventing the control system from initiating alleviating actions which would prevent the engine from deviating from the standard running line:

The first of the modifications was to override the control of the two bleed valves behind the second stage of the HPC. In normal operation a pressure sensing switch remains open until a minimum compressor pressure ratio is achieved. When that minimum is exceeded the switch closes, applying a voltage to the valves and forcing them to close. A switchable DC voltage supply was connected in parallel across the valves so the valves could be forced closed irrespective of compressor pressure ratio. Forcing the valves closed prevented them from being opened in response to diminished surge margin and also to keep them in the closed position during operation of the HPC at or below 82% rotational speed, where they would normally switch open. Once stall or surge occurred this override could be immediately switched out to assist alleviation via normal functioning of the bleed valves. Frequently, when stall or surge occurred at speeds well above 82%, where the bleed valve would normally always be closed, the compressor's effectiveness was severely reduced, so that the pressure ratio was sufficiently low to permit the bleed valve to instantly open and relieve the condition.

The second modification was provided to override the section of the controller sensing and limiting exit gas temperature, EGT. To do this, an operator controlled biasing voltage counteracting the signal from the EGT thermocouples was inserted into the thermocouple circuit. That is, by introducing a reverse voltage the controller sensed a reduced temperature signal implying a proportionately reduced EGT and was therefore prevented from reducing the fuel delivery rate with the result that the maximum limit temperature could be exceeded for the short period necessary until the initiation of compressor instability. Following onset of the instability, the override was switched out and the throttling device was quickly retracted to relieve the engine from the unstable stalled condition and to permit the engine to cool.

It was found with the Larzac engine on occasion, particularly with higher levels of intake distortion, that when the engine had stalled and surged and the overrides and blockage subsequently removed the engine would not return to normal operation. Instead, the EGT remained very high, the thrust remained low and the engine was unresponsive to normal power lever movements. When this condition was encountered it was imperative to reduce the temperature to acceptable levels as soon as possible. This could only be done by removing the source of the heat- cutting off the supply of fuel to reduce combustion intensity. This could not be safely achieved by simply shutting down the engine since this would leave the engine soaking at very high and potentially damaging temperatures without any internal cooling. Further, there was some evidence suggesting that a considerable excess of fuel might have pooled in the combustor or its outer liners, so that if the engine was shut down there was a risk of an uncontrollable, continuing, very destructive internal fire. In these circumstances it is most important to maintain as much air flow as possible whilst reducing available fuel. This was done by pulling back the power lever to below the fuel-off setting, thereby cutting off all fuel and allowing the engine speed to fall off. As the speed (N_{HPC}) fell below idle (54%) the starter motor was activated. Although from stationary the starter motor cannot accelerate the engine to more

than 16%, at higher rotational speed activating the starter motor reduces engine deceleration very markedly. It was found that with all fuel cut off and the starter motor operating, when the speed had dropped to about 35 to 30%, the cooling effect of the continuing airflow was sufficient to bring the EGT back to normal levels. Once the speed and temperature were adequately reduced the igniter system was reactivated and the power lever advanced to the ground idle position, thereby admitting sufficient fuel for ignition, just as in a normal engine start from stationary. Once the engine had returned to the normal idle condition the power lever was advanced sufficiently to raise the speed to about 65% to 70% to give enhanced airflow to aid cooling and was kept at that condition for 15 to 20 minutes to stabilize internal temperatures.

2.2.4 Test Program:

Steady state baseline data sets for the normal operating line were acquired from all the installed sensors, both low rate and high speed dynamic, at several different engine speeds using a clean inlet. These data sets defined the steady state operating line for both the LPC and HPC of the Larzac.

Starting with the steady state operating point on the operating line and ending with stall on the surge line for a given rotor speed, a series of data sets for different points at the same rotor speed was acquired, defining the traverse/excursion trajectory of the compressor operating point in the off design region in the compressor stall margin. This constant speed traverse was carried out using firstly, and in succession:

> Actuated core blockage mechanism,
> Actuated by-pass blockage mechanism,
> or both, and
> Clean inlet,

Followed, secondly, by:

> Actuated core blockage mechanism,
> Actuated by-pass blockage mechanism,
> or both, and
> Distortion screens at the inlet,

A series of tests were performed in which the core blockage bullet mechanism was slowly inserted into the engine core nozzle or the iris gradually closed at the by-pass duct exit until engine stall was achieved. The gradual activation of both the LPC and HPC throttling devices was carried out in a step by step fashion. Full recording from all sensors was carried out for each intermediate step, until the last step which characterised the engine stalled condition. The process was repeated a number of times at different rotor speeds thereby covering different parts of the compressor map, and with different inlet distortion conditions including clean inlet. These tests were repeated as far as possible several times (within limits arising from ambient conditions varying from day to day) thus demonstrating the consistency of the results obtained

For a restricted number of conditions of blockage and distortion the engine was also put through a series of tests in which the throttle was slammed to maximum from various starting power levels.

After each stall, the bleed valve and EGT overrides were switched out and the throttling device was quickly opened to help the engine recover from stall and to relieve the resulting very high temperature condition.

3. Test Results and Discussion

3.1 Pressure-Time Domain Traces

3.1.1 Actuated core blockage mechanism:

3.1.1.1 Tests with Clean Inlet Flow:

With clean inlet (no distortion screens installed in the intake duct), the stall inception is shown in the time domain for both LPC inlet and exit at fixed HPC speeds of 74%, 82% and 90% respectively in Figures 14-a, 14 -b and 14 -c. These results were acquired with the static and total pressure probes using the Kulite pressure transducers, with output signals low-pass filtered (1200 Hz cut-off).

As an example and to illustrate the effect, details of stall inception corresponding to N_{HPC} = 74% of the stall shown in Figure 14a above, are presented in Figure 15. Stall appeared to have occurred within one of the fan stages, as the stalled condition is indicated in Figure 15 by the blockage or build up of static pressure at the fan inlet (dP_{s-u}), and the drop in static pressure at the fan exit (dP_{s-d}) upstream of the HPC. Each of the pressure-time traces shown in this Figure, as well as those at other speeds in Figure 14 can be subdivided into three regions: a stable region prior to the inception of stall, the stall region, and finally, a region of stable operation of the engine (the third region). The start of stall always appears with a large step jump in pressure. The reduction or tapering in the pressure amplitude in the third region is due to the de-throttling of the core flow by the fast, continuous and complete withdrawal of the bullet or core blockage mechanism out of the engine nozzle, so alleviating stall and returning the engine to stable operation.

In the above raw pressure-time traces, in most of the stable region prior to stall, there is no readily apparent visible indication, sign or warning of the imminent stall that follows. The region of interest would be the one that actually defines the pressure transition step on the border of the stable/stall region. The duration of this step or region has order of magnitude similar to the thickness of the impulsive jump of the pressure trace line at the beginning of the stall region in Figure 15-a. The traces of the inlet static pressures in this region were expanded in the pressure-time domain into a 56 millisecond segment, as is shown in Figure 16.

The simultaneous static pressure traces obtained with the five Kulite static pressure transducers for the short period prior to and into the initiation of the first stall event are

shown in Figure 16. The pressure disturbances in each of these traces appear to exhibit both a temporal growth in time, and a temporal distribution for stall initiation, representing a spatial variation around the duct circumference at the inlet of the first stage of the fan. The spatial variation of the pressure pulses around the circumference appeared to move around the compressor face in the direction of motion of the rotor and grow in an orderly fashion between successive transducers in the same axially located cross-sectional plane, indicating the presence of classical rotating stall.

The presence of pressure disturbances that are visible in this very short-duration view of the steady state region in each of the traces, just prior to stall, are called "stall precursors", and provide an indication or warning of the impeding stall event. It can be seen that the pre-stall disturbances had very small amplitude compared to the disturbances of rotating stall. No remarkable precursors of significant amplitude were detectable in these pressure-time domain traces. However, some, with small amplitude, were detected and identified visually, but whenever this was possible, they were found to be too close to the initiation of stall to be of value for use as a warning for its inception.

Stall precursors have been sought to use as triggers to input to an active control system as warning of an impeding stall before it actually occurs. This warning could have significant practical benefit if the warning were sufficiently in advance of stall to permit adequate time for the control system to respond.

The important issues which therefore need to be resolved are the identification of suitable signals from stall and surge precursors. The earlier the control system is able to detect these precursors prior to the inception of stall the more effective the control system will be in increasing the stability of the machine through the suppression of surge and rotating stall. This increased stability would increase the potential for improved performance, operating range and pressure rise of the compressor.

Stall inception in the time domain, acquired with the conventional low speed pressure probes for the same stall event depicted in Figures 15 and 16, is shown in Figure 17. This shows pressures upstream and downstream of both the fan and the HPC for the same conditions- fixed $N_{HPC} = 74\%$, throttling the HPC with the core blockage mechanism and a clean inlet without distortion. In the total pressure traces downstream of the fan, or at the inlet of the HPC, the stall process is seen to always start with an overpressure spike, apparently caused by surging of the HPC. When this happens the stalled flow downstream of the fan simultaneously acts as a total pressure distortion in the inlet of the HPC leading to its further surging, and as an effective blockage to the fan exit, immediately leading to the commencement of stall in the fan. In this case then the spike in the inlet duct pressure trace would be caused by the subsequent stall of one of the fan stages.

3.1.1.2 Tests with Inlet Distortion Screens:

Similar results were obtained at the same fixed HPC speeds with distortion screens installed in the inlet. These screens were installed at the location shown in Figure 8, in the

duct at one duct diameter upstream of the LPC face, as is shown schematically in Figure 11. Tests were carried out for three different distortion setups, namely 120°, 180° and 240° out of 360° of the inlet duct cross sectional area, as is also shown in Figure 11. Each distortion setup was tested with the three fixed HPC rotational speeds of N_{HPC} = 74%, 82% and 90%. The corresponding results for stall inception in the time domain obtained with the same transducers as for the no distortion case are shown in Figures 18, 19 and 20 for 120°, 180° and 240° distortion screen sectors respectively.

In all of the traces in these Figures, including those in Figure 14, the steady state portion of the pressure time domain prior to stall appear to be the same. For the HPC speeds 74% and 82%, the stall inception during testing with inlet distortion also appeared in these traces to be almost the same as those recorded with clean inlet at the same speeds. For the higher speed of N_{HPC} = 87% and 240° distortion at the inlet however, the compressor was brought to stall, and stall that continued to promptly develop into surge with much less entry of the bullet into the nozzle during the throttling process of the HPC core flow. Tests with distortion screens indicated that the higher the speed and the larger the distortion, the less entry of the bullet into the nozzle needed to trigger stall. Traces for static pressures upstream and downstream of the fan are compared in Figure 21 for the surge condition (from Figure 15) with N_{HPC} = 74% and clean inlet versus the surge condition (Figure 20) for N_{HPC} = 87% with 240° of inlet distortion. Figure 22 shows this latter example of stall/surge inception in the time domain as acquired with conventional low-speed transducers and pressure probes upstream and downstream of the fan and the HPC.

3.1.2   Actuated By-Pass Blockage Mechanism

3.1.2.1   Tests with Clean Inlet Flow:

As was the case with the HPC and the core blockage mechanism, a similar series of tests was carried out on the engine in which compressor stall was initiated by throttling the LPC exit using the by-pass blockage mechanism shown in Figure 9.

Figure 23 shows stall inception in the time domain for several HPC speeds, all obtained with a clean inlet to the fan. The traces represent the low-pass filtered (1200 Hz) signals from the Kulite transducers mounted in the static ports and total pressure probes installed in the inlet and exit of the LPC.

In some of the traces, particularly those from the LPC exit, the pressure can be seen to rise with time, in the steady region prior to stall. This pressure rise was due to the continuous closing of the bypass blockage during the throttling process. In this case the blockage device was acting as does the conventional exhaust poppet damper frequently used in fan and compressor test rigs.

During testing with the by-pass blockage mechanism, the stability of the fan was found to be very sensitive to the movement of the throttling iris at the by-pass duct exit, in contrast to the comparative insensitivity of the engine to insertion of the bullet into the exhaust nozzle. A fan stall could easily be triggered with a small radial movement of the iris inward towards the engine centreline; this sensitivity increased markedly with HPC speed. The higher the HPC speed the more prone the fan to spontaneous inception of stall, and the sharper the transition region or boundary defining the stability limit of the

compressor. This effect was observed to become more pronounced at higher HPC speeds to the extent that ultimately the transition would pass directly to surge without the normally preceding stall being apparent, as is shown at N_{HPC} = 97% in Figure 23.

3.1.2.2   Tests with Inlet Distortion Screens:

The tests described in section 3.1.2.1, with a clean inlet, were repeated but with three different distortion screen setups, namely 120°, 180° and 240° of screen out of the total 360° of the inlet duct cross sectional area at the inlet. Each distortion setup was tested with the same fixed HPC rotational speeds of N_{HPC} = 75%, 85% and 90%. The corresponding results for the stall inception in the time domain obtained with the same transducers as for the no distortion case are shown in Figures 24, 25 and 26 for the 120°, 180° and 240° respectively.

It was observed that the higher the HPC speed and the larger the inlet distortion screen, the less inward travel of the by-pass duct iris needed to trigger an LPC stall. At HPC speeds of 85% or higher, the transition was always found to be directly into surge, as is apparent in successive traces of Figures 24, 25 and 26.

An example of stall precursors are shown in Figure 27, in this series of tests, which were recorded for N_{HPC} = 85%, and 180° distortion screen. The plot shows traces from the five Kulite static pressure transducers at the LPC intake and covers the short period prior to and into the initiation of the first stall event. It is similar to those traces shown in Figure 16, which were for clean inlet flow at N_{HPC} = 74%.

Figure 28 provides another example from this series of tests, and shows the behaviour of the compressor in the time domain during surge inception. These traces were acquired with the conventional pressure probes upstream and downstream of both the fan and the HPC at N_{HPC} = 75%, and with 180° distortion screen in the intake.

3.2 Fourier Transform and Pressure Spectra

3.2.1 Actuated core blockage mechanism:

Fourier spectra are presented in Figures 29a and 29b, for the initial stable steady state and for the stalled condition, for the same filtered static pressure signals presented in Figure 15 (clean inlet). The signals were obtained from the inlet and exit of the fan respectively, with a clean inlet and throttling of the core exit. In the steady state spectra both upstream and downstream of the fan, (apart from 50Hz mains hum), the dominant frequencies having quite large amplitudes were those corresponding to the rotor frequencies of both the Fan and the HPC and their harmonics. For the stalled condition, two new frequencies, f1 = 91.59 Hz and f2 = 137.7 Hz, each with its second harmonic, appeared to have come into play, and dominated the spectra of the traces both upstream and downstream of the fan. Neither of these new frequencies was related to either of the shaft rotational speeds, and must therefore originate with flow unsteadiness associated with the stall and surge phenomena.

Further spectra for the stalled region and derived from the same static pressure sensors used to generate Figures 15, 29a and 29b are displayed for comparison in Figure 30. The signals were captured for stalls at three different HPC speeds, again with clean intake and

core throttling. Spectra from upstream and downstream of the fan are shown in Figures 30a, and 30b respectively. Qualitatively, the spectra for the three HPC speeds (N_{HPC} = 74%, 82% and 92%) appeared to be almost the same. There was no significant difference visible from upstream to downstream of the fan. The spectra show f1 = 91.59 Hz making a constant appearance at all speeds. The only discernable difference was that the dominant frequency, f2 = 137.7 Hz, in the N_{HPC} = 74% spectrum, appeared to slightly drop to f2 = 134.7 Hz for N_{HPC} = 82%, and then to stay almost constant at f2 = 135 Hz at N_{HPC} = 92%. This shows that this dominant frequency arising during stall does not appear to be affected by the compressor rotational speed.

Fourier spectra for the stall and surge region and for the initial steady region prior to stall, obtained at N_{HPC} = 87% and 240° distortion, are compared in Figure 31. The spectra in Figure 31a derive from the static pressures measured at the fan inlet. Correspondingly, the signals providing the spectra of Figure 31b derive from the fan exit. For the initial steady region the dominant frequencies in the spectra (ignoring the 50Hz mains hum) at both upstream and downstream locations were found to be 169.4 Hz and 307.3 Hz and their harmonics. In the inlet signal there are also discernible frequency peaks at 335 Hz and at 670 Hz. Some of these frequencies may well correspond to the LPC and HPC speeds.

In the surge region spectra however, the dominant frequency at both the upstream and downstream locations was found to be 79.5 Hz and its second harmonic of 159 Hz. Another distinctive frequency (but with much less amplitude) was 123 Hz; its second harmonic is barely discernible at both locations. This is different from that was found in the stall spectra for the undistorted inlet flow.

3.2.2 Actuated By-Pass Blockage Mechanism

Fourier spectra for the LPC with clean intake, and stall invoked with the by-pass blockage mechanism are shown in Figure 32. Stall was invoked at three different HPC speeds- N_{HPC} = 75%, 80% and 90%. Figure 32a and Figure 32b present spectra from upstream and downstream of the fan respectively.

The dominant frequency in the N_{HPC} = 75% spectra clearly appears to be f = 87.5 Hz with up to six of its harmonics at the fan inlet and up to only the second harmonic at the fan exit. The other distinct frequency visible at both fan inlet and exit is f = 125.3 Hz.

In the case of N_{HPC} = 80% the dominant frequency appeared to be f = 102.1 Hz with up to five harmonics at the fan inlet, and up to the third harmonic at the exit. Two other frequencies appear in the spectra; f = 130.6 Hz and f = 151.4 Hz, but apparently without their harmonics.

As to the higher speed, N_{HPC} = 90%, six different frequencies appear at f = 16, 112, 139, 163.6, 239.2 and 339.5 Hz. Up to four harmonics of the 239 Hz frequency can be seen, while a second harmonic of 339 Hz is also apparent.

It can be seen from the above that the number and amplitude of significant frequencies increased with HPC rotational speed. In contrast, this outcome differs from the conclusion to be drawn from the spectra of Figure 30, obtained when stall was invoked with the core

blockage mechanism, where apart from a slight reduction in frequency with speed, the dominant frequencies appeared not to be affected by increasing N_{HPC}.

The effect of inlet flow distortion on the dominant frequencies in the Fourier spectra for fixed N_{HPC} = 90%, recorded by the same transducers upstream and downstream of the fan, is presented in Figures 33a, 33b, 33c and 33d for inlet flow distortion of 0º, 120º, 180º, and 240º respectively. The recorded frequencies for the various inlet distortions are presented and compared in the following table. The table shows the dominant frequencies for each inlet flow distortion, but displays no apparent trends from which can be drawn or correlated as to the effect of distortion on the dominant frequencies.

Distortion extent	LPC	f1	f2	f3	f4	f5	f6	F7	f8	f9
0º	inlet	**16**	**40**	**112**	**139**	**163.6**	**239.2**	**339.5**		
	Exit	"		"	"	"	"	"		
120º	inlet	**25**	**39.7**	**74.45**	**114.4**	**160.8**	**219.1**	**274.6**	**391.3**	**506.2**
	Exit	"	**40.6**	**74.45**	"	"	**367.7**	**675.7**		
180º	inlet	**43.89**	**76.48**	**107.1**	**134.5**	**149.2**	**164.8**	**513.9**	**526.4**	**676.2**
	Exit	**42.36**	**75.61**	**106.7**	"	"	"			
240º	inlet		**78.51**	**134.2**	**161.6**	**319.9**	**436.3**	**587.5**	**655**	**677.1**
	Exit		**78.48**	"	"	"	"			"

4. Concluding Remarks

This report describes how the Larzac engine was fully instrumented in those locations that could be accessed without special tooling, with both conventional low and very fast response transducers installed, and a data acquisition system providing a wide selection of sampling speeds.

The engine instrumentation demonstrated the capability to detect flow instabilities which are considered as precursors for stall and surge in the engine.

The engine operation was extended to the region between the operating and surge lines of engine compressor operation through the use of the designed and manufactured core and by-pass blockage mechanisms installed on the engine exhaust nozzles and operating either separately or together.

Compressor stall was initiated through the use of either of the throttling devices, both with and without distortion screens installed in the inlet. It was found that to initiate a stall using any of these means, it was necessary to override some of the engine controller functions, such as compressor bleed actuation, and rotational speed and turbine exit gas temperature limiters.

Transient data showing the transition to stall were examined and analysed. Preliminary analyses indicate that stall precursor pressure pulses exist in the compressor inlet region at the compressor face. These pressure pulses move around the compressor face and in time, grow into rotating stall. The pressure pulses almost always develop into surge at the higher range of compressor rotational speeds.

In the steady state range of the recorded pressure trace prior to stall, the dominant frequencies found in the Fourier spectra were those corresponding to the LPC and HPC rotational speeds and their harmonics.

However, in the stall region, the dominant frequencies could not be correlated to either of the shaft speeds. The dominant frequencies were found to be different for different shaft rotational speeds, and for different combinations of throttling mechanism and inlet flow distortion.

Stall precursors were observed and can be detected visually from the pressure traces. However, the precursor pulses were of small amplitude and occur only milliseconds prior to the point of stall initiation, too close to be of value for use in stall warning and control. Additional analysis will be required to decide if it is possible to identify stall precursors which would provide more warning time. Further work is needed to completely describe a stall and surge event. This further analysis will probably require the use of advanced signal processing and analysis.

Future work would include non-contacting blade deflection and tip clearance sensors to detect compressor stall precursors, and to compare results from these with measurements obtained with the Kulite pressure transducers. It would be particularly useful if through-the-case sensors were to prove to be applicable.

One further observation is of interest. In almost every case, as the engine was coaxed toward the surge line, a very loud, almost musical, sound was emitted from the engine intake. This sound was so intense that it was objectionable in the sound proofed control room and was in the range 10 to 140 Hz and apparently comprised only one or two very dominant frequencies. Very quickly the test personnel came to recognize this sound as a warning that the compressor was close to stalling. On several occasions whilst taking a data recording when this sound was readily apparent, with the blockage mechanism stationary and with some distance to travel before stall was expected to occur, the engine suddenly and quite spontaneously stalled and even went into surge without any apparent external trigger. Thus, in some way the sound itself appeared to provide a warning that the compressor was operating in a flow region where stall should be anticipated. Since the experimental program was focussed on the detection and identification of stall precursor pulsations this observed phenomena was not pursued. However, it is possible that detection of such acoustic tones may provide the sought after warning and trigger for an active stall prevention system. Therefore it is recommended that this observed phenomena be further investigated.

5. Acknowledgements

6. References

1. Cumpsty, N.A., 1994, 2004, "Compressor Aerodynamics", Longmans.

2. Emmons,H.W., Pearson, C.F., Grant, H.P., 1955, "Compressor Surge and Stall Propagation", Transactions of the ASME, vol. 79.

3. McDougall, N.M., Cumpsty, N.A., Hynes, T.P., 1990, "Stall Inception in Axial Compressors", ASME Journal of Turbomachinery, vol.112, pp 116-125.

4. Day, I.J., 1993, "Stall Inception in Axial Flow Compressors", ASME Journal of Turbomachinery, vol. 115, pp 1-9.

5. Herpel, T., Fottner, L., 1993, "A System for Monitoring, Measurement and Analysis of Transient Performance and Stall Phenomena of Gas Turbine Engines", ICIASF '93 Record, IEEE Publications 93CH3199-7.

6. Hoess, B., Fottner, L., 1997, "Experimental Setup, Measurement and Analysis of the Onset of Compressor Flow Instabilities in an Aeroengine", ICIASF '97 Record, IEEE Publications 1997.

7. Hoess, B., Leinhos, D., Fottner, L., 2000, "Stall Inception in the Compressor System of a Turbofan Engine", ASME Journal of Turbomachinery, vol. 122, pp 32-44.

8. Leinhos, D.C., Schmid, N.R., Fottner, L., 2001, "The Influence of Transient Inlet Distortions on the Instability Inception of a Low-Pressure Compressor in a Turbofan Engine", ASME Journal of Turbomachinery, vol. 123, pp 1-8.

7. Figures
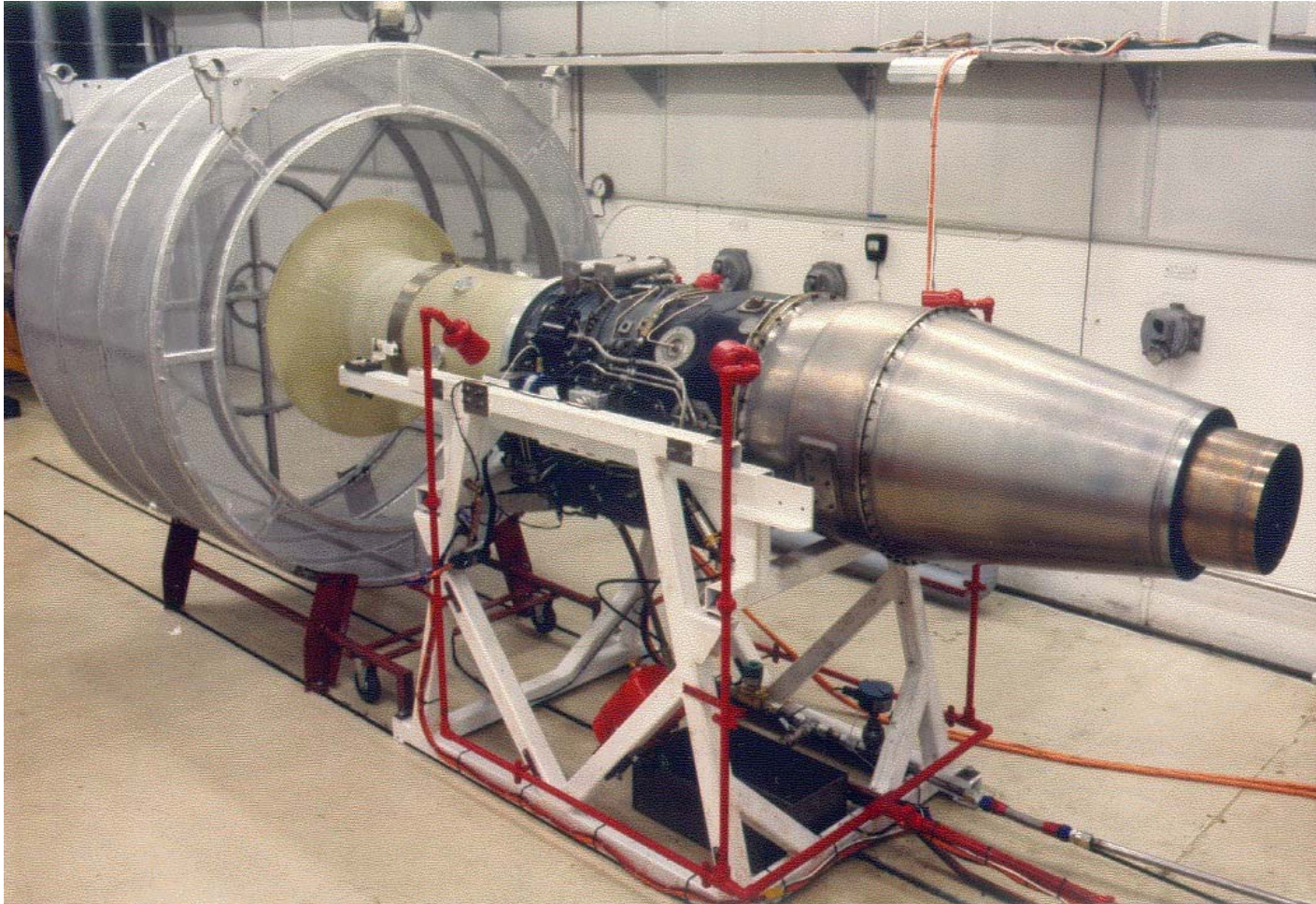
Figure 1: The original Larzac test rig in Small Engine Test House at DSTO Melbourne prior to modification

Figure 2: Schematic of the Larzac test rig with location of initial conventional low speed instrumentation
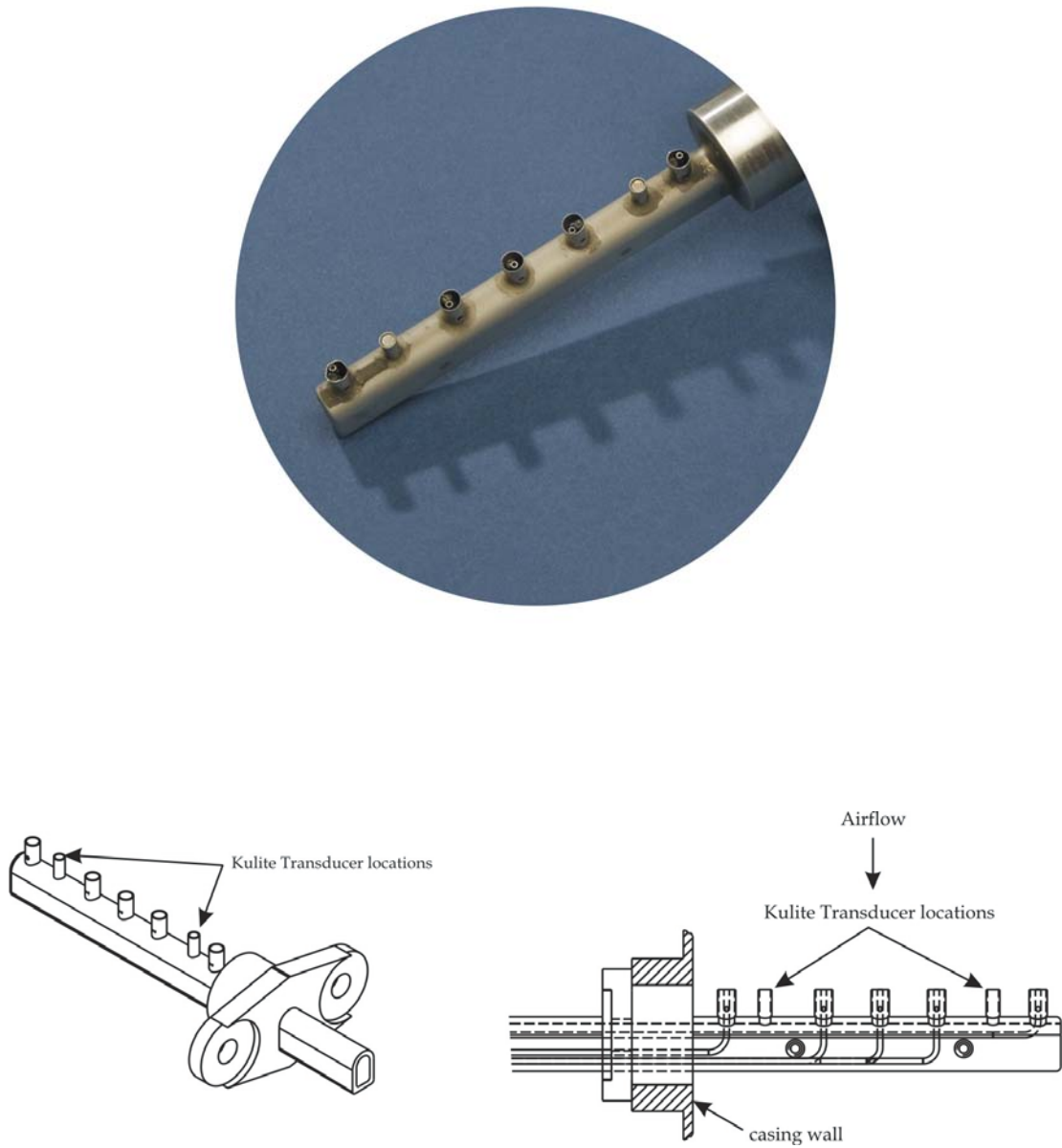
Figure 3: Total pressure and temperature rake at the fan exit
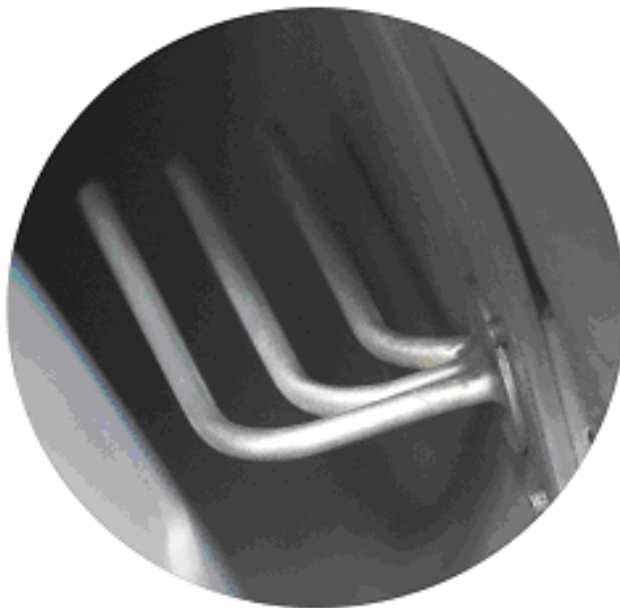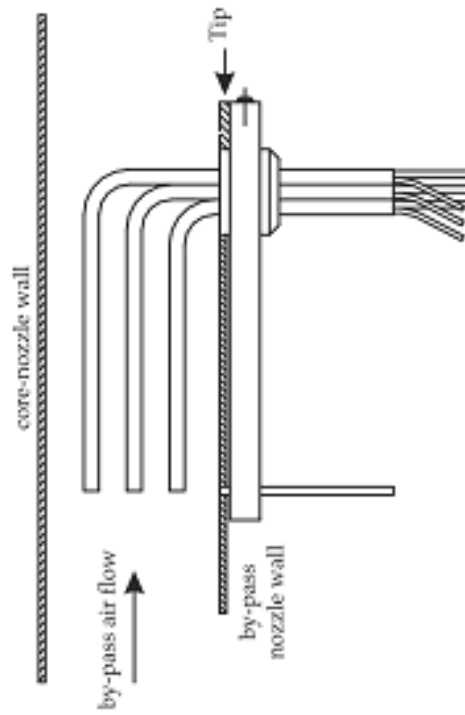
Figure 4: Measurement of total pressure, temperature and static pressure at the exit of the by-pass duct
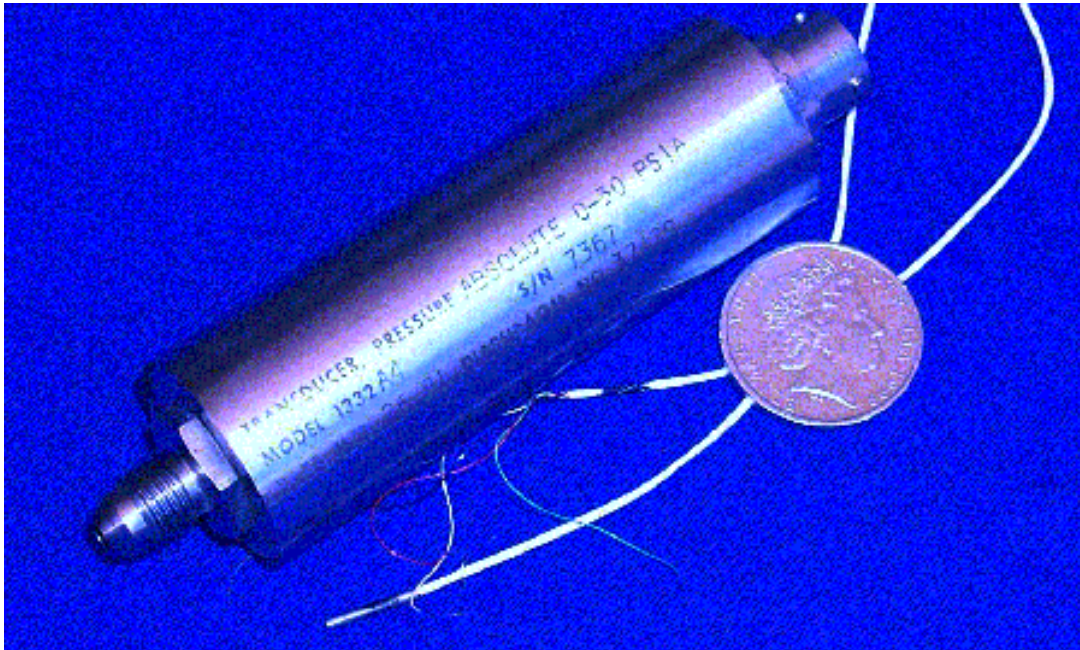
Figure 5: The miniature Kulite transducer compared in terms of size with the conventional low speed transducer

Figure 6: Miniature Kulite transducer static pressure probe at the exit of the fan upstream of the HPC inlet

Station number	Type	Angle	Serial #
1.	Static	1.5 °	40
2.	Total	11.5 °	none fitted
3.	Total	52.5 °	none fitted
4.	Static	73.5 °	39
5.	Total	116.5 °	406
6.	Static	145.5 °	42
7.	Total	191.5 °	none fitted
8.	Static	217.5 °	43
9.	Total	232.5 °	none fitted
10.	Static	289.5 °	407
11.	Total	296.5 °	405

Figure 7: The Larzac fan ring probe holder for the miniature Kulite transducers at the fan inlet, and angular probe location as viewed from the front and numbering starts at TDC and runs clockwise
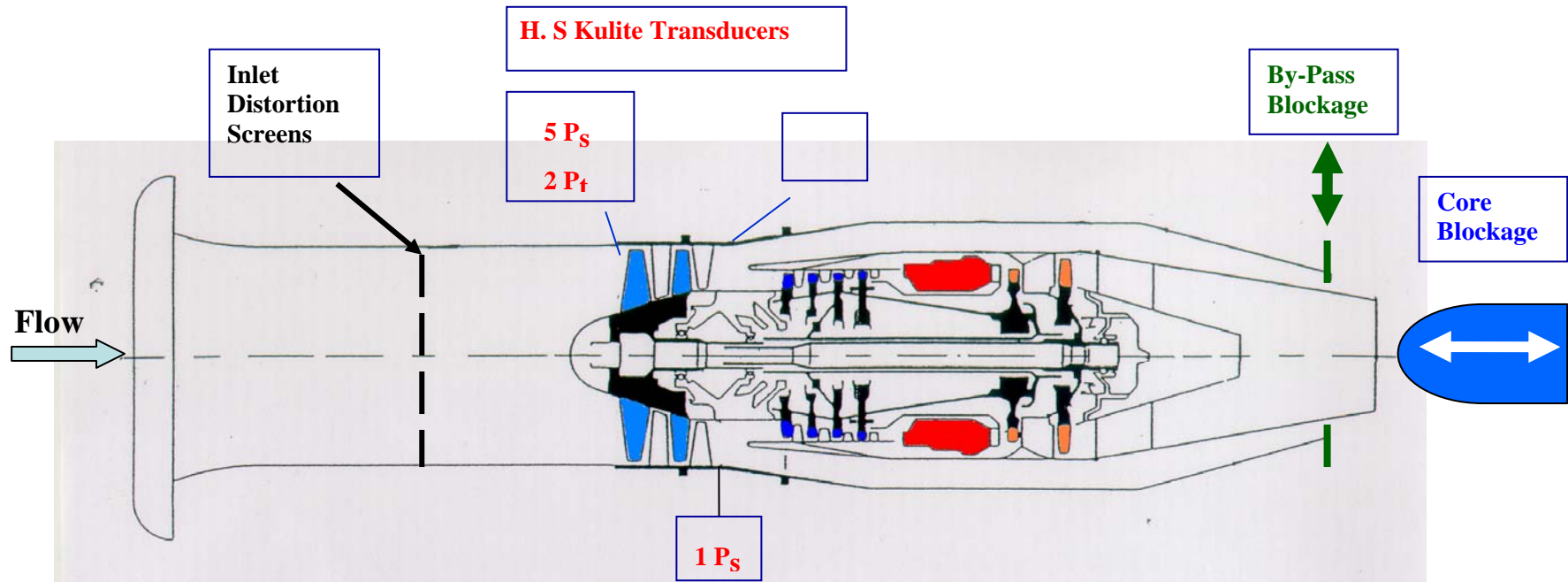
Figure 8: Schematic of the Larzac test rig illustrating the location of stall initiating mechanisms, with the new dynamic high speed instrumentation
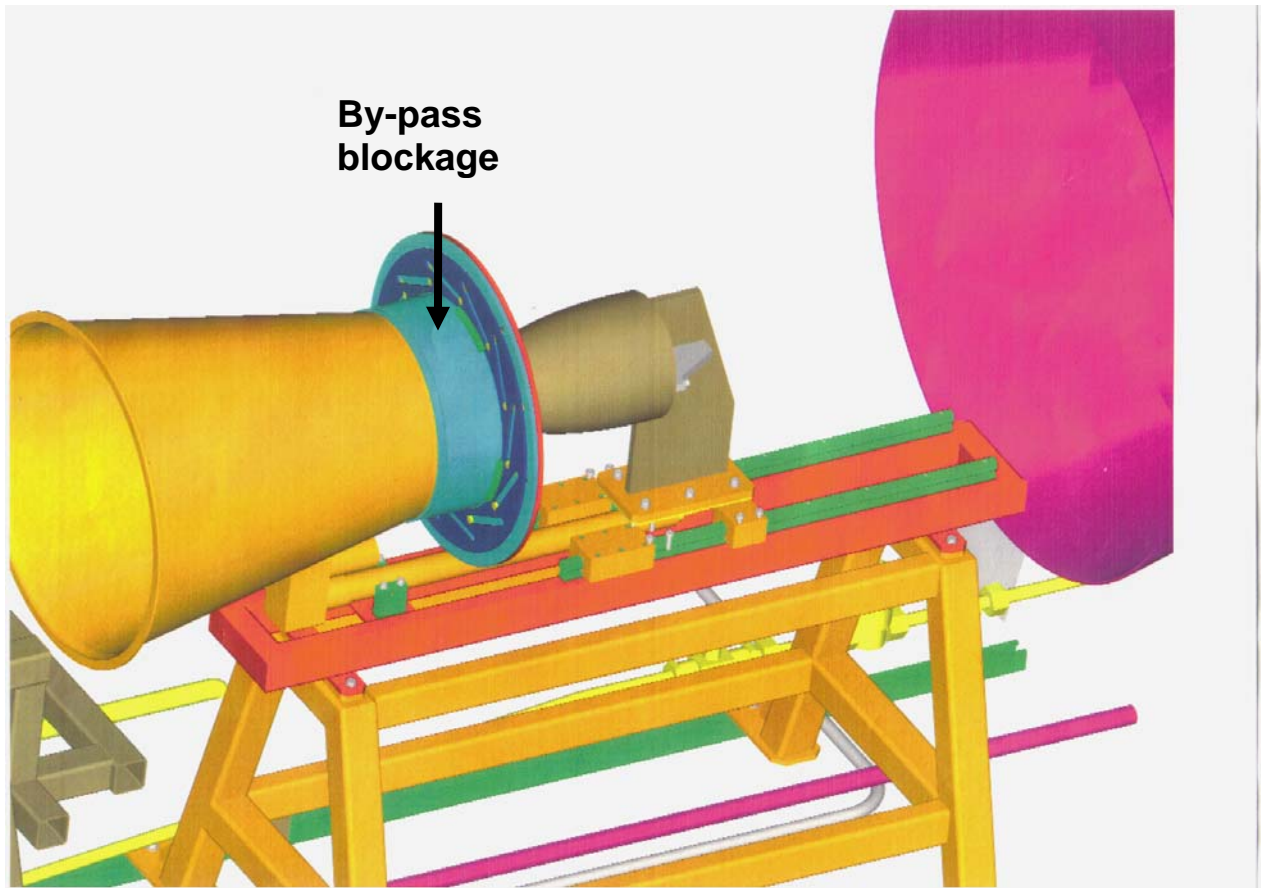
Figure 9: Schematic of the by-pass throttling mechanism
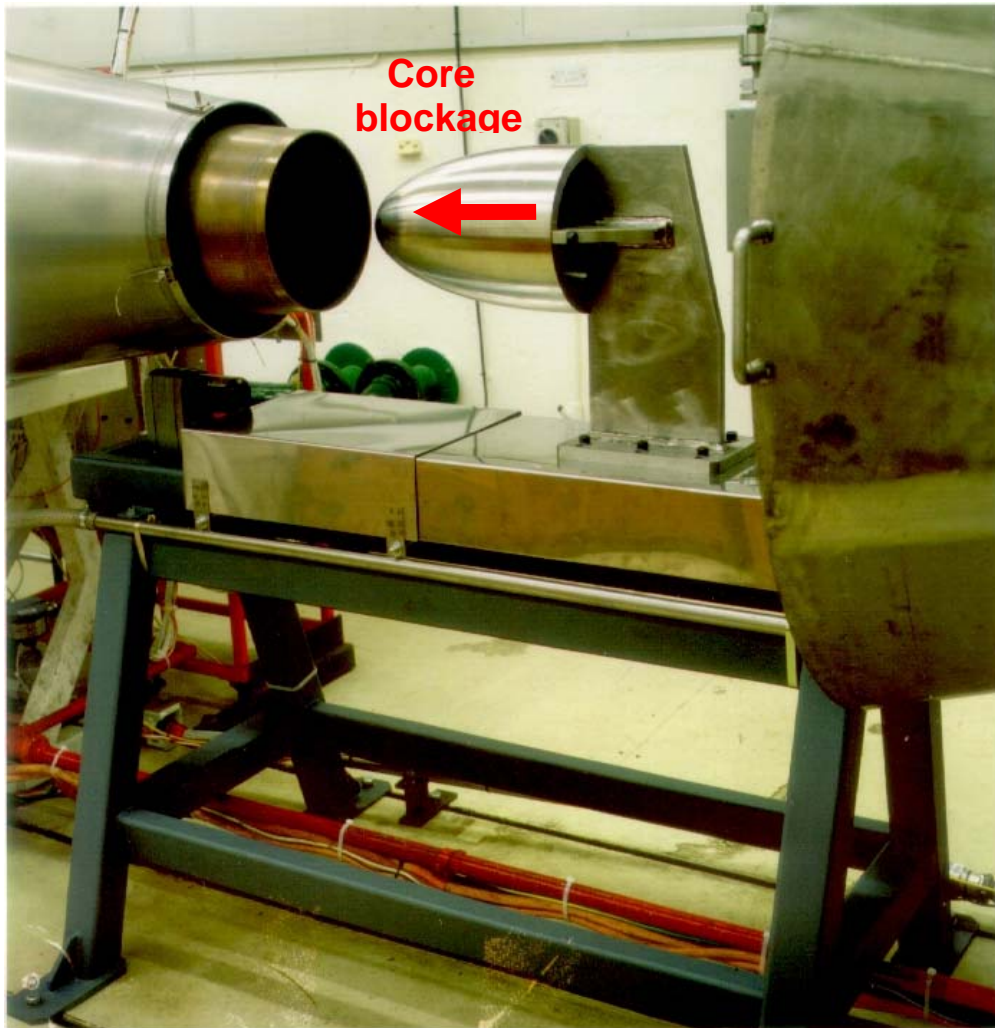
Figure 10: The core or HPC throttling mechanism
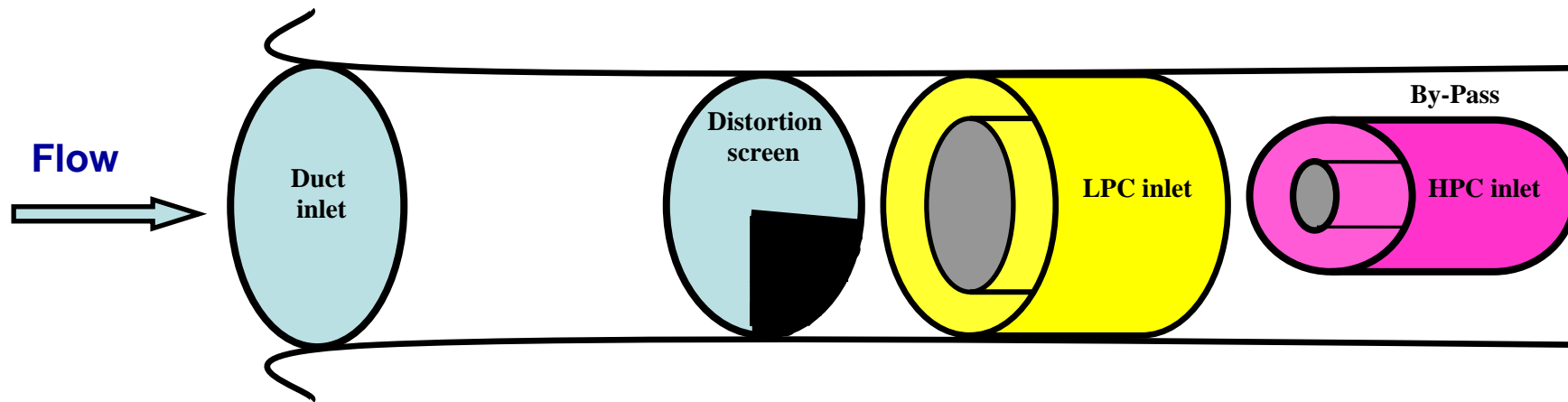
Figure 11: Inlet flow distortion with combination of 60^0 distortion screen sectors

Engine

High Speed Signal (16 CHS)

Low Speed Signal (35 CHS)

First 16 Low speed Channels

Amplifiers

Low - Speed Signal Distribution- Collection Interface Box

Display

Operators Computer

High - Speed Signal Distribution- Collection Interface Box

Cu-toff Freq 1250 Hz

All 35 Low speed Signals

Individual Channel Filters Chs 0 - 7

Individual Channel Filters Chs 8 - 15

Sampling Synchronisation Signal

High Speed Card 1 12500 Samples/s/Ch

High Speed Card 2 12500 Samples/s/Ch

Low -Speed Card 32 Samples/s/Ch

DMA

DMA

DMA

File HI-SPD 1

File HI-SPD 2

File Low-SPD

Display

DAQ Computer

Figure 12: Schematic of signal distribution, collection and data acquisition

```
┌──────────────┐          ┌──────────────┐                    ┌────────────────────────┐
│ DT3003       │          │ DT2839       │      Ext Clk       │ DT3003 x 2 (Both Cards) │
│ C/T 1        │   Clk    │ C/T 1        │ ─────────────────▶ │ Sampling 8 channels @ 12.5Khz │
│ Generate Rate│ ───────▶ │ Divide By 3200│                   │ Each                    │
│ 100Khz       │          │ Ie Generate  │                    │ Base Clock is 100Khz    │
└──────────────┘          │ 31.25Hz Rate │                    │ Ext Clock Used          │
                          │ Using Ext    │                    └────────────────────────┘
                          │ Clock 4% Duty│
                          │ Cycle        │
                          └──────────────┘
                                 │ Gate
                                 ▼
                          ┌──────────────┐                    ┌────────────────────────┐
                 Clk      │ DT2839       │                    │ DT2839                  │
         ───────────────▶ │ C/T 2        │     Ext Clk        │ Sampling 128 Channels   │
                          │ Generate 100Khz│ ───────────────▶ │ At 100Khz Channel Skew  │
                          │ Rate         │                    │ Ext Clock               │
                          │ Using Ext Gate│                   │ Repetition Rate is 31.25 Hz │
                          └──────────────┘                    └────────────────────────┘
```

```
┌──────────────┐          ┌──────────────┐                    ┌────────────────────────┐
│ DT3003       │          │ DT2839       │     Ext Trigger    │ DT3003 x 2 (Both Cards) │
│ C/T 1        │   Clk    │ C/T 1        │ ─────────────────▶ │ Sampling 8 channels @ 12.5Khz │
│ Generate Rate│ ───────▶ │ Divide By 800│                    │ Each                    │
│ 12.5Khz      │          │ To Create 32 Hz│                  │ Internal Base Clock is 100Khz │
└──────────────┘          │ from 12.5Khz │                    │ External Trigger        │
                          │ Input        │                    └────────────────────────┘
                          └──────────────┘
                                 │
                                 │         Ext Trigger        ┌────────────────────────┐
                                 │ ─────────────────────────▶ │ DT2839                  │
                                 │                            │ Sampling 1-128 Channels │
                                 │                            │ At 224Khz               │
                                 │                            │ Ext Trigger (Trig Scan Mode) │
                                 │                            │ Repetition Rate is 32 Hz │
                                 │                            └────────────────────────┘
```

*Figure 13: The Data Acquisition Software synchronisation problem*
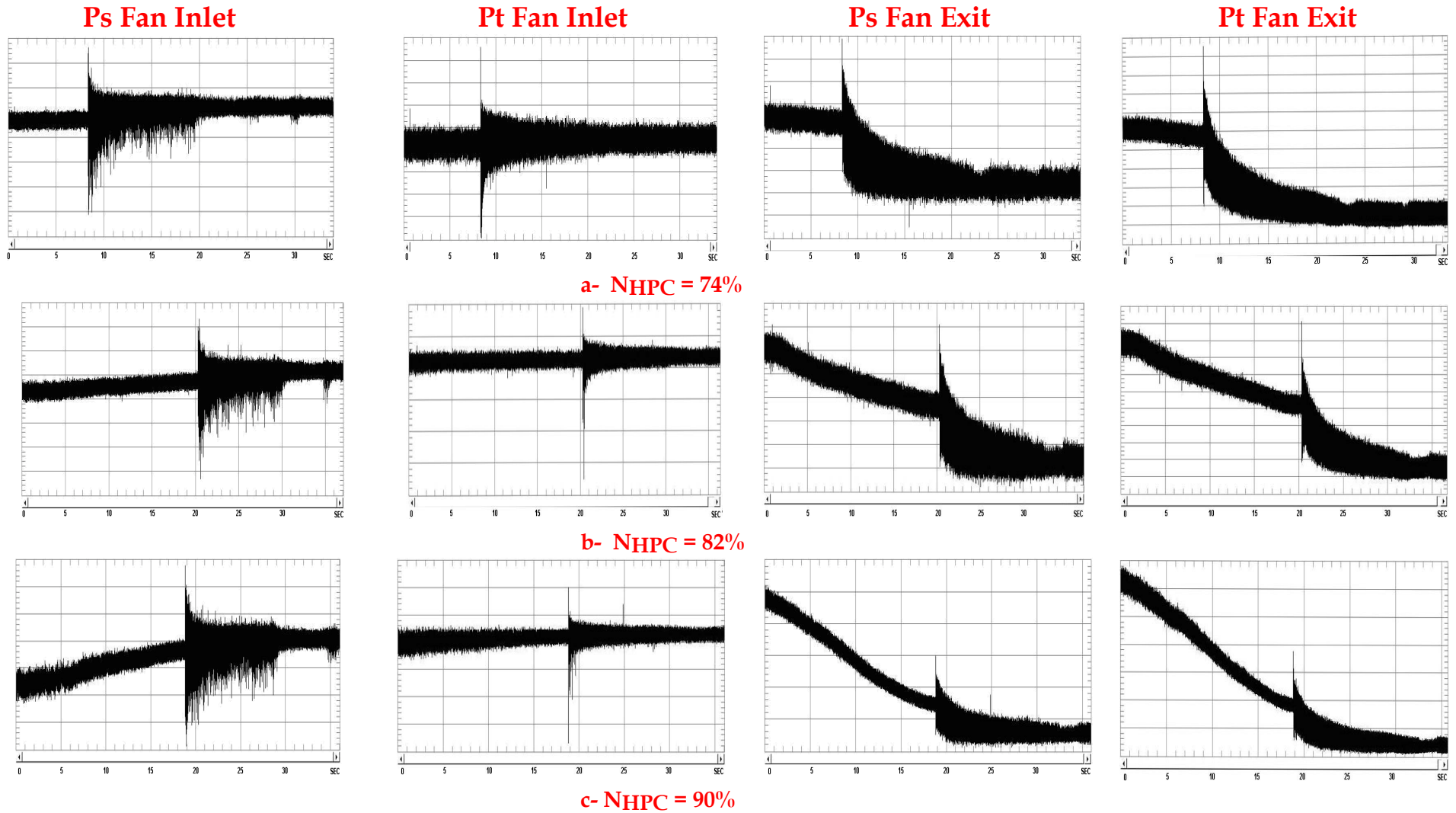
Figure 14: Stall inception in the time domain as acquired with the Kulite, for different rotational speeds of the HPC, obtained by throttling the HPC with the Core blockage mechanism, and with no inlet flow distortion.

(a): Upstream of the fan

(b): Downstream of the fan
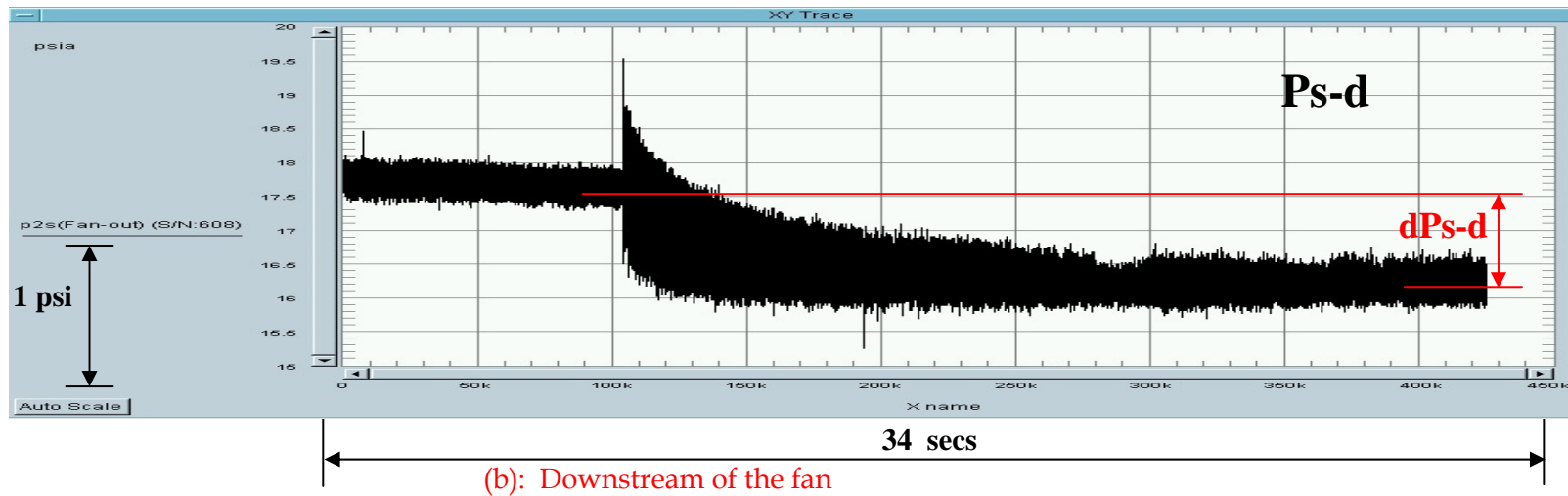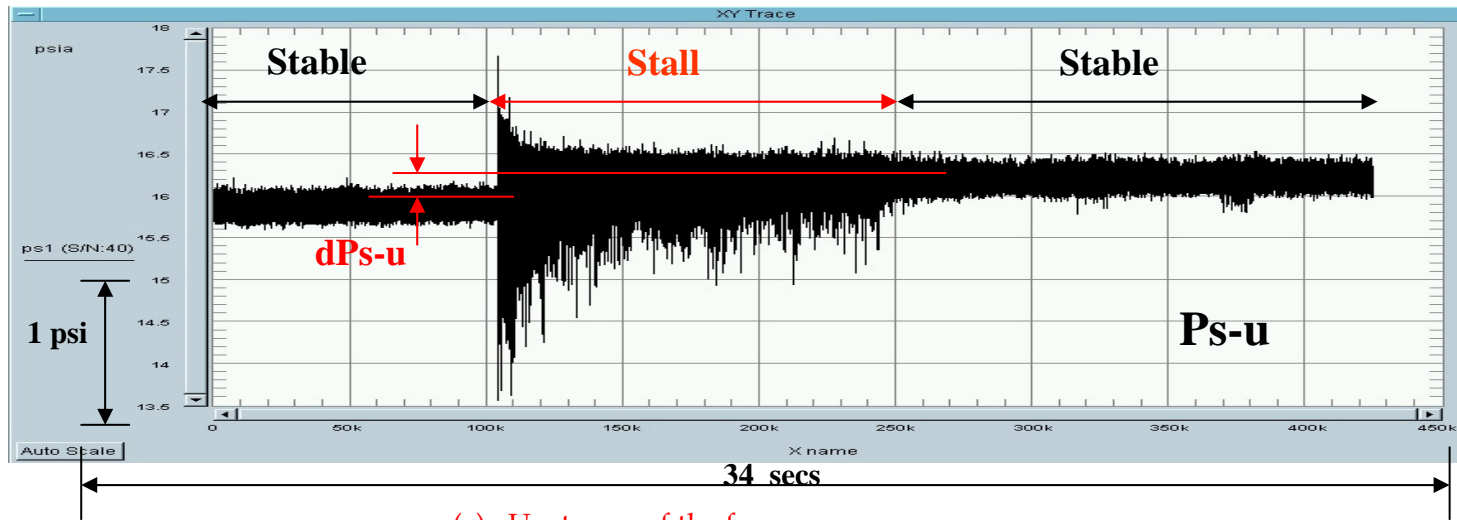
Figure 15: Stall inception in the time domain as acquired with the Kulite, and N_{HPC} = 74% throttling of the HPC with the Core blockage mechanism
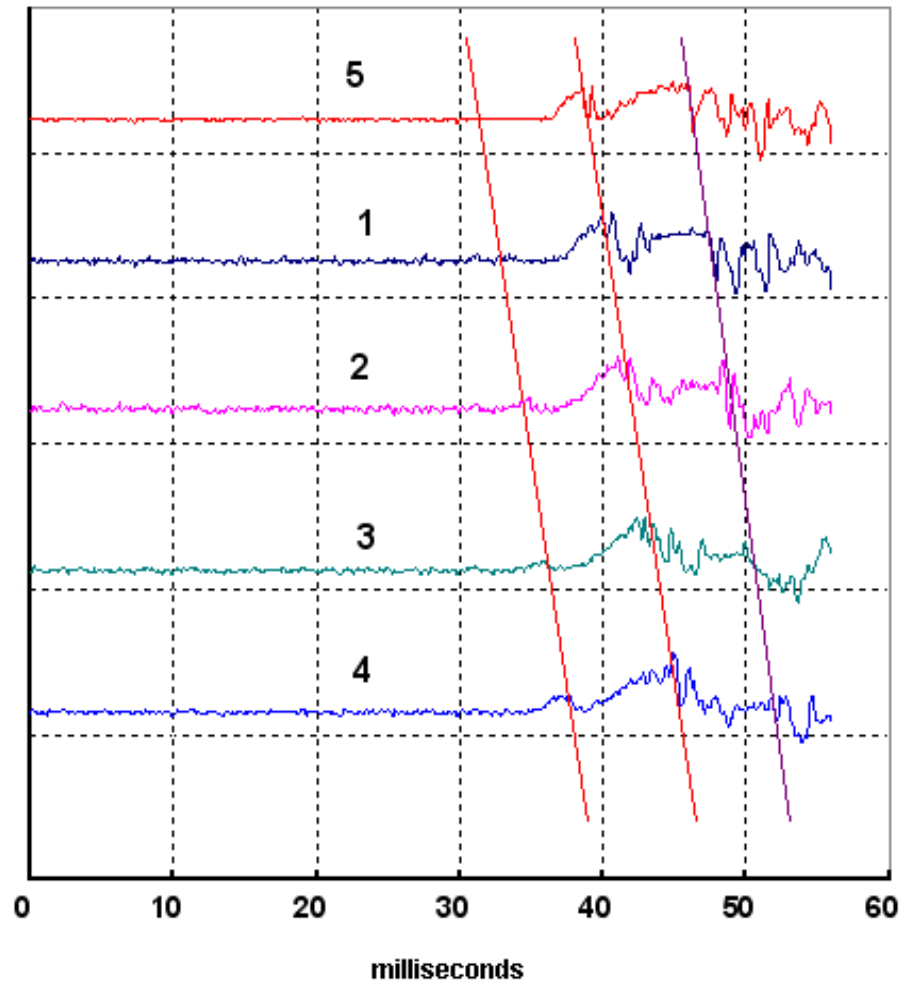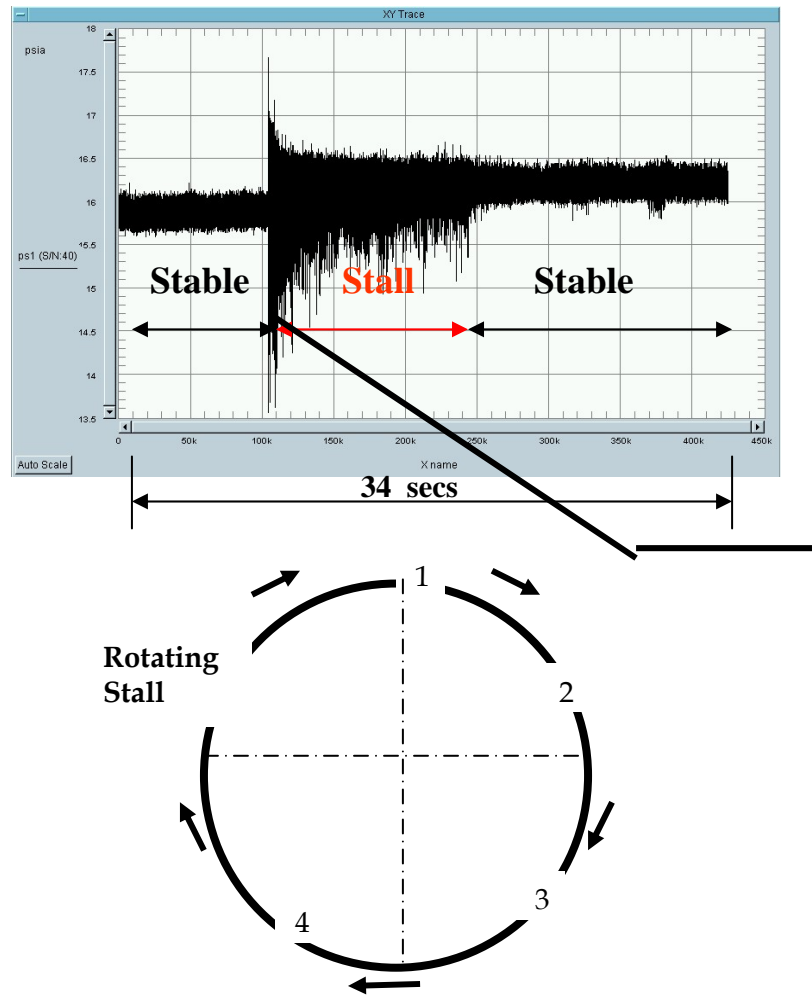
Figure 16: The simultaneous static pressure traces obtained with the five Kulite static pressure transducers of the short period prior and into the initiation of the first stall event, at the fan inlet for N_{HPC} = 74%, with no inlet flow distortion and throttling of the HPC with Core blockage mechanism.
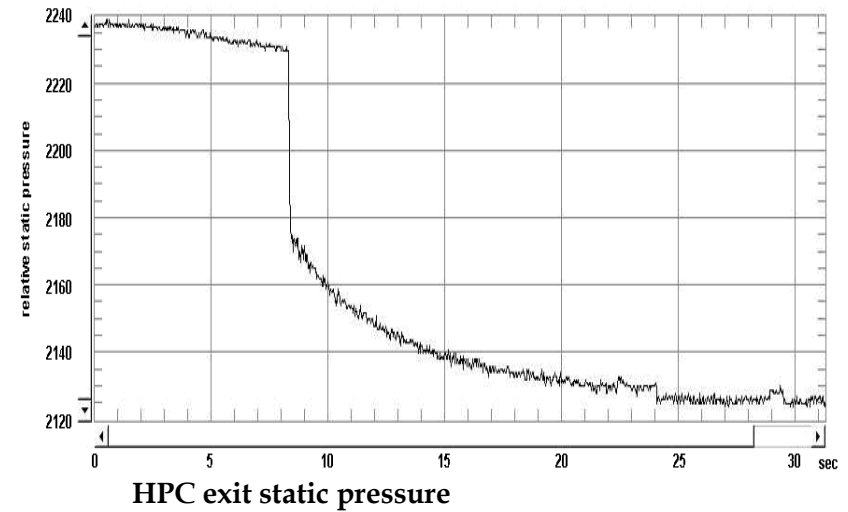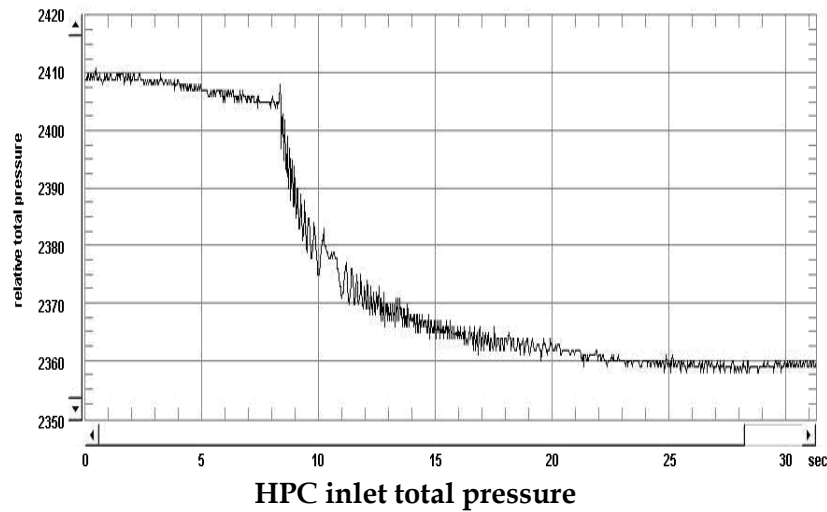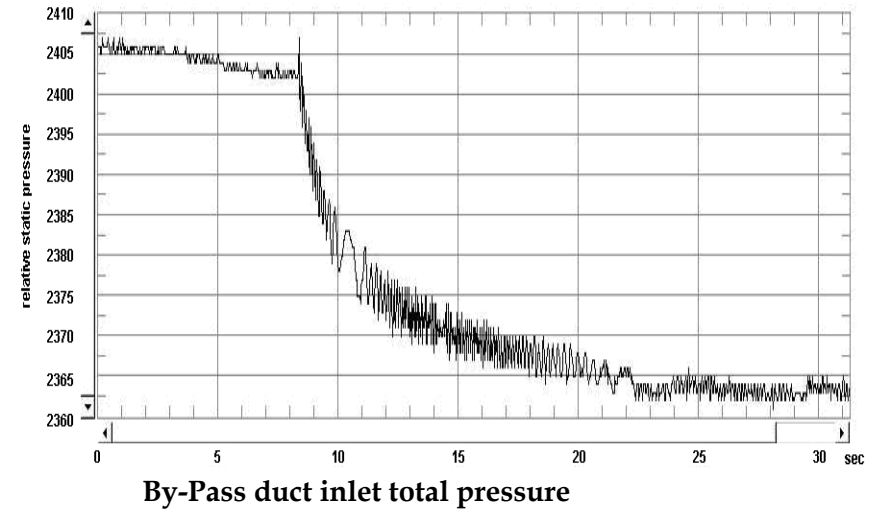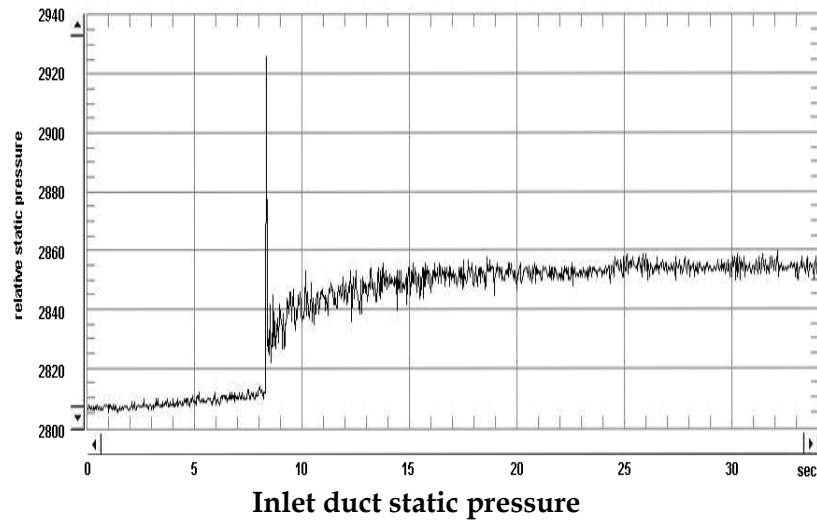
Figure 17: Stall inception in the time domain acquired with the with the conventional pressure probes. For N_{HPC} = 74%, with no inlet flow distortion and throttling of the HPC with Core blockage mechanism.

DSTO-RR-0377

Vertical axis - relative pressure
Horizontal axis - time
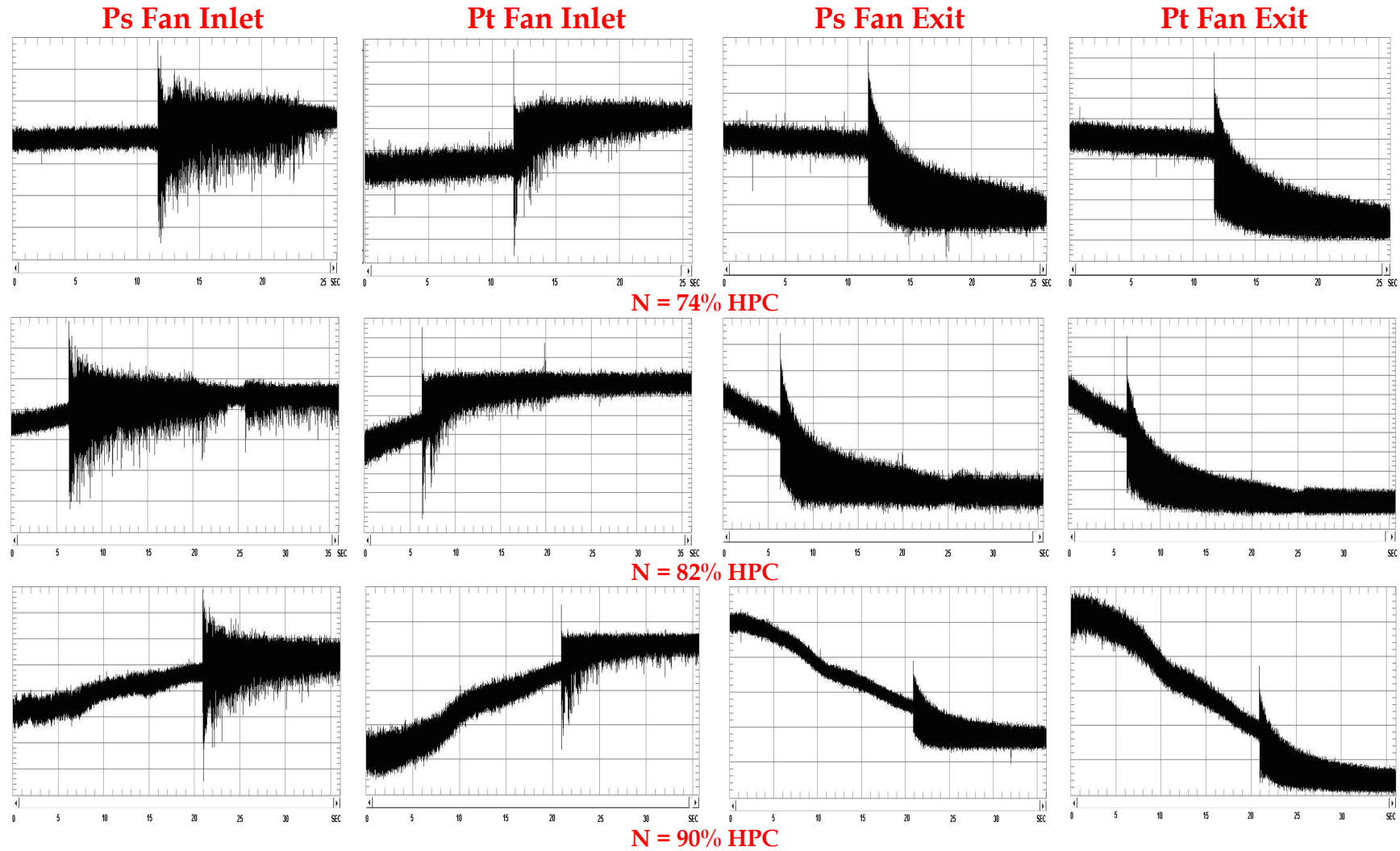
Figure 18: Stall inception in the time domain as acquired with the Kulite, for different rotational speeds of the HPC, obtained by throttling the HPC with the Core blockage mechanism, and with 120º inlet flow distortion.
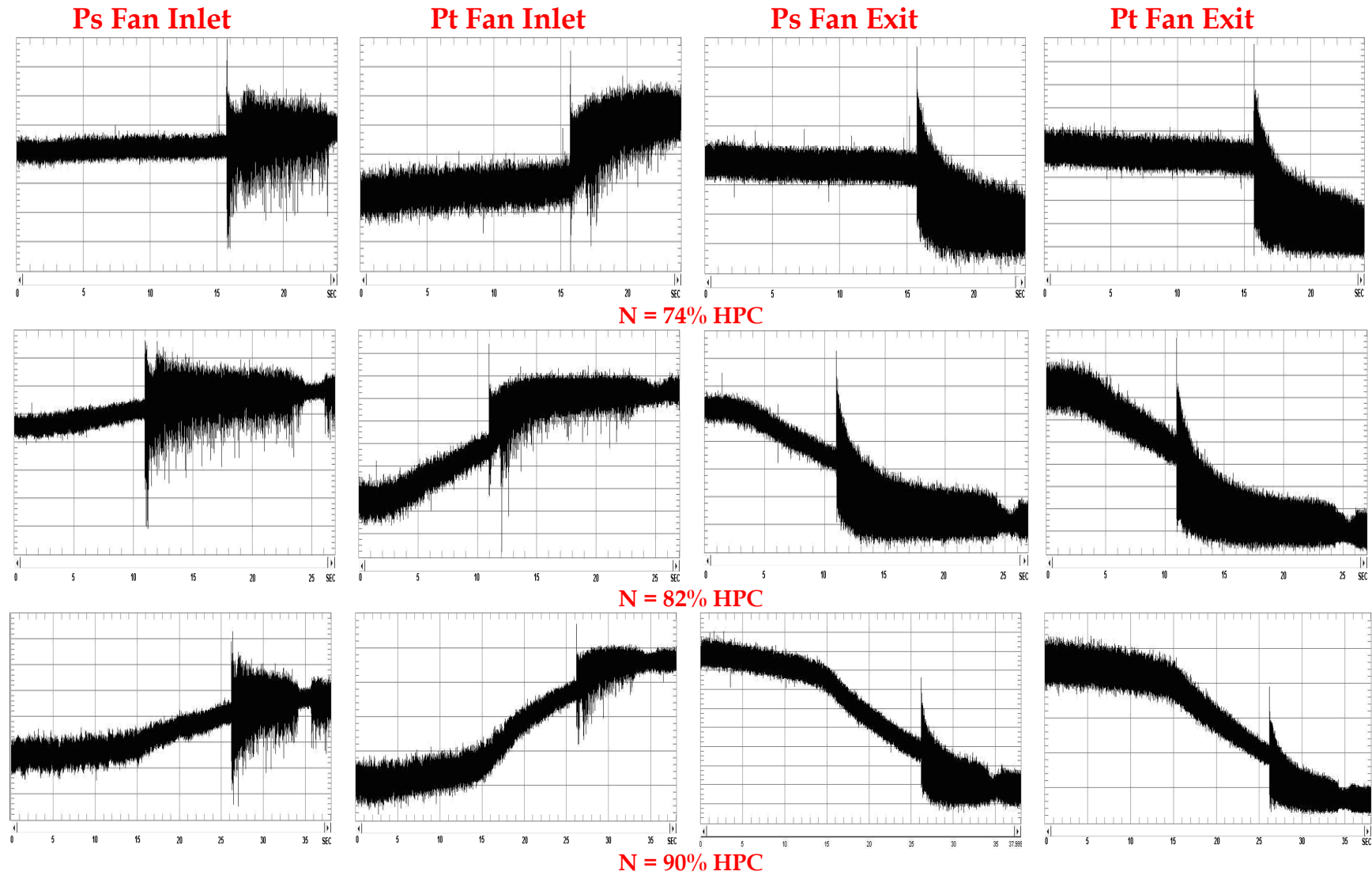
Figure 19: *Stall inception in the time domain as acquired with the Kulite, for different rotational speeds of the HPC, obtained by throttling the HPC with the Core blockage mechanism, and with 180º inlet flow distortion*

Vertical axis - relative pressure
Horizontal axis - time

Ps Fan Inlet   **Pt Fan Inlet**   **Ps Fan Exit**   **Pt Fan Exit**

N = 74% HPC

N = 82% HPC

N = 87% HPC
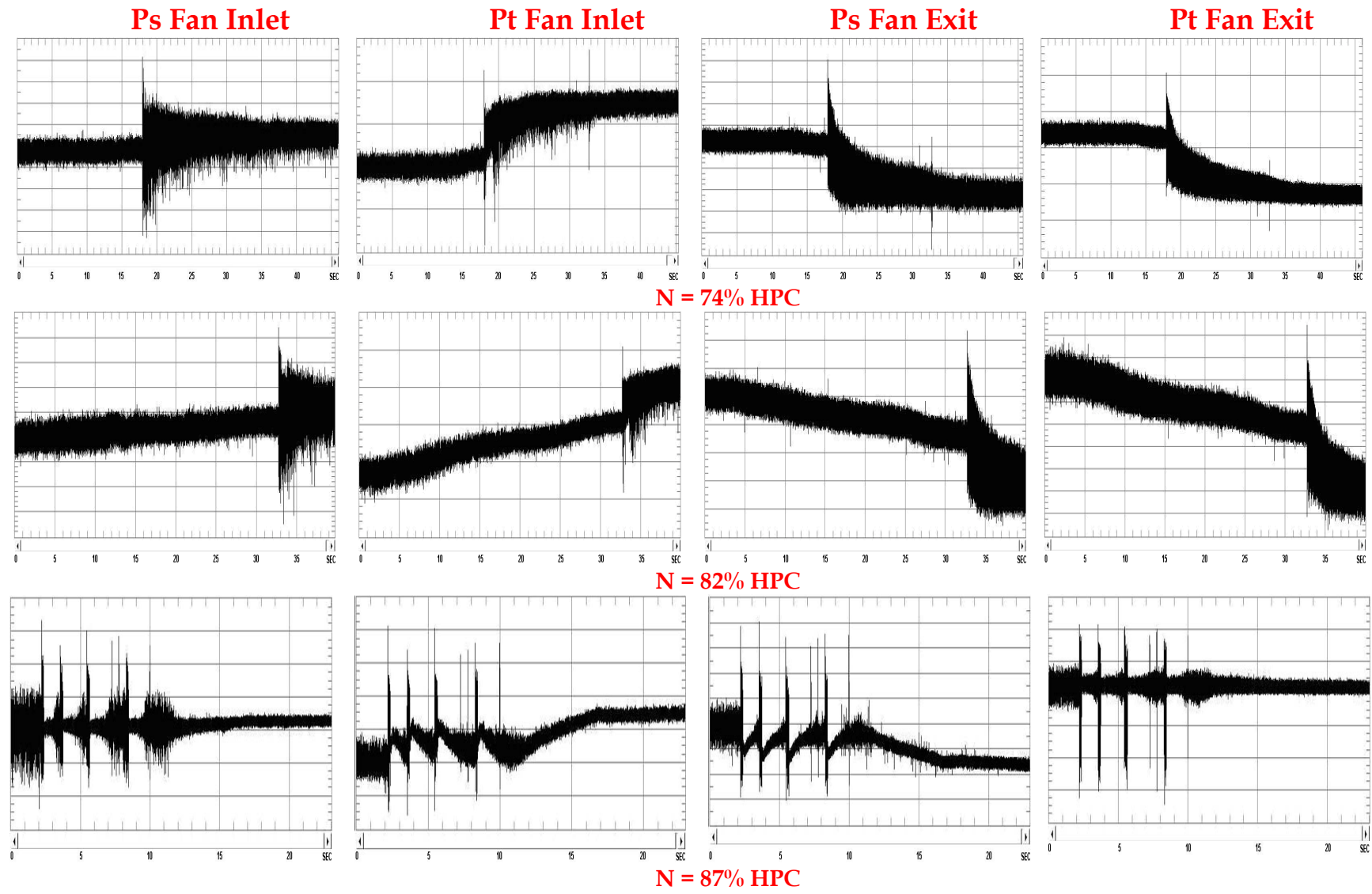
Figure 20: Stall inception in the time domain as acquired with the Kulite, for different rotational speeds of the HPC, obtained by throttling the HPC with the Core blockage mechanism, and with 240° inlet flow distortion
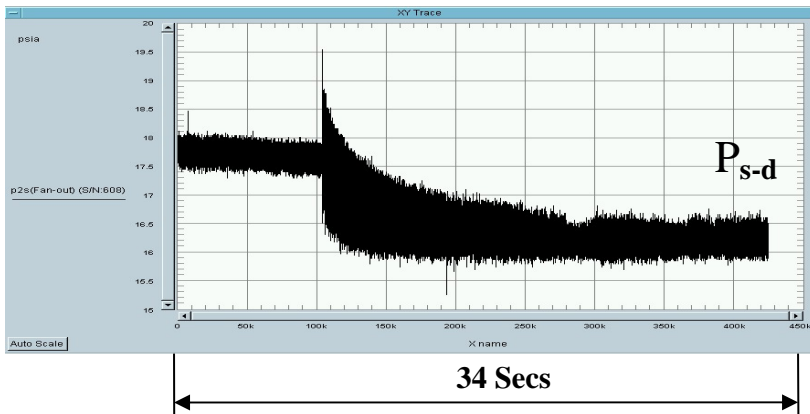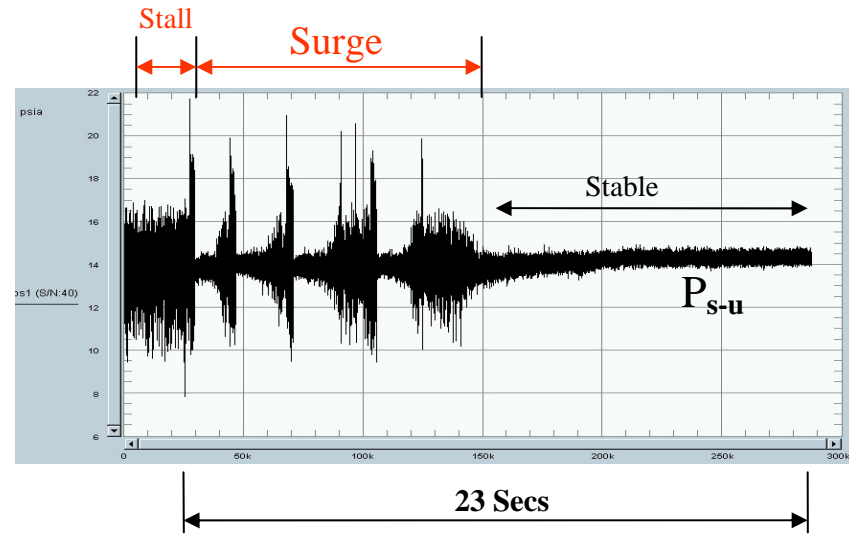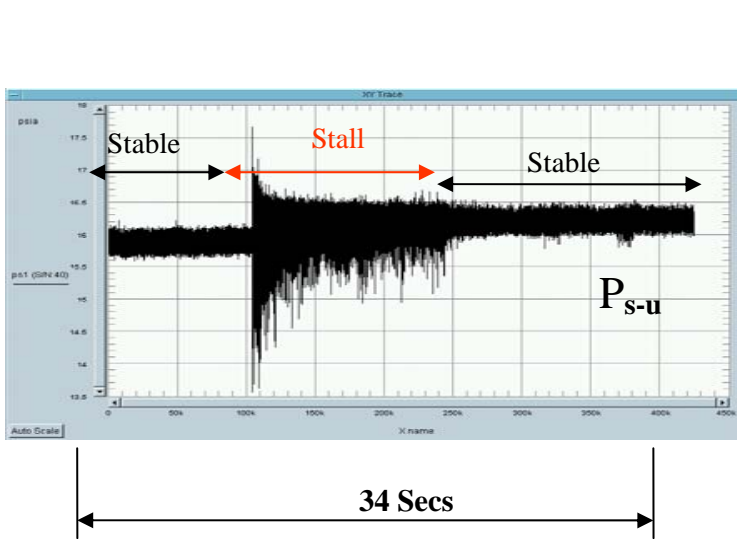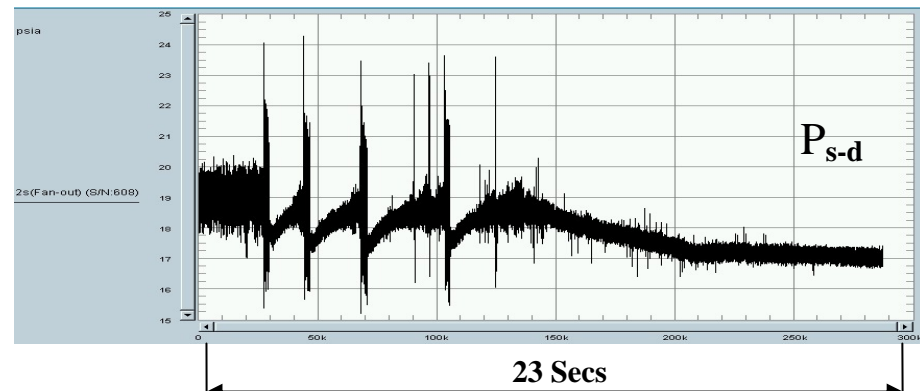
Figure 21: Stall inception in the time domain compared with that of surge as acquired with the Kulite transducer at the fan face. Throttling of the HPC with Core blockage mechanism
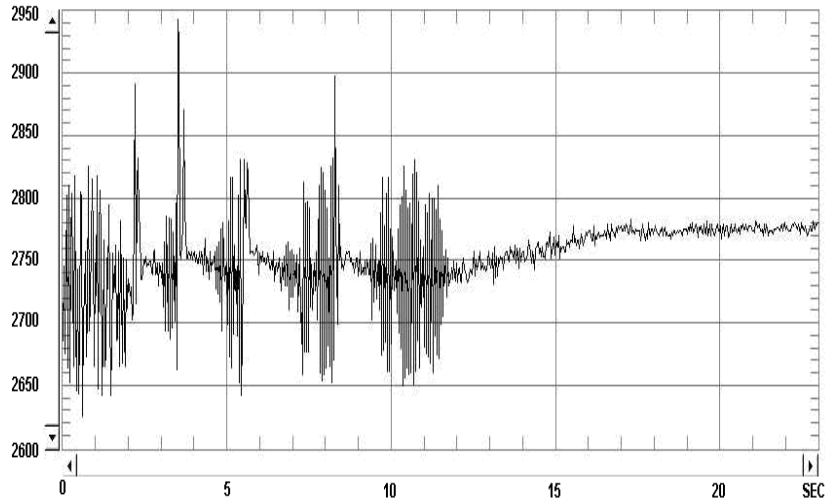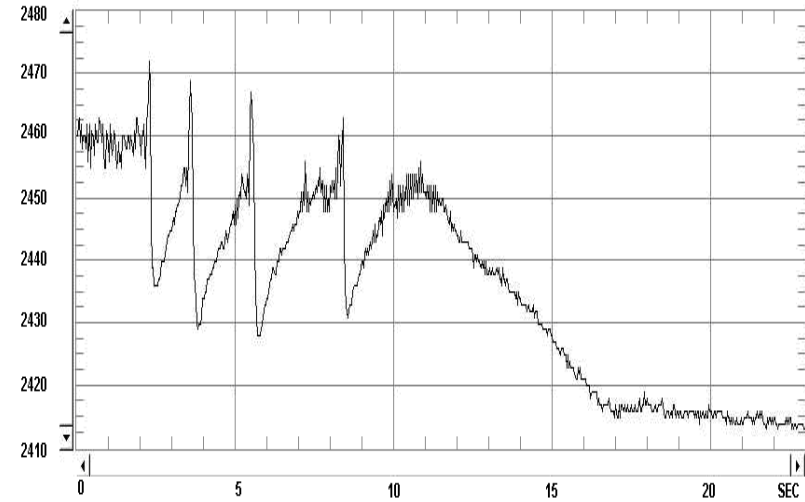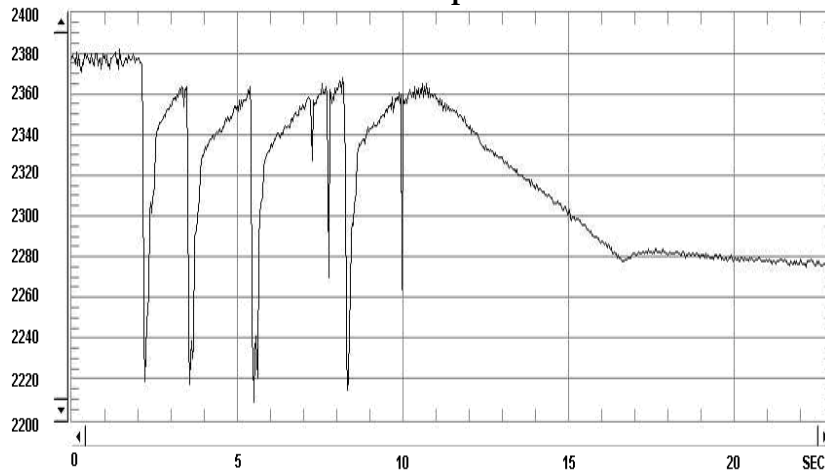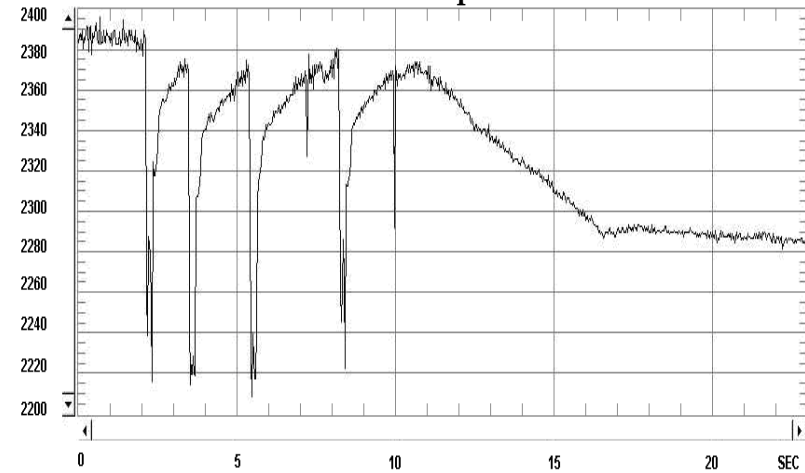
Figure 22: Surge inception in the time domain acquired with the conventional pressure probes, obtained by throttling of the HPC with Core blockage mechanism, for NHPC = 87% and 240° inlet flow distortion.

Vertical axis - relative pressure
Horizontal axis - time
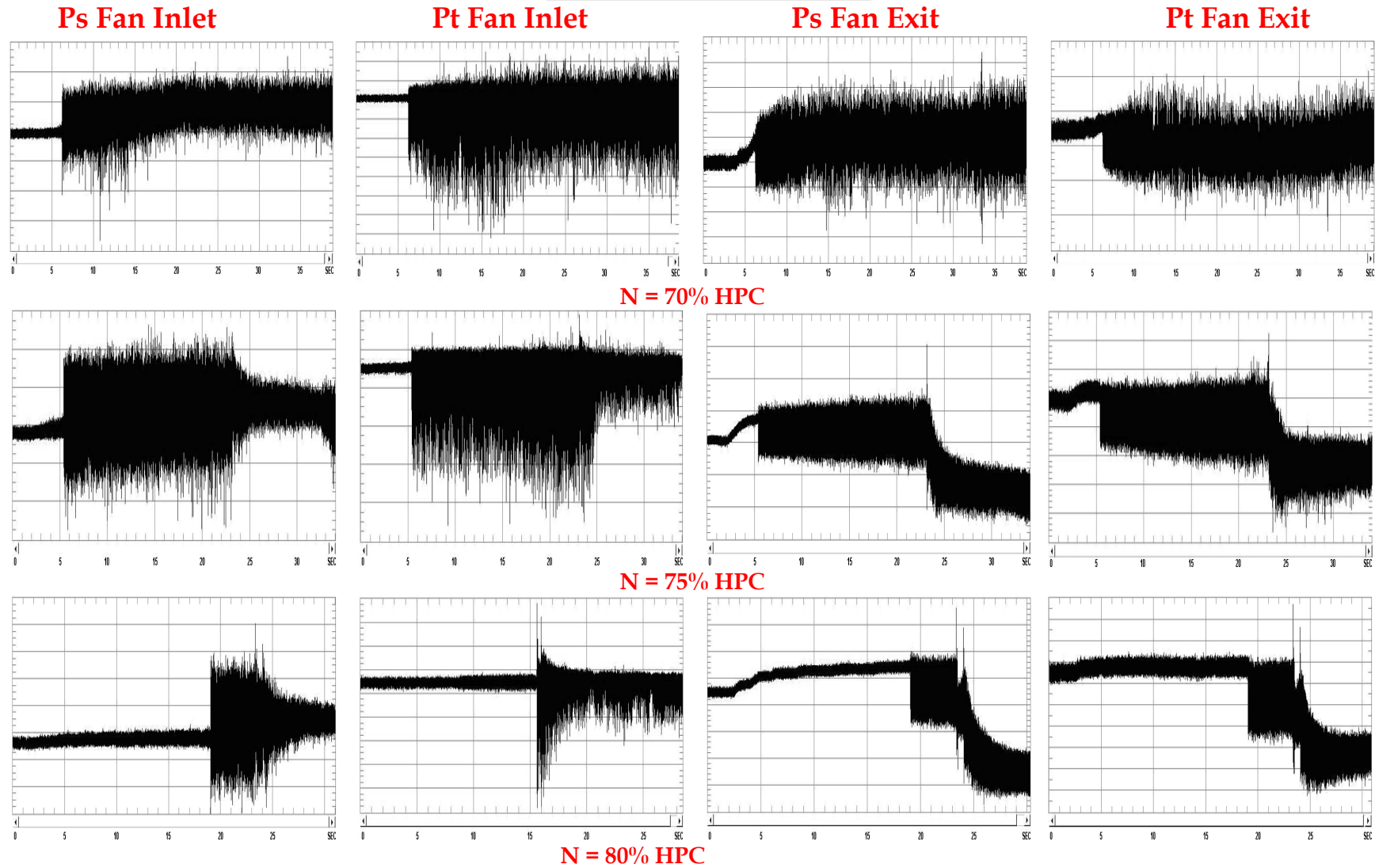
Figure 23a: Stall inception in the time domain as acquired with the Kulite, for different rotational speeds of the HPC, obtained by throttling the HPC with the by-pass blockage mechanism, and with no inlet flow distortion.

DSTO-RR-0377

| Vertical axis - relative pressure |
| Horizontal axis - time |

Ps Fan Inlet   **Pt Fan Inlet**   **Ps Fan Exit**   **Pt Fan Exit**

N = 85% HPC

N = 90% HPC

N = 97% HPC
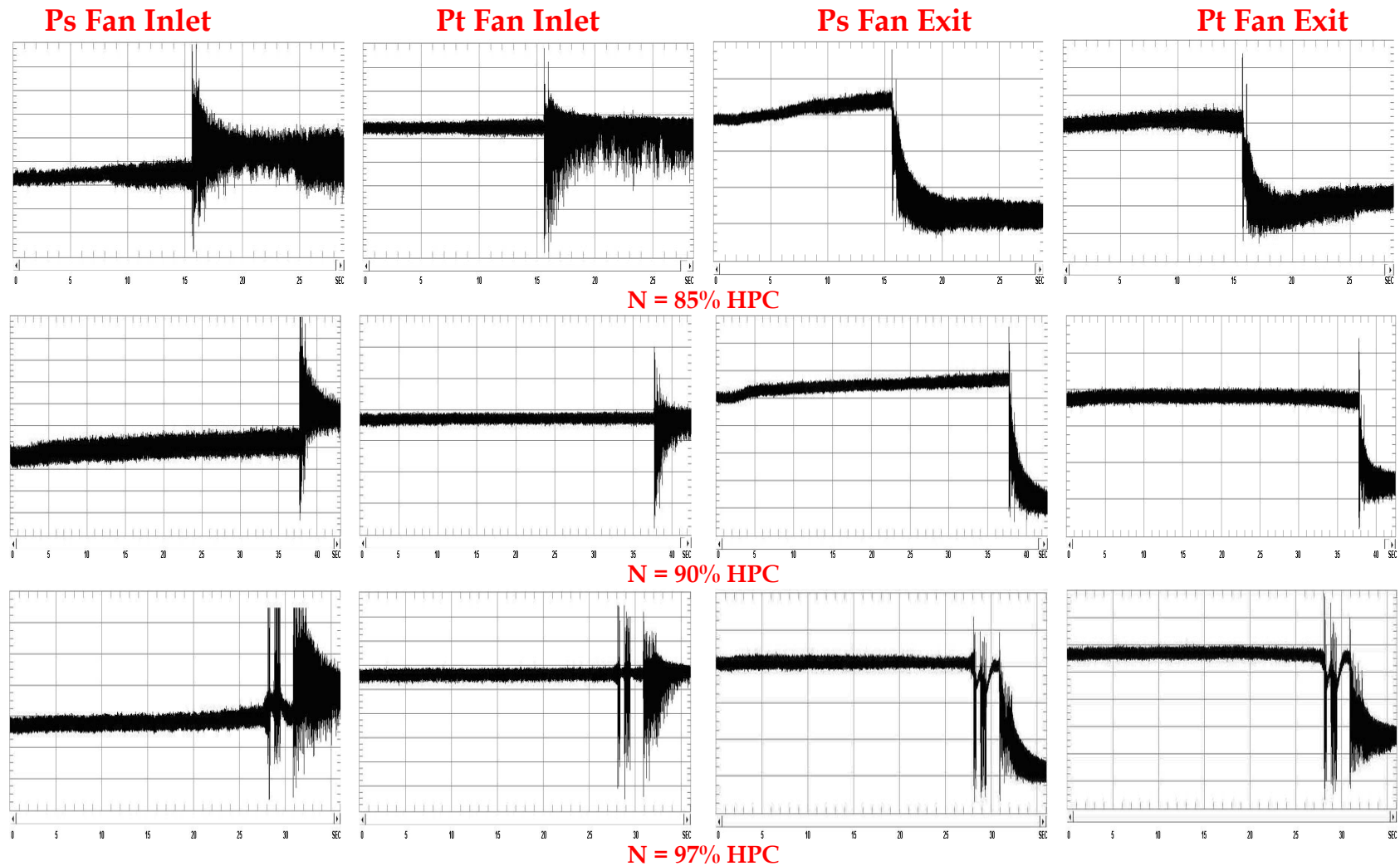
Figure 23b: Stall inception in the time domain as acquired with the Kulite, for different rotational speeds of the HPC, obtained by throttling the HPC with the by-pass blockage mechanism, and with no inlet flow distortion.

| **Vertical axis** - relative pressure |
| **Horizontal axis** - time |
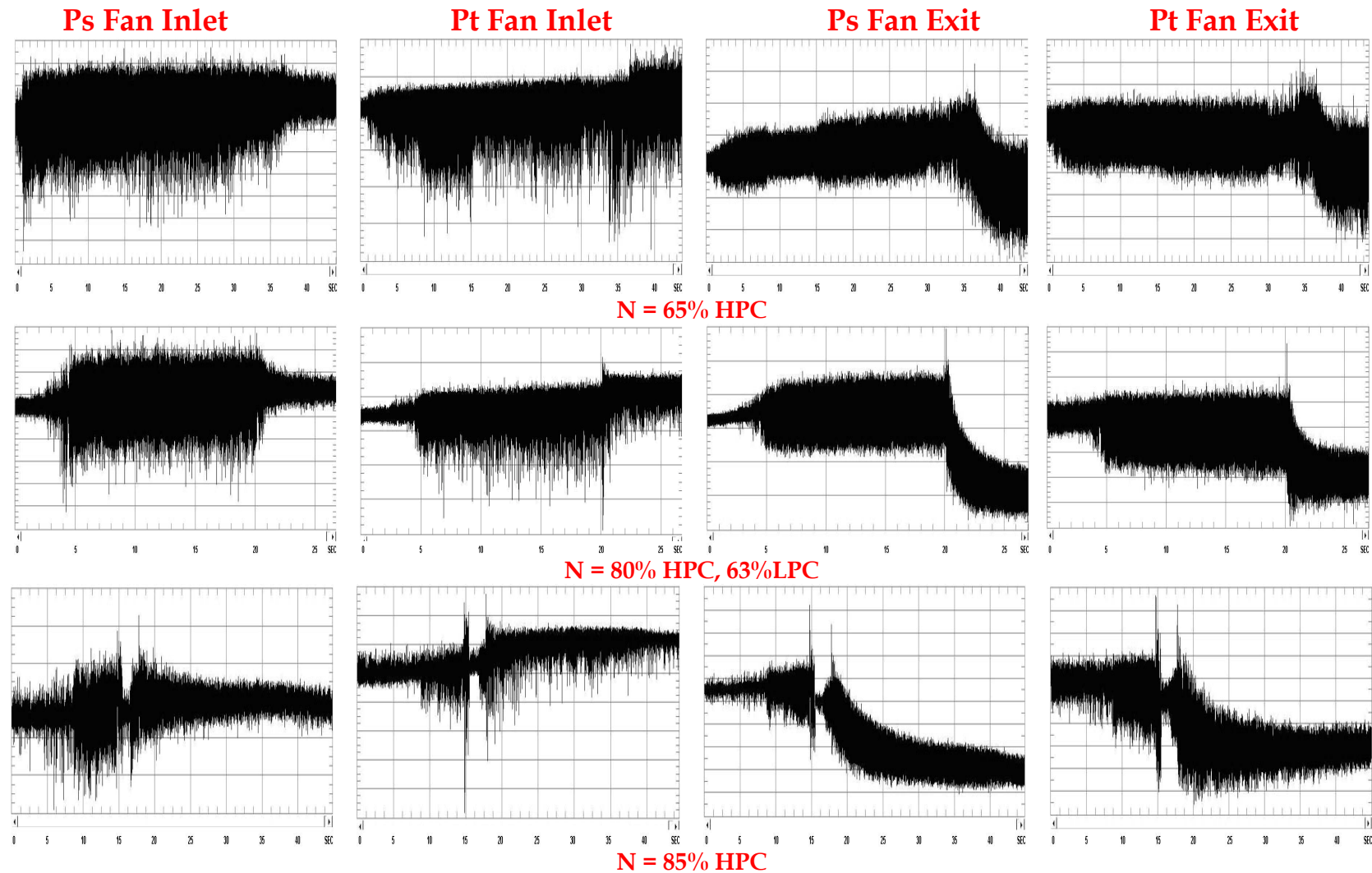
Figure 24a: Stall inception in the time domain as acquired with the Kulite, for different rotational speeds of the HPC, obtained by throttling the HPC with the by-pas blockage mechanism, and with 120o inlet flow distortion.
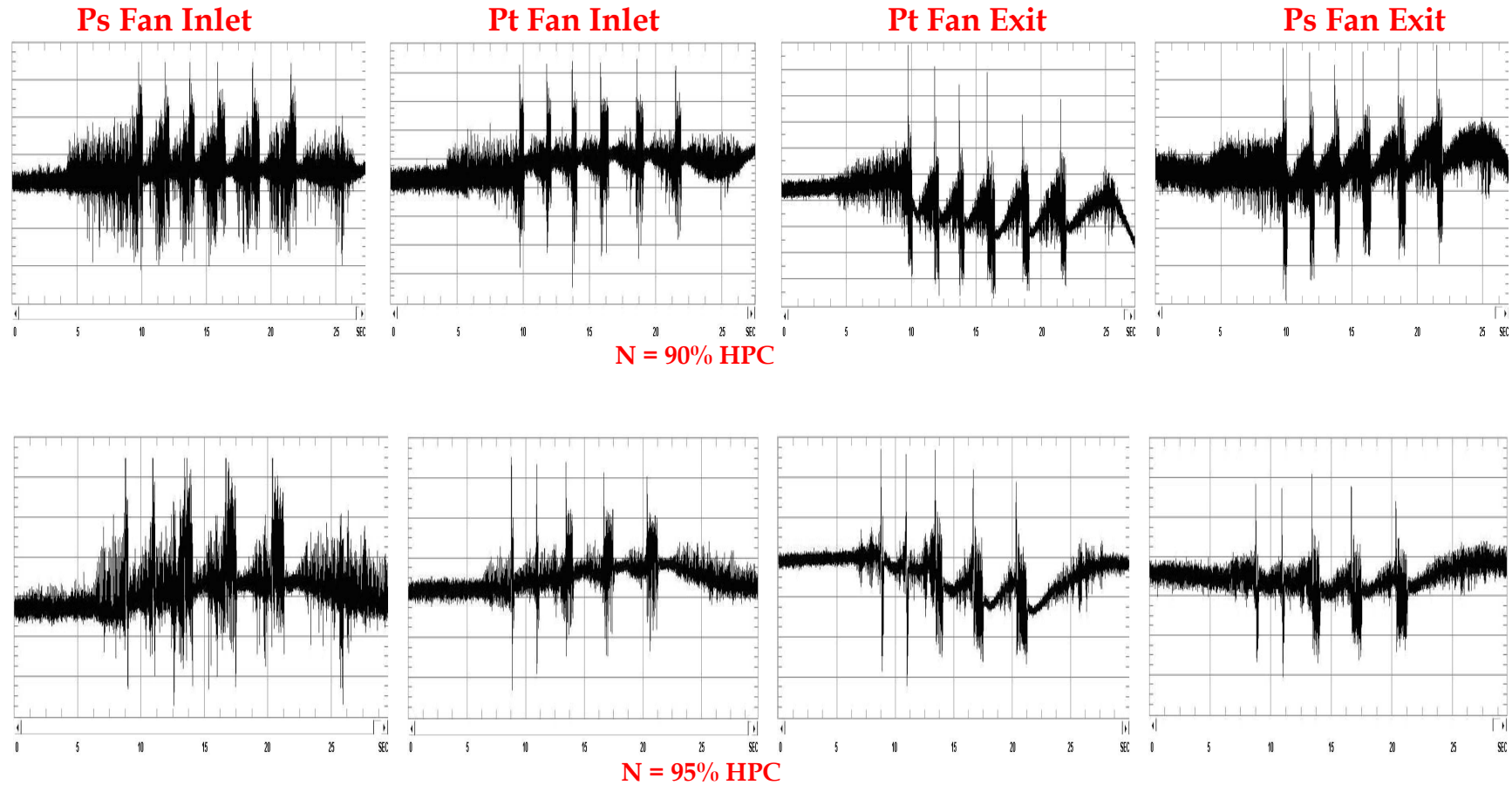
Figure 24b: Stall inception in the time domain as acquired with the Kulite, for different rotational speeds of the HPC, obtained by throttling the HPC with the by-pas blockage mechanism, and with 120º inlet flow distortion

Vertical axis - relative pressure
Horizontal axis - time
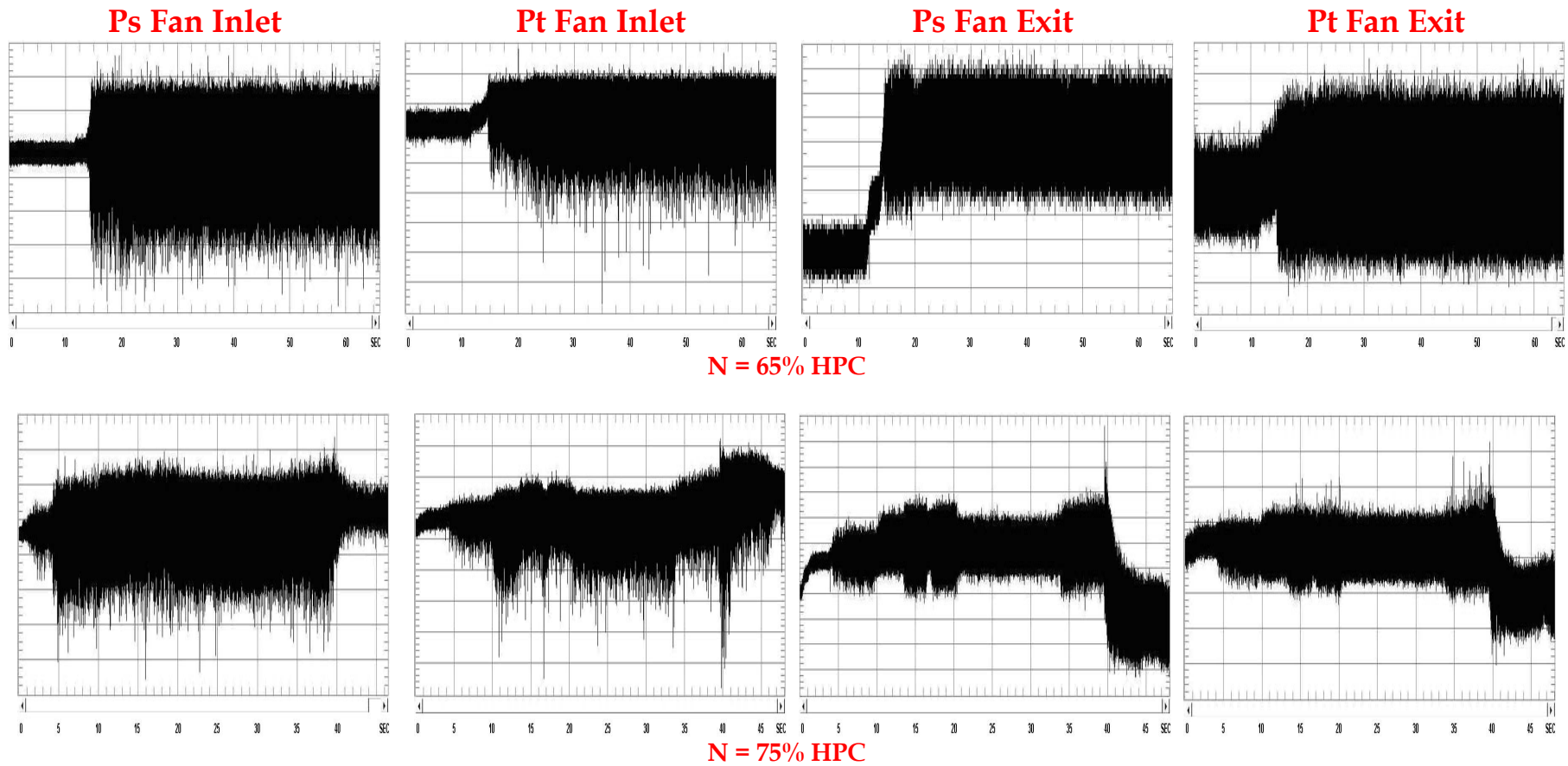
Figure 25a: Stall inception in the time domain as acquired with the Kulite, for different rotational speeds of the HPC, obtained by throttling the HPC with the by-pas blockage mechanism, and with 180° inlet flow distortion

Vertical axis - relative pressure
Horizontal axis - time
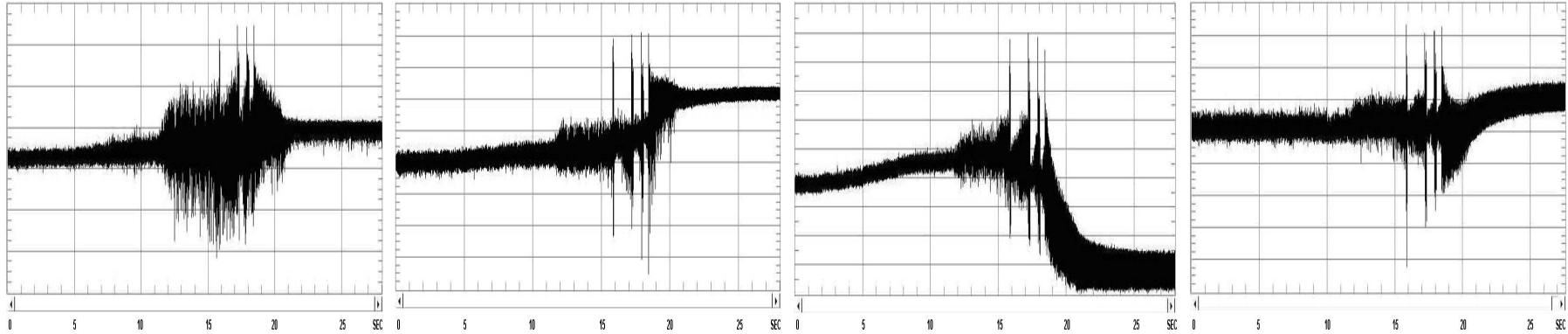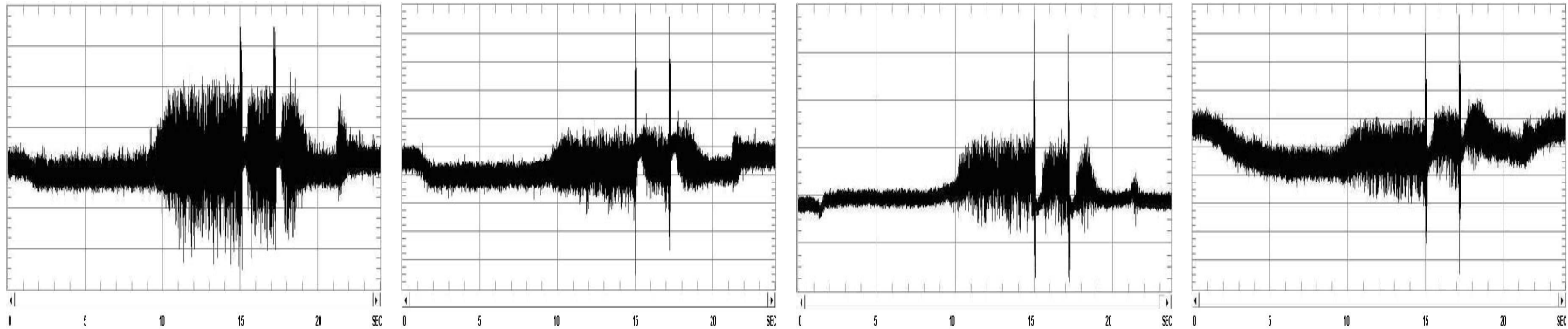
Figure 25b: Stall inception in the time domain as acquired with the Kulite, for different rotational speeds of the HPC, obtained by throttling the HPC with the by-pas blockage mechanism, and with 180º inlet flow distortion

Vertical axis - relative pressure
Horizontal axis - time
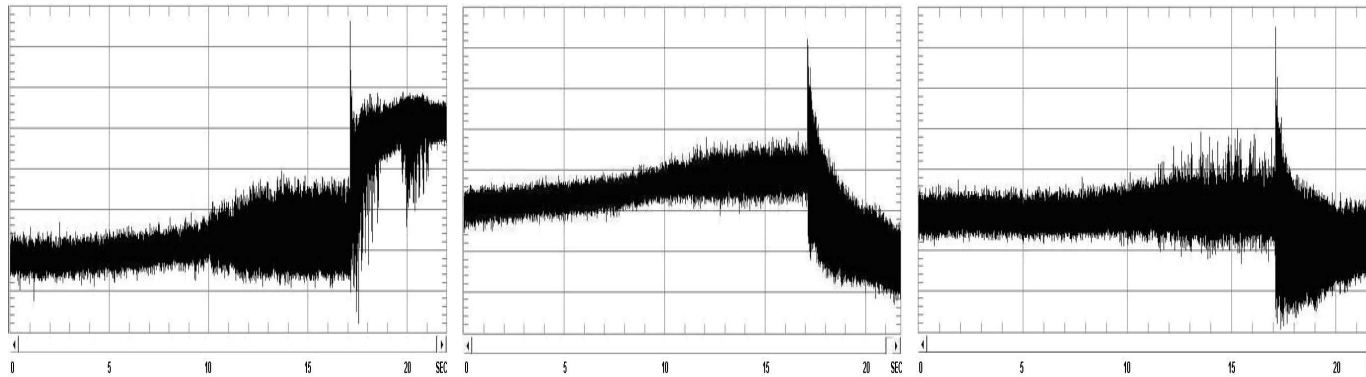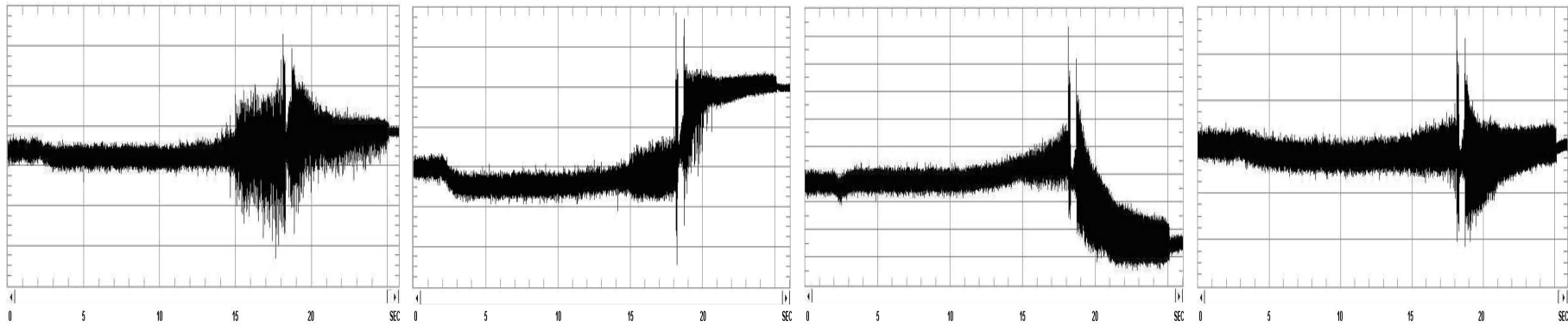
Figure 26: Stall inception in the time domain as acquired with the Kulite transducers, for different rotational speeds of the HPC, obtained by throttling the HPC with the by-pas blockage mechanism, and with 240º inlet flow distortion

DSTO-RR-0377

Vertical axis - relative pressure
Horizontal axis - time
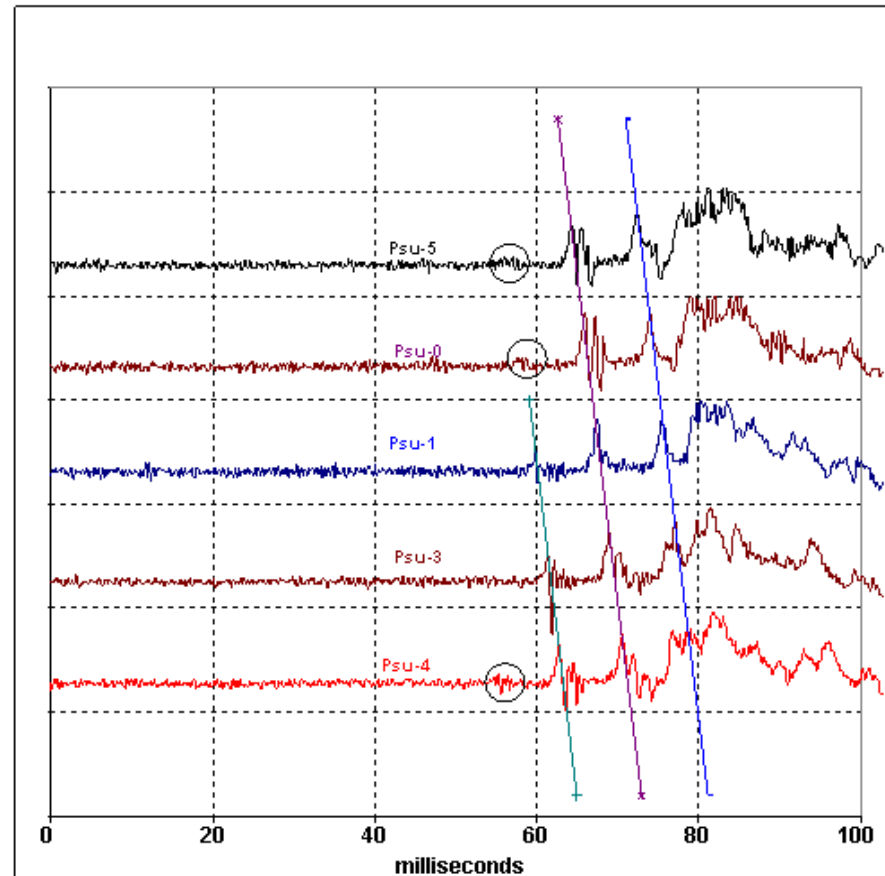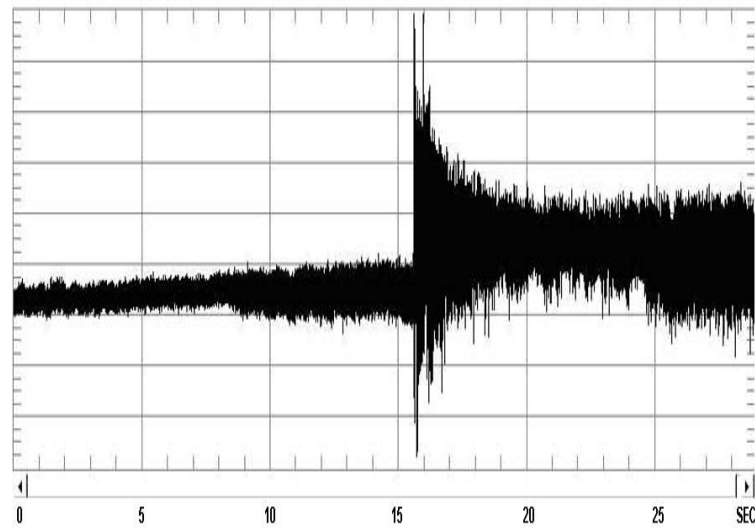
Figure 27: The simultaneous static pressure traces obtained with the five Kulite static pressure transducers of the short period prior and into the initiation of the first stall event, at the fan inlet for N_{HPC} = 85%, with no inlet flow distortion and throttling of the HPC with Core blockage mechanism.

Vertical axis - relative pressure
Horizontal axis - time
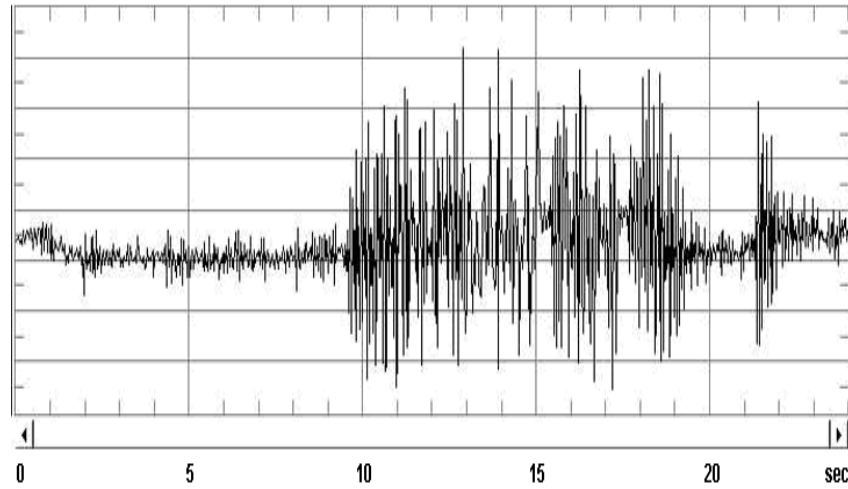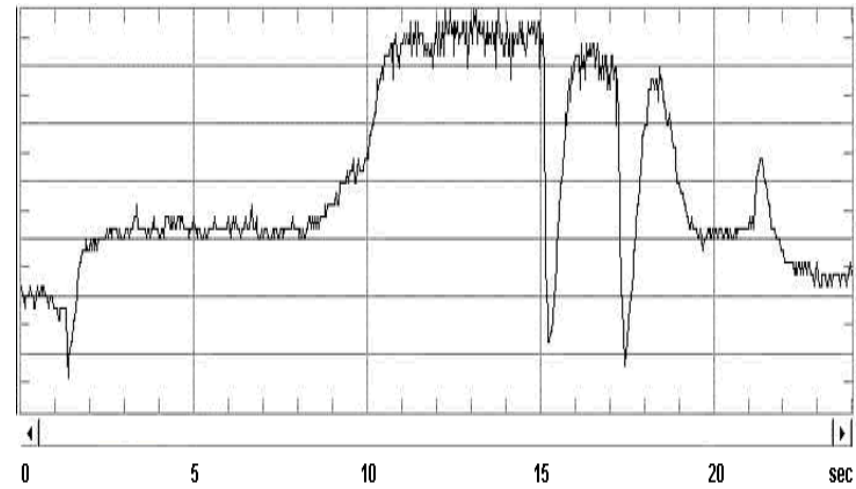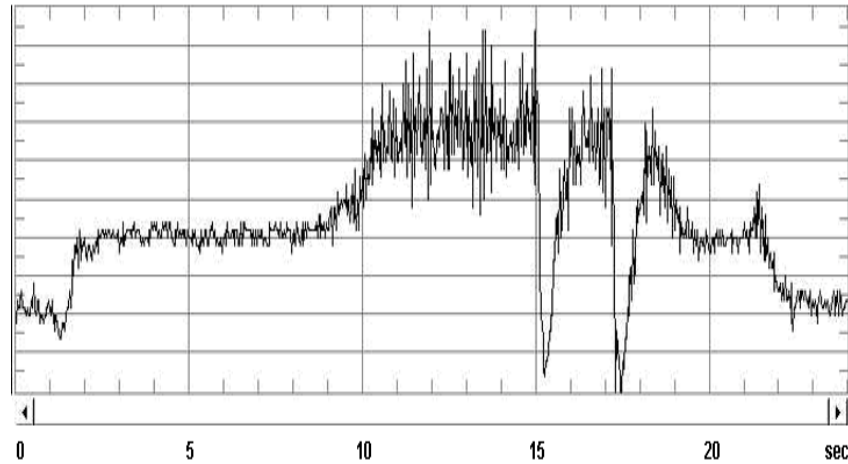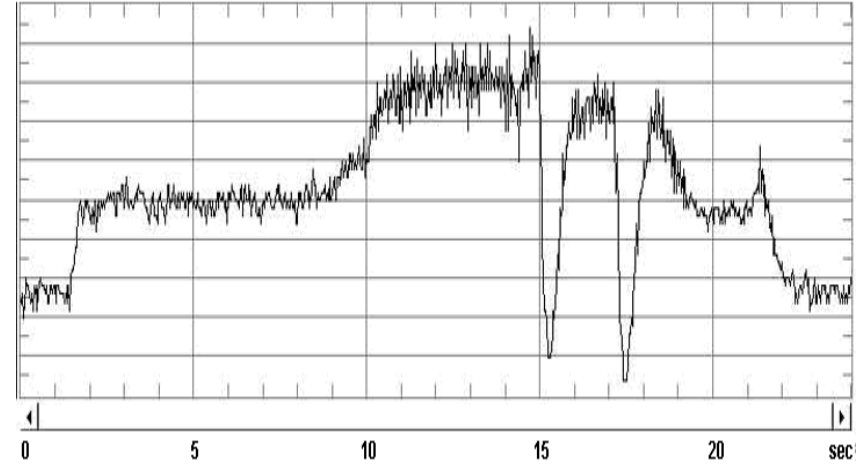
Figure 28a: Stall inception in the time domain acquired with the with the conventional pressure probes. For N_{HPC} = 75%, with 180° inlet flow distortion and throttling of the HPC with Core blockage mechanism.
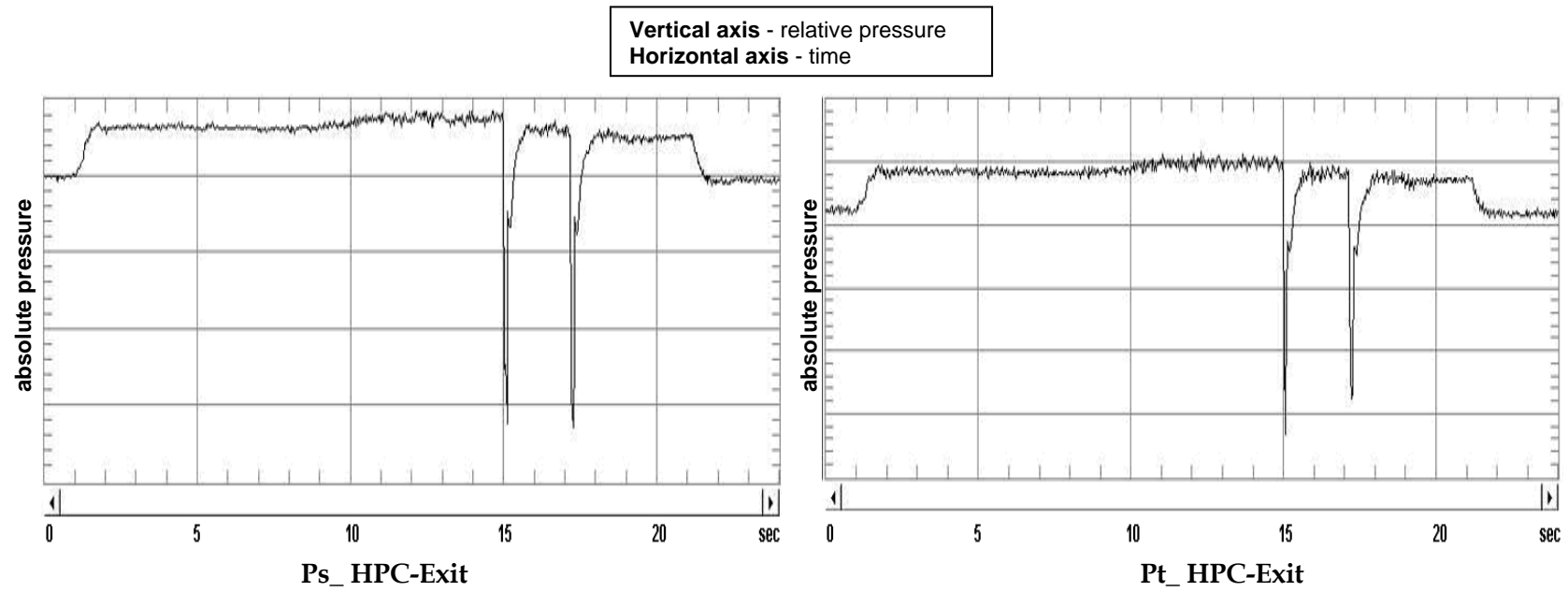
Figure 28b: Stall inception in the time domain acquired with the with the conventional pressure probes. For $N_{HPC} = 75\%$, with 180° inlet flow distortion and throttling of the HPC with Core blockage mechanism
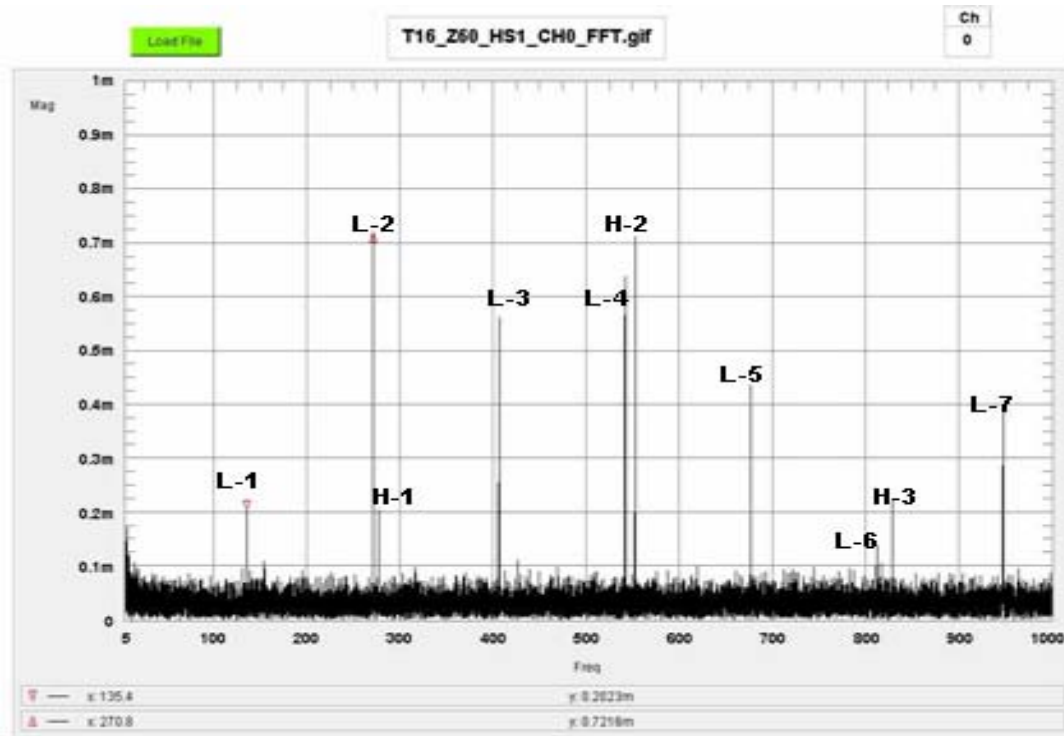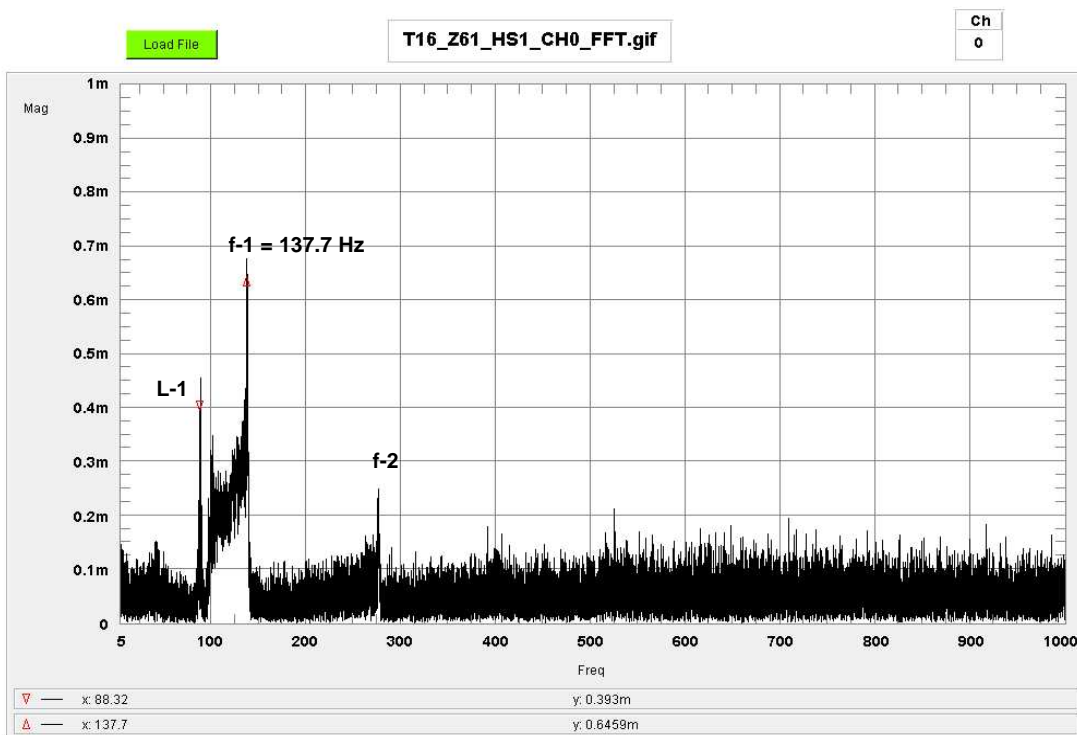
Z60 - S-S

Z61 - Stall

Figure 29a: Temporal Fourier spectrum for the Kulite static pressure probe signals, at the fan inlet, with no inlet flow distortion, for $N_{HPC} = 74\%$, and throttling of the HPC with the Core blockage mechanism
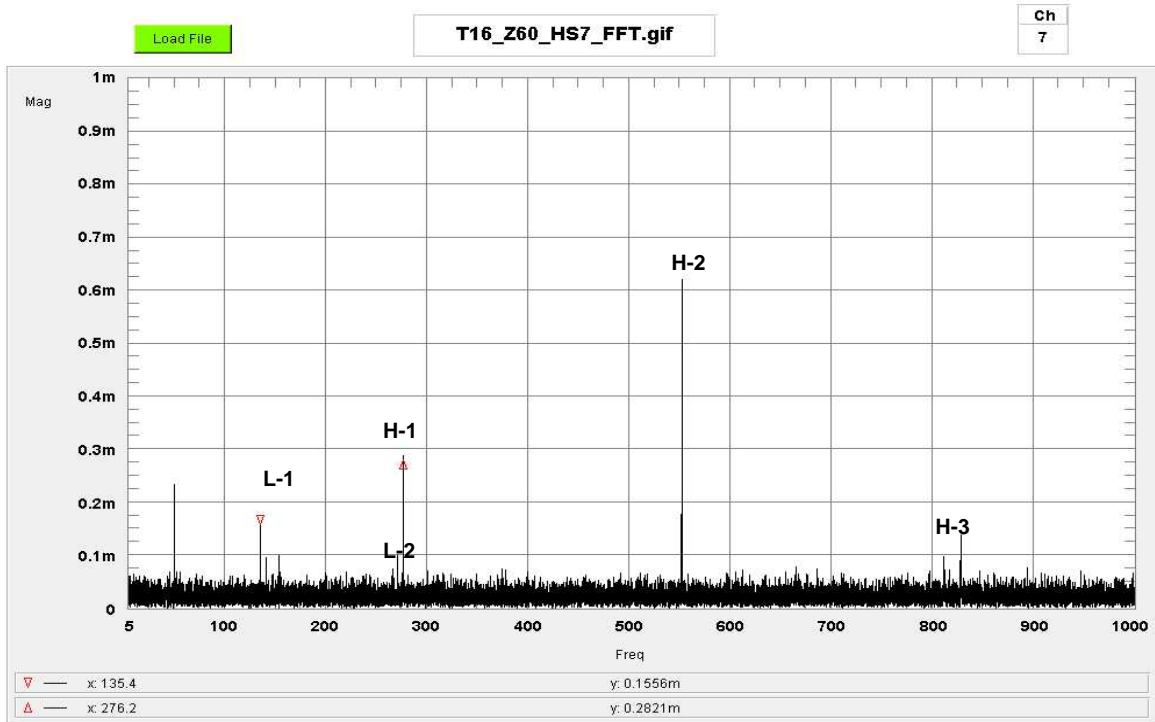
**Z60 - S-S**
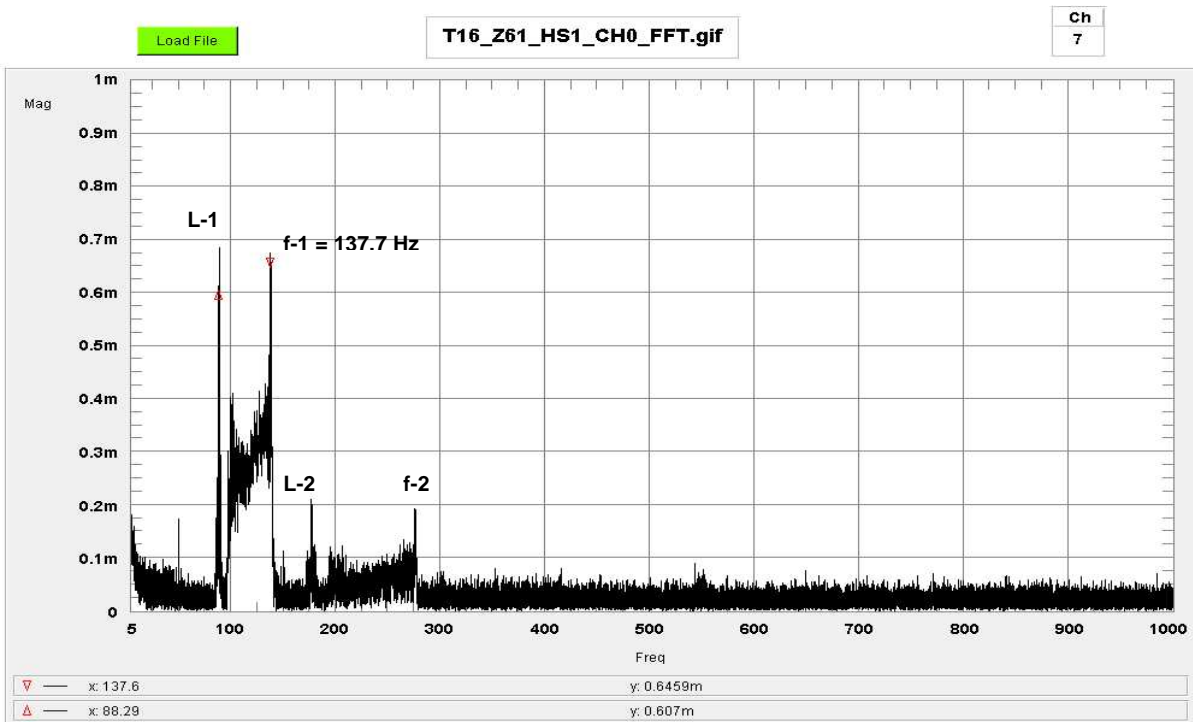
Z61 - Stall

Figure 29b: Temporal Fourier spectrum for the Kulite static pressure probe signals, at the fan exit, with no inlet flow distortion, for N_{HPC} = 74%, and throttling of the HPC with the Core blockage mechanism.
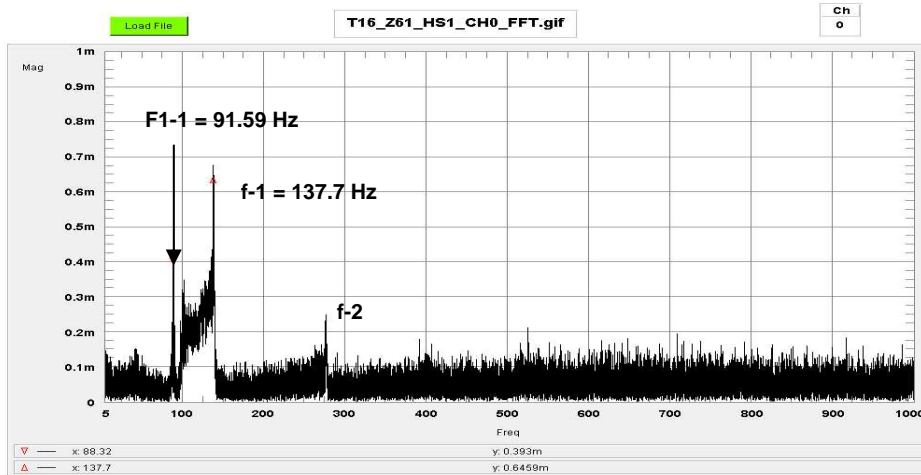
N$_{HPC}$ = 74%.
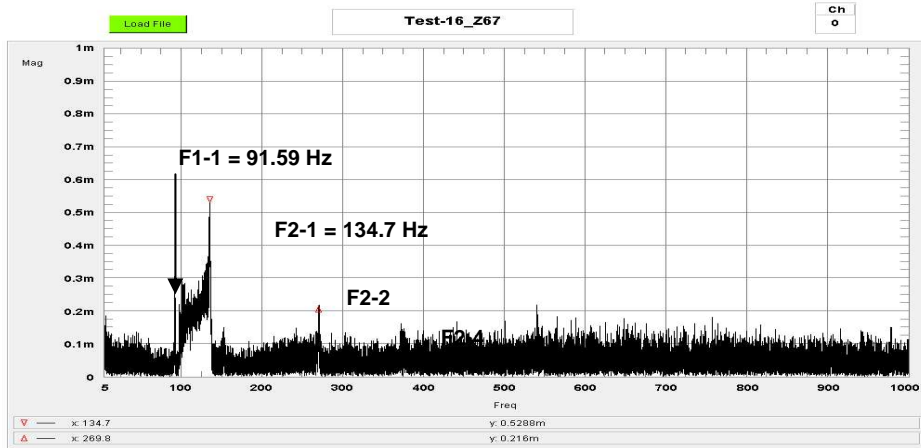
N$_{HPC}$ = 82%.
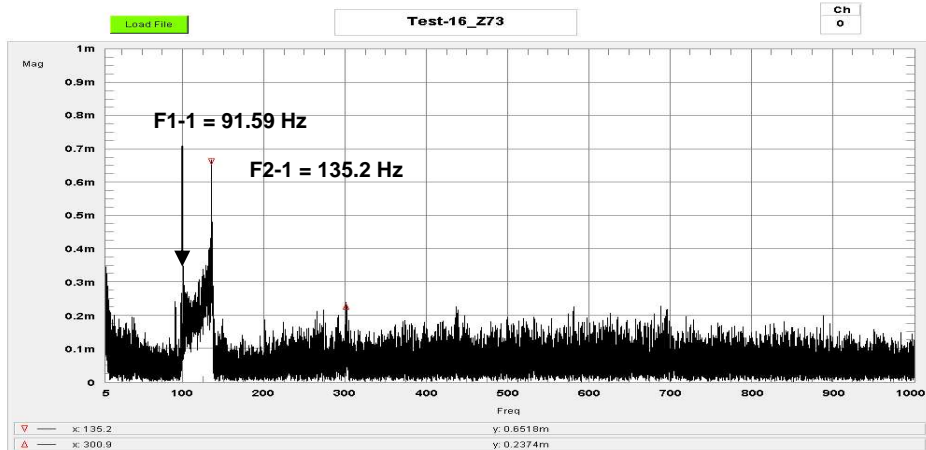
N$_{HPC}$ = 92%.

Figure 30a: Temporal Fourier spectrum for the Kulite static pressure probe signals, at the fan inlet, for different HPC rotational speeds, no inlet flow distortion, and throttling of the HPC with the Core blockage mechanism
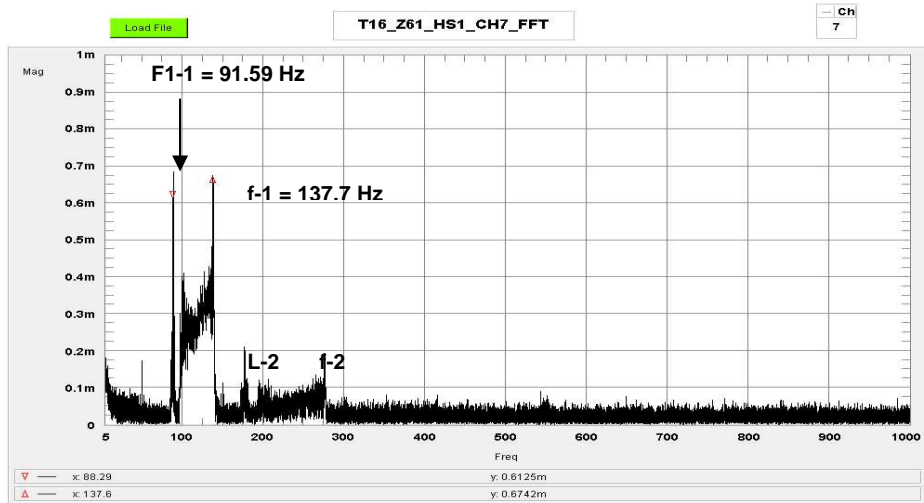
N_{HPC} = 74%.
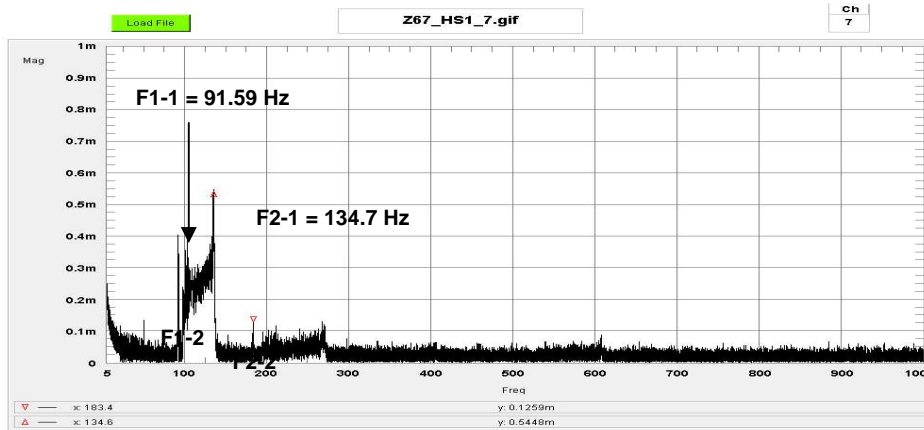
N_{HPC} = 82%
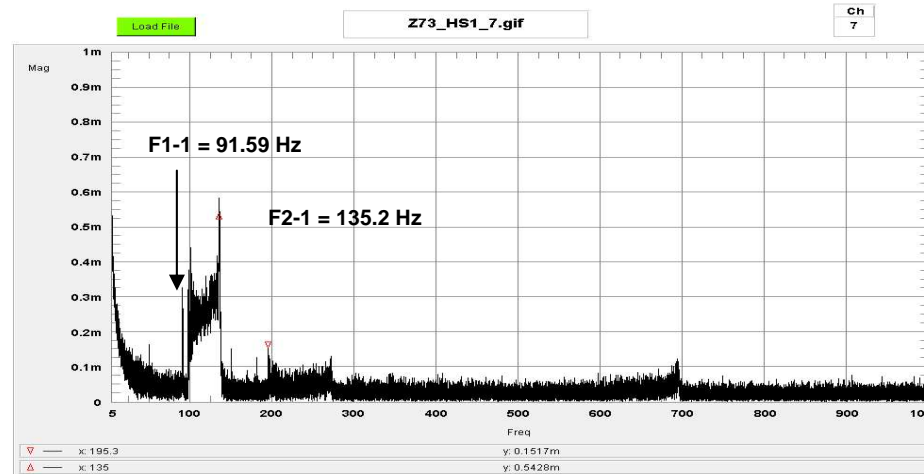
N_{HPC} = 92%.

Figure 30b: Temporal Fourier spectrum for the Kulite static pressure probe signals, at the fan exit, for different HPC rotational speeds, no inlet flow distortion, and throttling of the HPC with the Core blockage mechanism
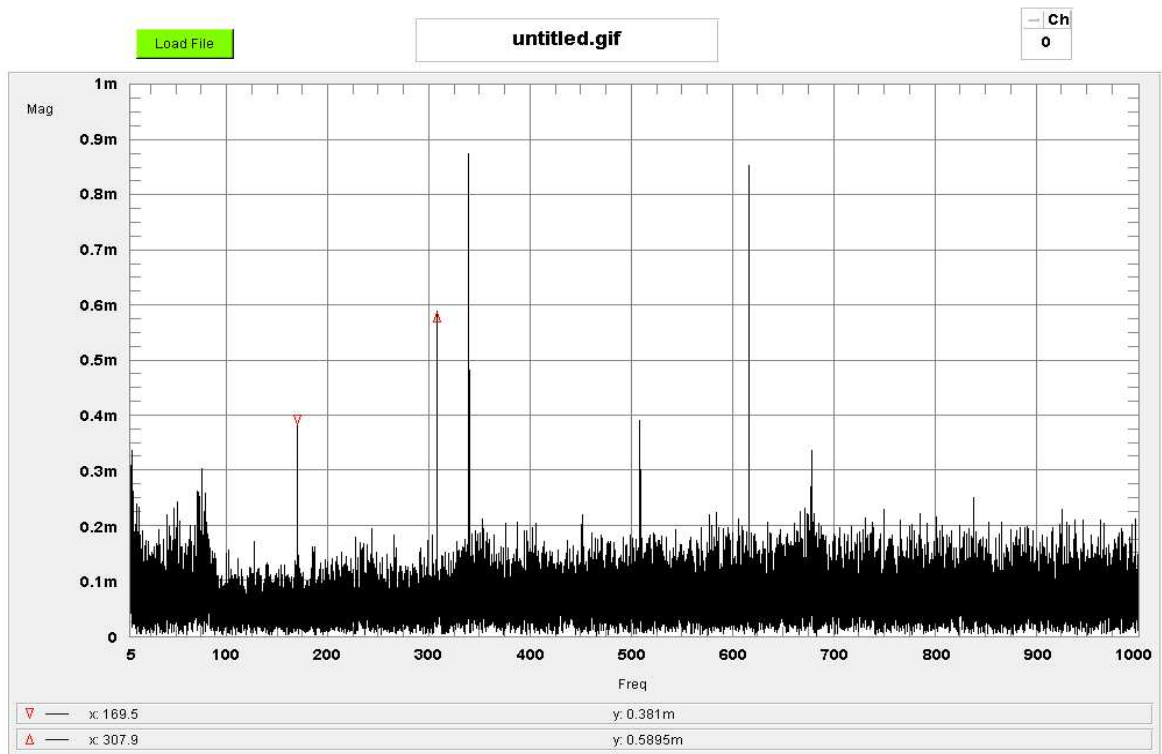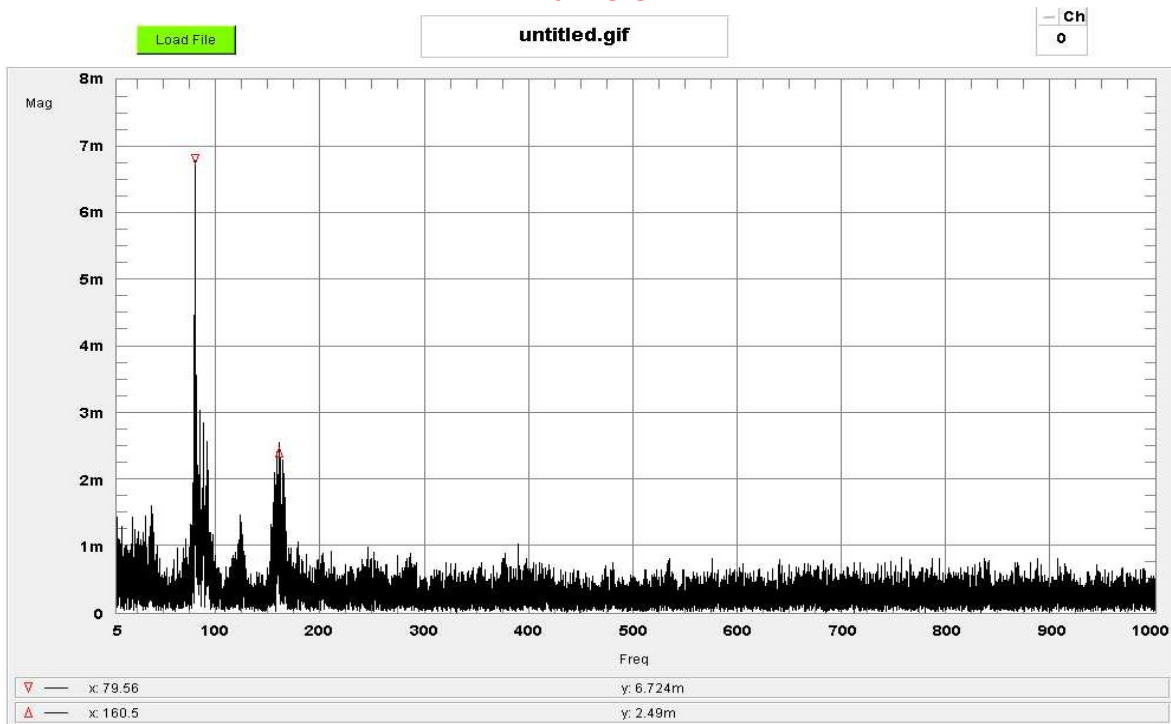
X64 - S-S

X66 - Surge

Figure 31a: Temporal Fourier spectrum for the Kulite static pressure probe signals, at the fan inlet, with 240º inlet flow distortion, for N_{HPC} = 87%, and throttling of the HPC with the Core blockage mechanism.
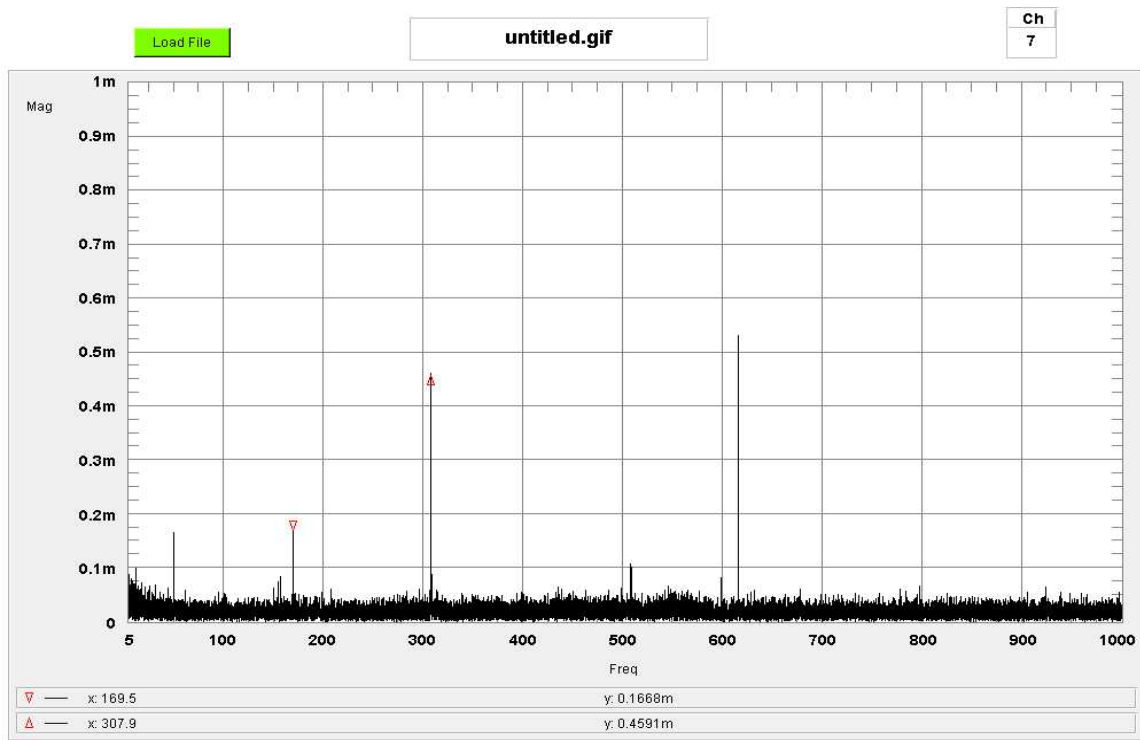
X64 - S-S
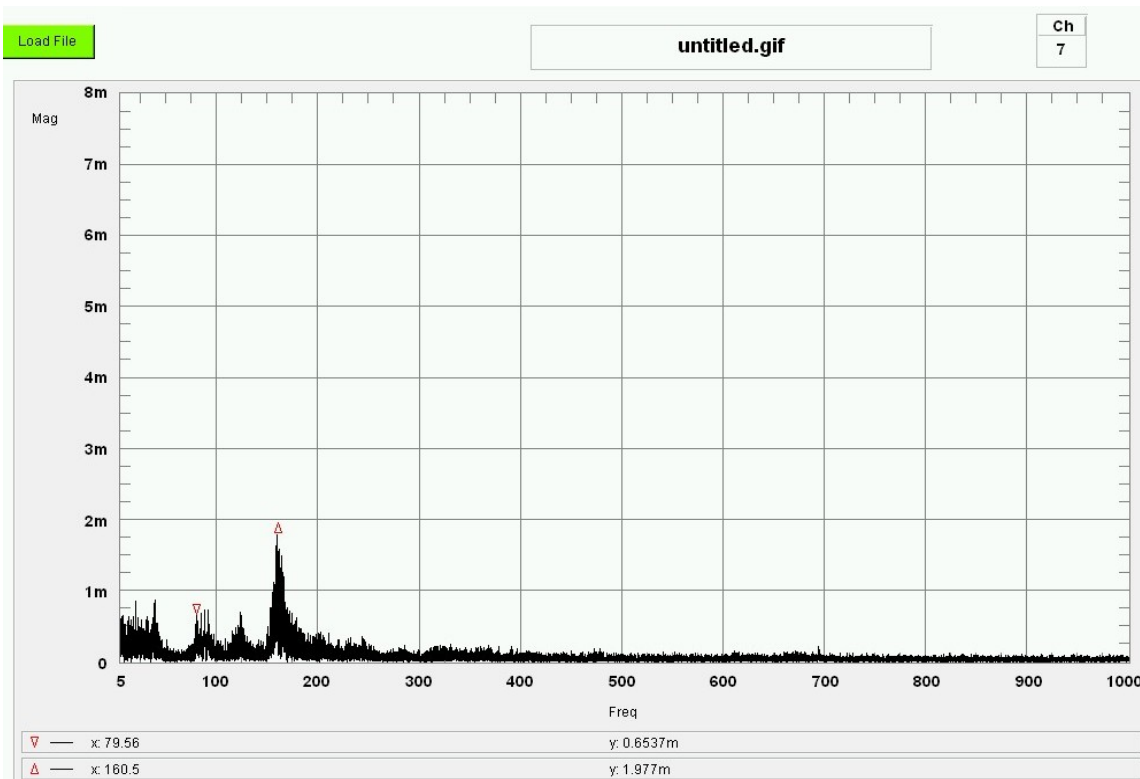
X66 – Surge -

*Figure 31b: Temporal Fourier spectrum for the Kulite static pressure probe signals, at the fan exit, with 240°
inlet flow distortion, for N_{HPC} = 87%, and throttling of the HPC with the Core blockage
mechanism*
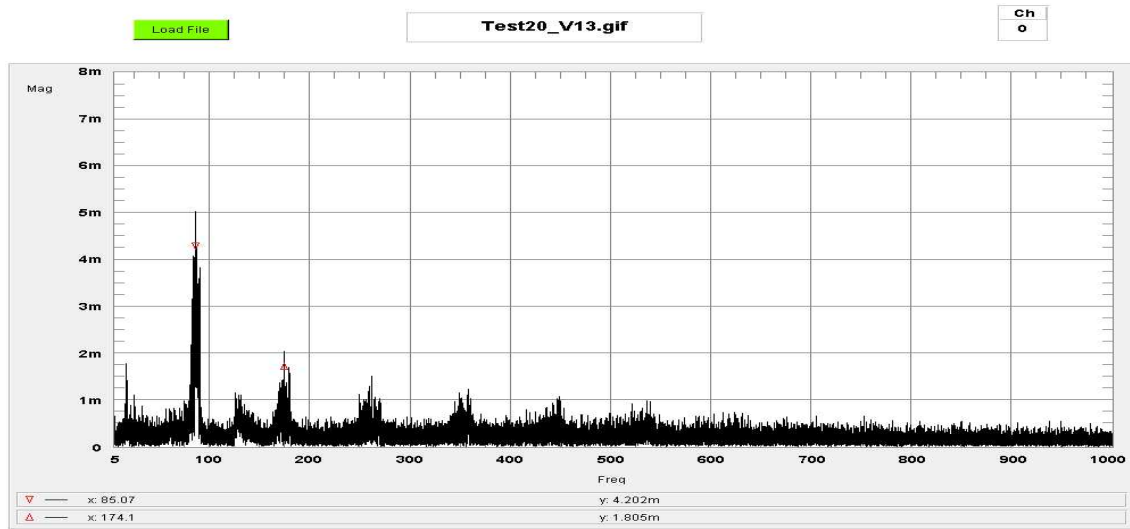
**V13** $N_{HPC} = 75\%$
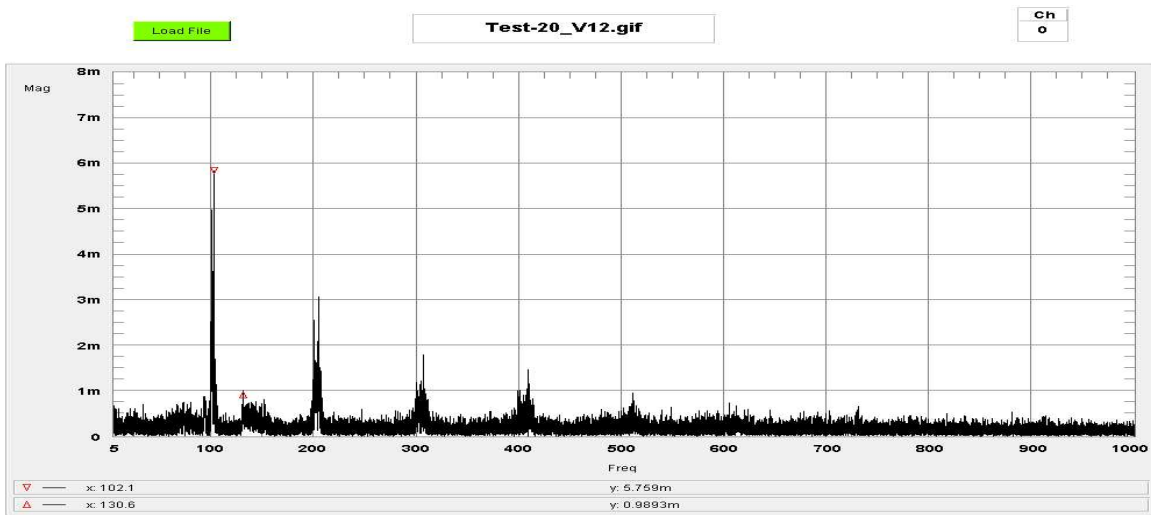
V12 $N_{HPC} = 80\%$
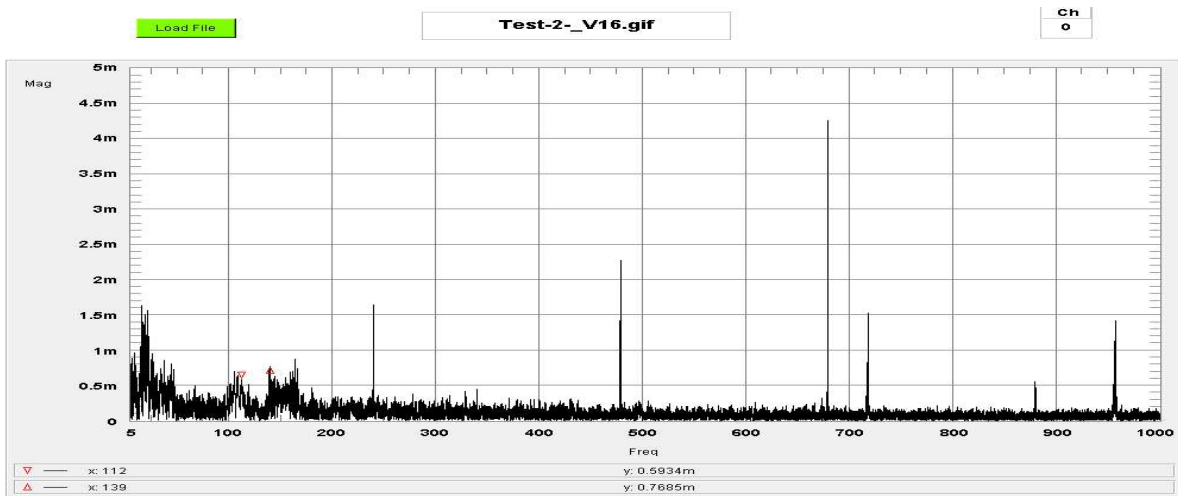
Figure 32a: Temporal Fourier spectrum for the Kulite static pressure probe signals, at the fan inlet, for different HPC rotational speeds, no inlet flow distortion, and throttling of the HPC with the by-pass blockage mechanism

DSTO-RR-0377
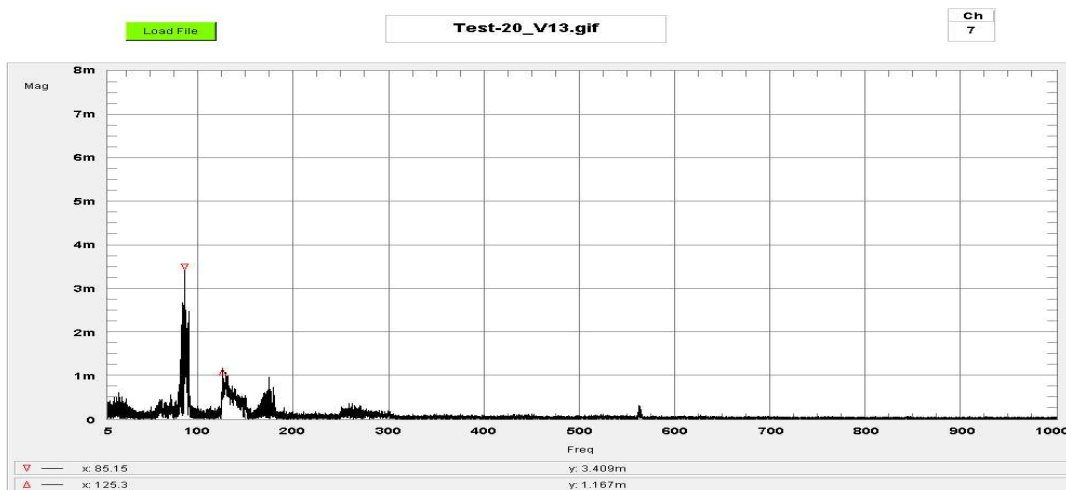
V13 $N_{HPC} = 75\%$
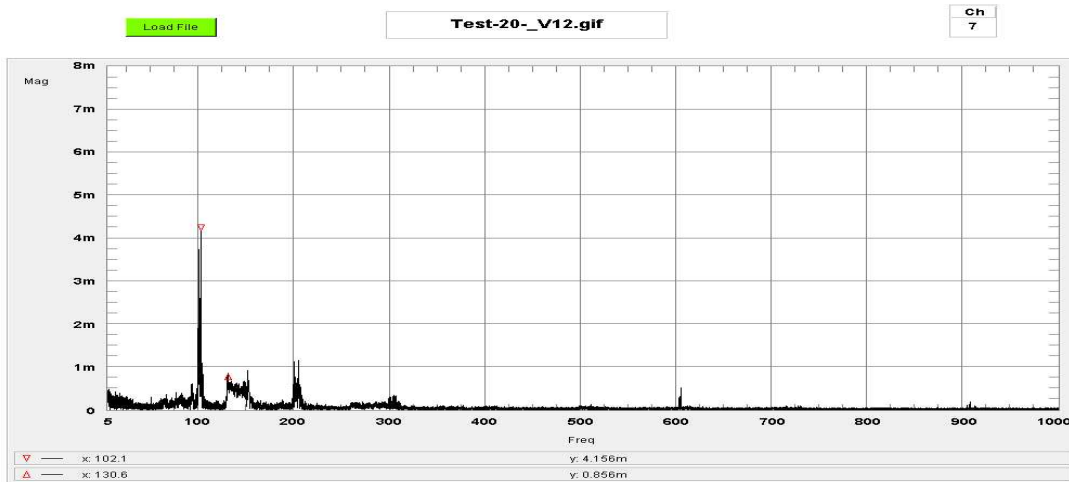
V12 $N_{HPC} = 80\%$
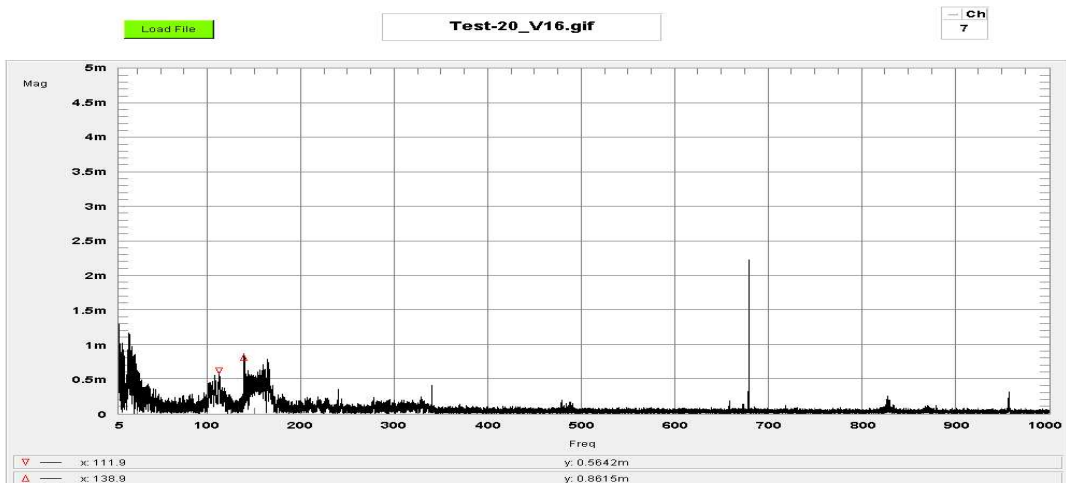
V16 $N_{HPC} = 90\%$

Figure 32b: Temporal Fourier spectrum for the Kulite static pressure probe signals, at the fan exit, for different HPC rotational speeds, no inlet flow distortion, and throttling of the HPC with the by-pass blockage mechanism
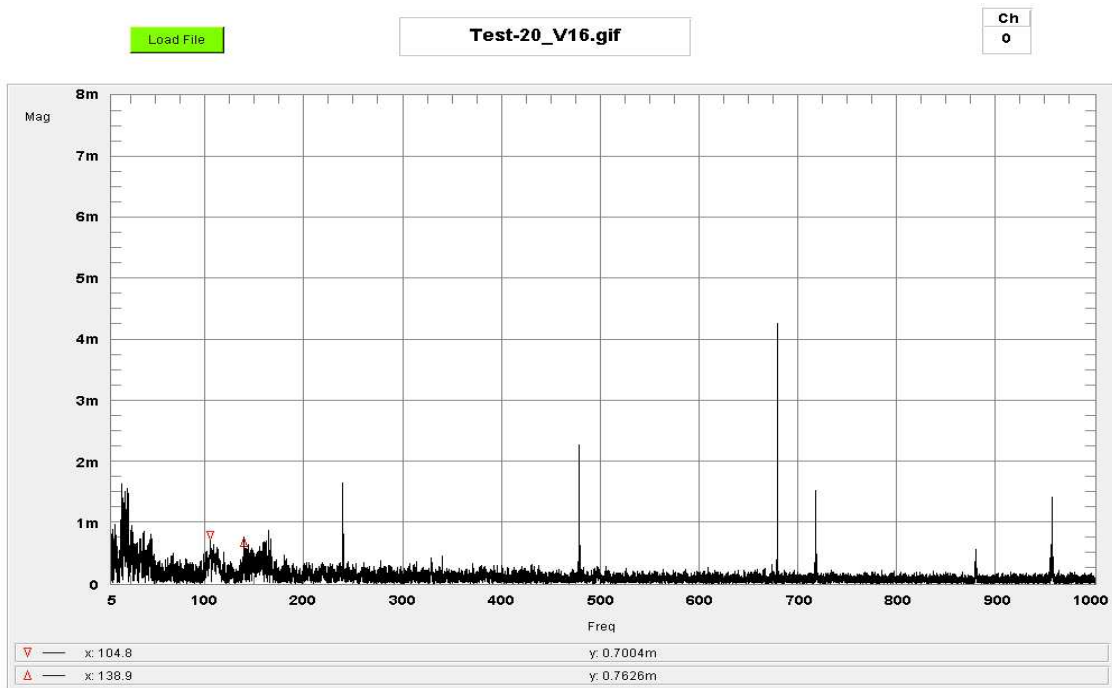
V16   0° – Distortion – Fan Inlet
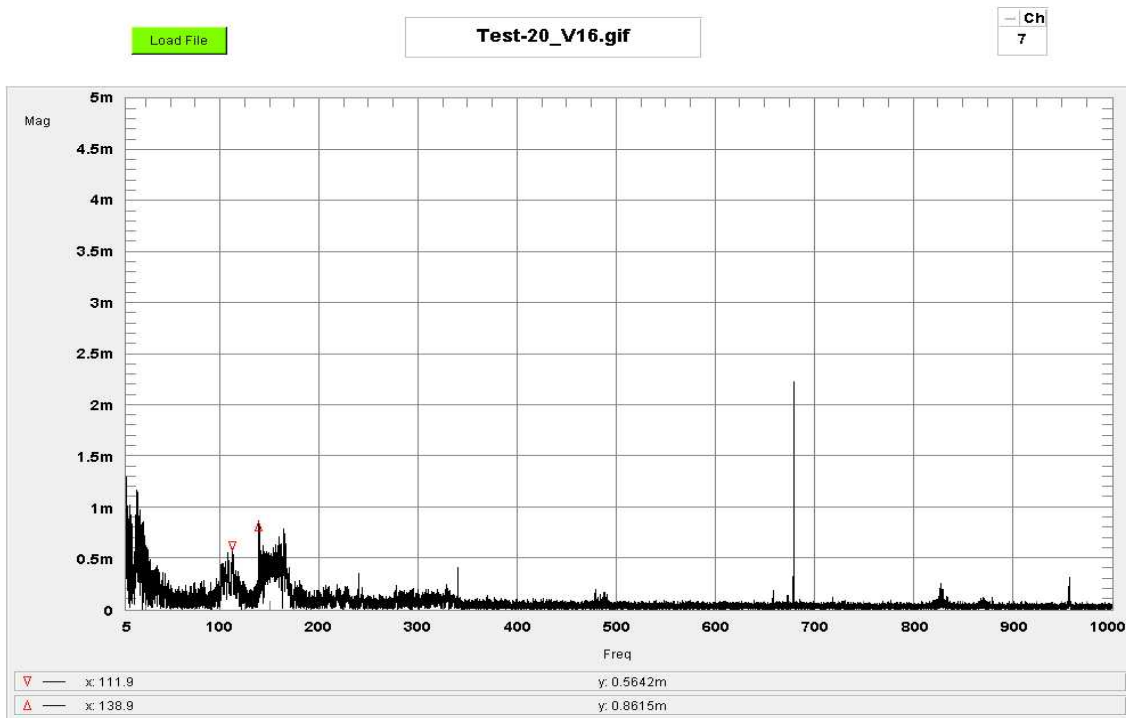
V16   0° – Distortion – Fan Exit

Figure 33a: For caption see page
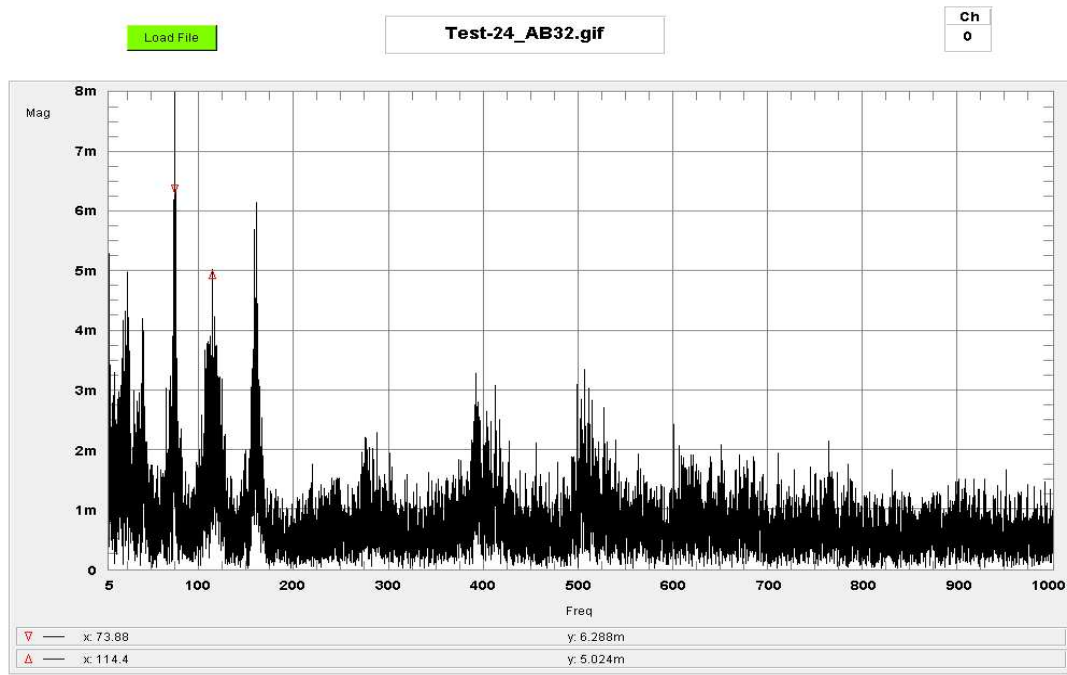
AB32   120$^\text{O}$ – Distortion – Fan Inlet
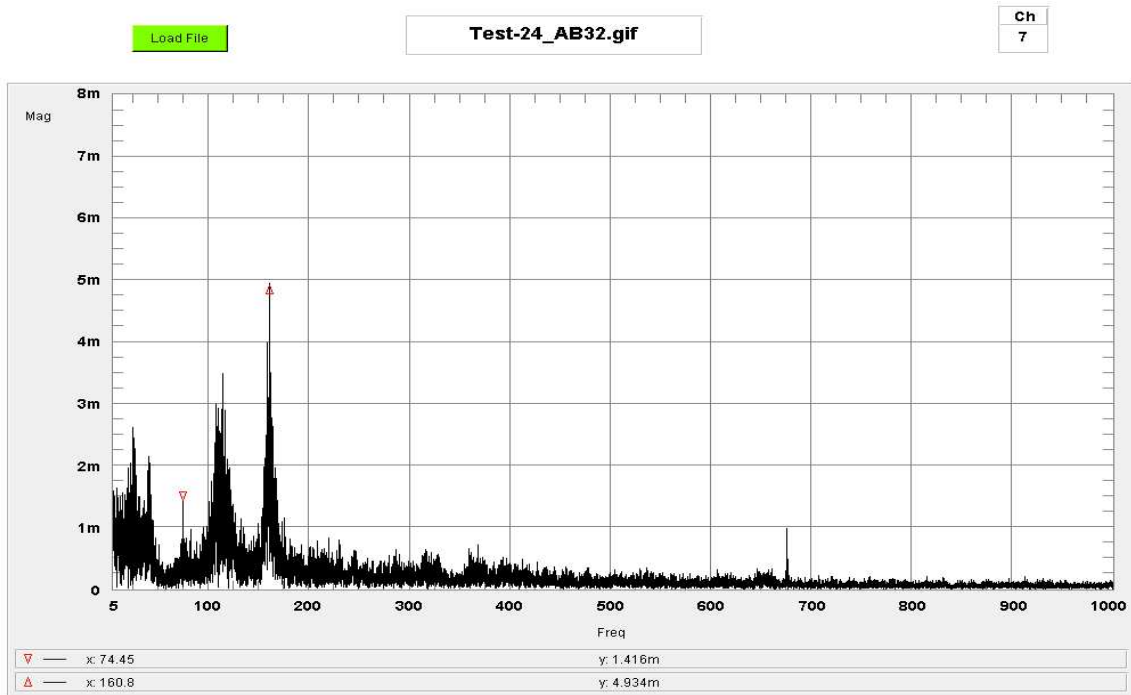
AB32   120$^\text{O}$ – Distortion – Fan Exit

*Figure 33b: For caption see page*
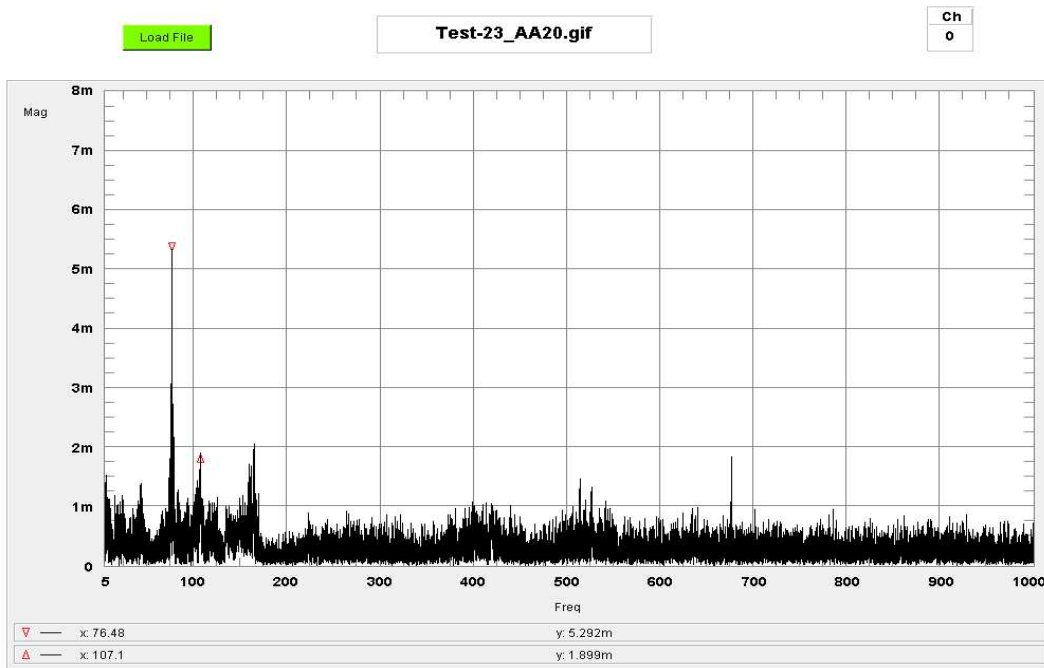
**AA20**   180° – Distortion – Fan Inlet
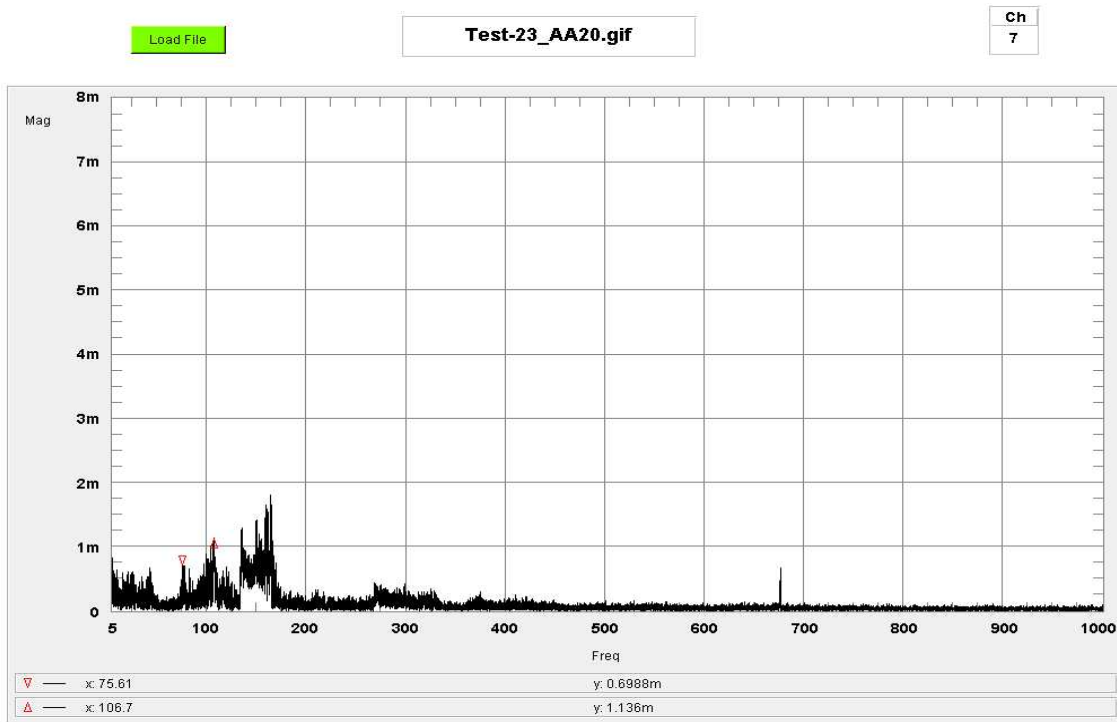
**AA20**   180° – Distortion – Fan Exit

Figure 33c: For caption see page
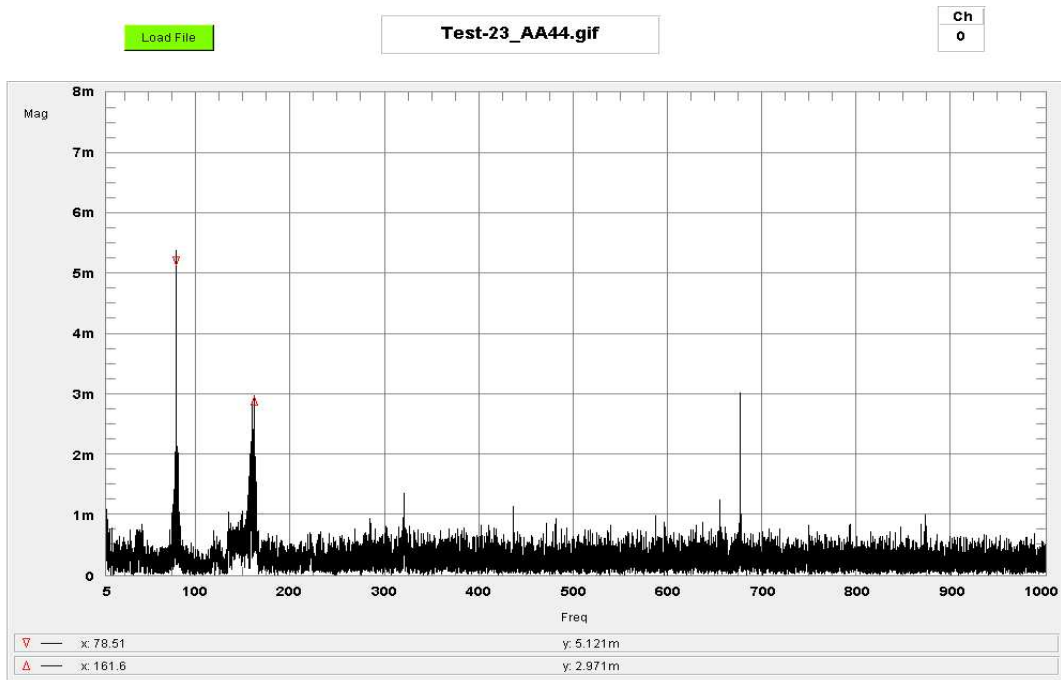
AA44   240° – Distortion – Fan Inlet
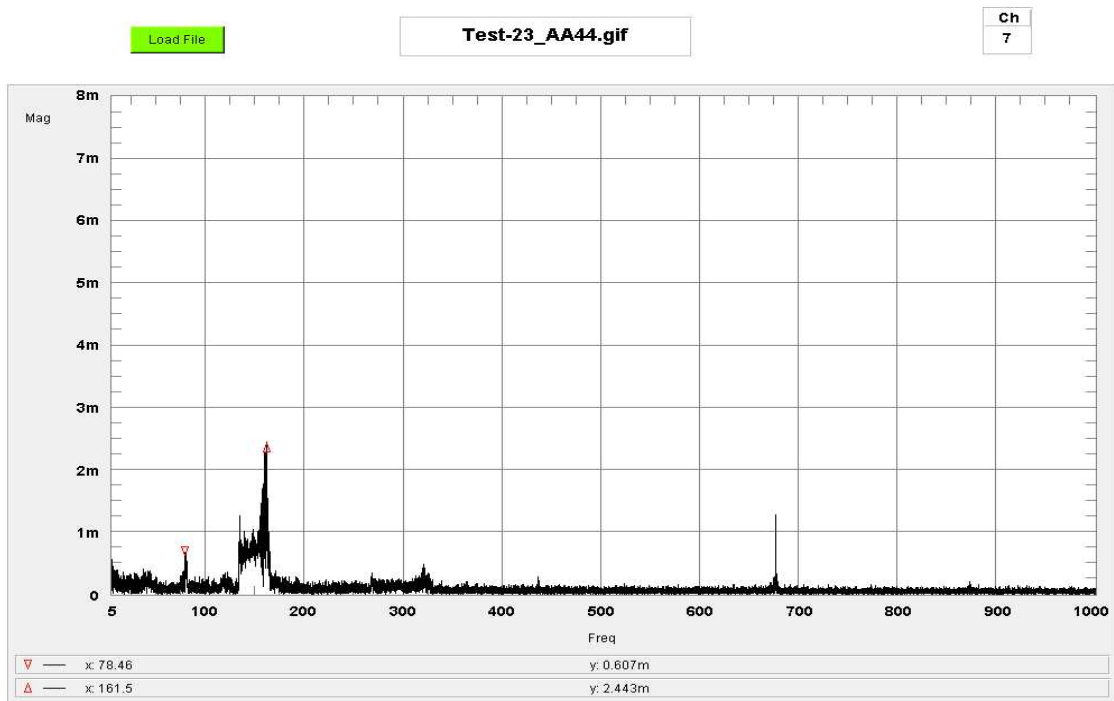
AA44   240° – Distortion – Fan Exit

Figure 33d: Temporal Fourier spectrum for the Kulite static pressure probe signals, at the fan inlet, for different inlet flow distortions at N_{HPC} = 90%, and throttling of the HPC with the by-pass blockage mechanism

DEFENCE SCIENCE AND TECHNOLOGY ORGANISATION DOCUMENT CONTROL DATA		1. PRIVACY MARKING/CAVEAT (OF DOCUMENT)

2. TITLE Development of the Larzac Engine Rig for Compressor Stall Testing	3. SECURITY CLASSIFICATION (FOR UNCLASSIFIED REPORTS THAT ARE LIMITED RELEASE USE (L) NEXT TO DOCUMENT CLASSIFICATION) Document (U) Title (U) Abstract (U)

4. AUTHOR(S) A M Abdel-Fattah and A S Vivian	5. CORPORATE AUTHOR DSTO Defence Science and Technology Organisation 506 Lorimer St Fishermans Bend Victoria 3207 Australia

6a. DSTO NUMBER DSTO-RR-0377	6b. AR NUMBER AR-015-222	6c. TYPE OF REPORT Technical Report	7. DOCUMENT DATE December 2011

8. FILE NUMBER 2010/1124003	9. TASK NUMBER 07/050	10. TASK SPONSOR	11. NO. OF PAGES 64	12. NO. OF REFERENCES 8

13. DSTO Repository of Publications http://dspace.dsto.defence.gov.au/dspace/	14. RELEASE AUTHORITY Chief, Air Vehicles Division

15. SECONDARY RELEASE STATEMENT OF THIS DOCUMENT

Approved for public release

OVERSEAS ENQUIRIES OUTSIDE STATED LIMITATIONS SHOULD BE REFERRED THROUGH DOCUMENT EXCHANGE, PO BOX 1500, EDINBURGH, SA 5111

16. DELIBERATE ANNOUNCEMENT

No Limitations

17. CITATION IN OTHER DOCUMENTS	Yes

18. DSTO RESEARCH LIBRARY THESAURUS http://web-vic.dsto.defence.gov.au/workareas/library/resources/dsto_thesaurus.htm

Gas Turbine engines; Testbed; Data acquisition

19. ABSTRACT
The development and upgrade of test installations, instrumentation and the data acquisition system of an existing turbofan engine test rig are described for an experimental program which was planned and initiated to investigate the transient unsteady operation of gas turbine engines with an emphasis on compressor operation. The objective of the program was to examine aerodynamic instabilities such as stall and surge. Of particular interest were the pre-stall behaviour of the compressor and the generation and the detection of gas-path stall/surge precursors. Methods used to invoke compressor stall/surge and to detect stall/surge precursors are described and examples of results of the observed stall/surge phenomena and their precursors are included. However, the precursor pressure pulses are of small amplitude and occur only several milliseconds prior to the point of stall initiation. Additional work is required to incorporate these results in a practical stall warning device.